Diss.ETH No. 17871

The role of EXECUTER1- and EXECUTER2-dependent retrograde signaling after release of singlet oxygen in *Arabidopsis thaliana*

A dissertation submitted to the
SWISS FEDERAL INSTITUTE OF TECHNOLOGY ZURICH
for the degree of
DOCTOR OF SCIENCES

presented by

Keun Pyo Lee

M.Sc. in Applied Biology, University of Dongguk, Republic of Korea

Date of birth: April 07, 1975
Citizen of the Republic of Korea

Accepted on the recommendation of
Prof. Dr. K. Apel, examiner
Prof. Dr. N. Amrhein, co-examiner

March, 2009

Contents

List of original publications

This thesis is based on the following publications.

I. Keun Pyo Lee, Chanhong Kim, Frank Landgraf, and Klaus Apel (2007) EXECUTER1- and EXECUTER2-dependent transfer of stress-related signals from the plastid to the nucleus of *Arabidopsis thaliana*. *Proc Natl Acad Sci* USA 104(24), 10270-10275.

II. Keun Pyo Lee, Chanhong Kim, Aiswarya Baruah, Christophe Laloi, Mena Nater, Ivo Feussner and Klaus Apel (2008) EXECUTER1 AND EXECUTER2-dependent retrograde signaling during late embryogenesis primes plastid development in seedlings of *Arabidopsis thaliana*. In preparation.

III. Chanhong Kim, Keun Pyo Lee, Ashok M.L., Karolina Blajecka, Magdalena Obazanek-Fojt, Hyesung Jeon, Rasa Meskauskiene, Hye Min Ham, Ji Young Kim, Diana Marcela Pazmiño Mantilla, Mena Nater, Karin Krupinska and Klaus Apel (2008) A new role of chloroplast as the *alpha* and *omega* of a plant-specific programmed cell death pathway. In preparation.

Own contributions

I performed the most experiments in these researches. I was, however, assisted by my co-authors. The detailed my own contributions for each part are following;

I. Keun Pyo Lee*, Chanhong Kim*, Frank Landgraf, and Klaus Apel (2007) EXECUTER1- and EXECUTER2-dependent transfer of stress-related signals from the plastid to the nucleus of *Arabidopsis thaliana*. *Proc Natl Acad Sci* USA 104(24), 10270-10275. (* first co-authors)

- Identification of homozygous mutants (ex1/flu, ex2/flu, ex1/ex2/flu) by PCR based genotyping.
- RNA extraction from mature plants for microarray analysis and Real-time PCR, and data analysis.
- Extraction and measurement of protochlorophyllide.
- Vector constructions to identify the localization in vivo for EXECUTER1 and EXECUTER2.
- Growth measurements for mutants to determine their growth inhibition under long-day condition.
- Computer based data analysis for homology searches and prediction of protein structure.

II. Keun Pyo Lee*, Chanhong Kim*, Aiswarya Baruah, Christophe Laloi, Mena Nater, Ivo Feussner and Klaus Apel (2008) EXECUTER1 AND EXECUTER2-dependent retrograde signaling during late embryogenesis primes plastid development in seedlings of *Arabidopsis thaliana*. In preparation. (* first co-authors)

- Identification of homozygous mutants (ex1, ex2, ex1/ex2, cyp707a3, ex1/ex2/cyp707a3) by PCR based genotyping.
- RNA extraction from seedlings and immature seeds for microarray analysis, Real-time PCR and RT-PCR.
- Extraction and measurement of chlorophyll, and determination of chlorophyll autofluorescence by FluorCam system and confocal laser scanning microscope, and measurement of plastid size.
- Protein extraction and Western blot analysis to determine the level of plastid protein.
- Sample preparations for transmission electron microscopy to observe chloroplasts and etioplasts.
- Isolation of immature seeds from different stages of siliques to detect singlet oxygen production.
- Germination tests and determination of plastid differentiation on abscisic acid-containing medium.
- Computer based data analysis.

III. Chanhong Kim*, Keun Pyo Lee*, Ashok M.L., Karolina Blajecka, Magdalena Obazanek-Fojt, Hyesung Jeon, Rasa Meskauskiene, Hye Min Ham, Ji Young Kim, Diana Marcela Pazmiño Mantilla, Mena Nater, Karin Krupinska and Klaus Apel (2008) A new role of chloroplast as the *alpha* and *omega* of a plant-specific programmed cell death pathway. In preparation. (* first co-authors)

- In planta transformation and identification of transgenic lines.

- RNA extraction from seedlings for RT-PCR and computer based gene expression analysis.

- Determination of cell death by trypan blue staining.

- Growth measurements for mutants to determine their growth inhibition under short-day condition.

- Extraction and measurement of protochlorophyllide.

- Determination of photo-inhibitory stress conditions (low temperature / high light stress).

- Chlorophyll a fluorescence measurements by FluorCam system.

Abbreviations

AAA	ATPase associated with various cellular activities
ABA	Abscisic acid
ATP	adenosine triphosphate
bp	base pair
BLAST	Basic Local Alignment Search Tool
Chl	Chlorophyll
Col	Columbia
cDNA	complementary deoxyribonucleic acid
DAA	Day After Anthesis
dNTP	deoxyribonucleotide triphosphate
DTT	dithiothreitol
D/L	dark/light
EDTA	ethylenediaminetetraacetic acid
E. coli	*Escherichia coli*
EX	EXECUTER
HPLC	high performance liquid chromatography
HR	hypersensitive response
Ler	*Landsberg erecta*
LL	continuous light
mRNA	messenger ribonucleic acid
MS	Murashige and Skoog
NCBI	National center for biotechnology information
OD	optical density
ORF	open Reading frame
PCR	polymerase chain reaction
PCD	programmed cell death
Pchlide	Protochlorophyllide
POR	NADPH-protochlorophyllide oxidoreductase
PSII	photosystem II
ROS	reactive oxygen species
Rpm	revolution per minute
RT-PCR	reverse transcriptase polymerase chain reaction
TAIR	The Arabidopsis Information Resource
Vs	*versus*
wt	wild type

Summary

The conditional *flu* mutant of Arabidopsis, which generates $^1O_2$ in plastids during a dark-to-light transition, has been used to study the biological activity of this reactive oxygen species. Upon the release of $^1O_2$, seedlings of the *flu* mutant bleach and die, whereas mature *flu* plants stop their growth. These $^1O_2$-mediated stress responses were abrogated in a suppressor mutant of *flu, flu/executer1*. In addition to visible phenotypic changes, generation of $^1O_2$ in the *flu* mutant led also to a rapid and drastic change in nuclear gene expression. Inactivation of EXECUTER1 (EX1) attenuated upregulation of $^1O_2$-responsive genes, but did not fully eliminate these changes. In the present study a second closely related EXECUTER protein, EX2, has been identified that has been also implicated with the signaling of $^1O_2$-dependent nuclear gene expression changes. Like EX1, EX2 is confined to the plastid. The primary function of EX2 seems to be that of a modulator attenuating and controlling the activity EX1. Only when both EX proteins are inactive in an *ex1/ex2/flu* triple mutant was the upregulation of the vast majority of $^1O_2$-responsive genes abolished.

In the second part of this thesis *ex1/ex2* double mutants have been used in a wild-type background to verify the physiological significance of EX1/EX2-dependent signaling. Plastid differentiation was severely impaired in cotyledons of *ex1/ex2* seedlings. This developmental arrest of plastid formation could be attributed to the release of $^1O_2$ during late embryogenesis activating signaling pathways prior to seed dormancy that predetermined the fate of plastid differentiation during seedling development. Unexpectedly, EX1/EX2-dependent signaling during late embryogenesis implicated abscisic acid (ABA) in playing a key role during early plastid differentiation. Normal plastid differentiation in *ex1/ex2* seedlings could be rescued by the addition of ABA.

Finally, in the third part of this thesis a novel form of programmed cell death has been described that implicates chloroplasts rather than mitochondria with being the source and the target of a cell death pathway that leads to a genetically controlled rapid loss of chloroplast integrity and triggers the collapse of the affected cell. Inactivation of EX1 and EX2 blocked the execution of this $^1O_2$-mediated cell death program.

Zusammenfassung

Die konditionierbare *flu* Mutante von Arabidopsis, die während eines Dunkel- Lichtwechsels $^1O_2$ in Plastiden freisetzt, wurde benutzt um die biologische Aktivität dieser reaktiven Sauerstoffspecies zu beschreiben. Nach Freisetzung von $^1O_2$ bleichen Keimlinge der *flu* Mutante aus und sterben, während reife *flu* Pflanzen ihr Wachstum einstellen. Diese durch $^1O_2$ ausgelösten Stressantworten wurden in einer Suppressor Mutante von *flu, flu/ex1,* ausgelöscht. Neben den sichtbaren phänotypischen Veränderungen führt die Freisetzung von $^1O_2$ in der *flu* Mutante auch zu schnellen Veränderungen der Kerngenexpression. Inaktivierung von EXECUTER1 reduziert zwar die Hochregulation der durch $^1O_2$ stimulierbaren Kerngene, unterdrückt sie aber nicht vollständig. In der vorliegenden Arbeit wurde ein zweites, eng verwandtes EXECUTER Protein, EXECUTER2 (EX2) gefunden, das ebenfalls an der Auslöschung von $^1O_2$-abhängigen Änderungen der Kerngenexpression beteiligt ist. Ähnlich wie EX1 tritt EX2 nur in den Plastiden auf. Die Hauptfunktion von EX2 scheint die eines Modulators von EX1 zu sein, der die Aktivität von EX1 unterdrückt und kontrolliert. Nur wenn beide EX Proteine in einer *ex1/ex2/flu* Triple-Mutante inaktiv sind, wurde die Hochregulation fast aller $^1O_2$-abhängigen Gene ausgelöscht.

Im zweiten Teil dieser Arbeit wurden *ex1/ex2* Doppelmutanten im Wildtyphintergrund benutzt, um die physiologische Relevanz der EX1/EX2-abhängigen Signalübertragung zu überprüfen. Die Differenzierung von Plastiden in den Keimblättern von *ex1/ex2* Keimlingen war stark gestört. Dieser Stop der Plastidenentwicklung konnte auf die Freisetzung von $^1O_2$ während der späten Embryogenese zurückgeführt werden. Somit werden Signalwege vor Erreichen der Dormanz der Samen aktiviert, welche den weiteren Verlauf der Plastidenentwicklung vorherbestimmen. Überraschenderweise zeigt die Untersuchung des *ex1/ex2*-abhängigen Signalweges, dass Abscisinsäure während der frühen Plastidenentwicklung eine Schlüsselrolle spielt. Die normale Differenzierung der Plastiden in der *ex1/ex2* Mutante konnte durch Zugabe von exogener ABA wieder hergestellt werden.

Im dritten und letzten Kapitel dieser Dissertation wurde eine neue Form von programmiertem Zelltod gefunden, bei der Chloroplasten statt Mitochondrien den Anfang und das Ziel eines Signalweges darstellen. Diese Signalwege führen zu einem genetisch kontrollierten Verlust der Chloroplastenintegrität und bewirken den Zusammenbruch der physiologischen Lebensprozesse der betroffenen Zelle. Die Inaktivierung von EX1 und EX2 blockiert die Durchführung dieses durch $^1O_2$ ausgelösten Zelltodprogramms.

1. Introduction

In organisms adapted to aerobic life conditions, the continuous production of reactive oxygen species (ROS) is an unavoidable consequence of various metabolic pathways such as respiration and photosynthesis (Neill et al. 2002; Apel and Hirt 2004). While oxygen in its ground state is chemically inert, it may be converted to ROS either by electron or energy transfer reactions. The former leads by stepwise reduction to the formation of superoxide radical ($O_2^{\bullet-}$), hydrogen peroxide (H_2O_2) and hydroxyl radical ($HO^{\bullet}$) (Halliwell 2006), whereas the latter results in the formation of singlet oxygen ($^1O_2$) (Foote 1968; Gollnick 1968). Generally ROS have been proposed to function in two different ways. ROS may react with various biomolecules such as proteins, lipids and nucleic acids and in this way cause irreversible damage that triggers necrotic responses and ultimately may kill the organisms (Rebeiz et al. 1988; Girotti 2001). On the other hand, organisms have evolved strategies to utilize ROS as signals that activate and control a variety of stress-related responses to environmental variation (Foyer and Noctor 2000; Gechev and Hille 2005).

Plants are sessile organisms that frequently encounter changes in their environment. They perceive these changes probably through a large number of sensors with different specificities that jointly activate several signaling pathways. How these signaling pathways interact and how the multitude of signals is integrated and leads to specific responses is the topic of intense research (Fujita et al. 2006). One of the first reactions of plants under environmental stress is the enhanced production of chemically distinct reactive oxygen species (ROS) (Apel and Hirt 2004). In plants, chloroplasts and peroxisomes have been shown to be major sites of ROS production (Foyer and Noctor 2000). The enhanced generation of ROS in these cellular compartments has been attributed to the disturbance of the light-driven photosynthetic electron transport by a variety of environmental factors that trigger stress responses (Niyogi 1999). Under these environmental conditions, plants are exposed to light intensities that exceed their capacity to assimilate CO_2 and that lead to the over-reduction of the electron transport chain and ultimately may result in the inhibition of photosynthesis. Plants may use two different strategies to protect their photosynthetic apparatus: first, the thermal dissipation of excess excitation energy in the photosystem II antennae (non-photochemical quenching) (Muller et al. 2001), and second the transfer of electrons from PSII to various acceptors that act as alternative sinks for electrons, thereby sustaining partial oxidation of PSII acceptors and preventing photo-inactivation of PSII (photochemical quenching). Photochemical quenching may be achieved in chloroplasts through the direct reduction of oxygen to the ROS superoxide radical by reduced electron transport

components associated with PSI (Asada 1999; Rizhsky et al. 2003) and by reactions linked to the photorespiratory cycle that result in the enhanced production of the ROS hydrogen peroxide in peroxisomes (Kozaki and Takeba 1996). A third ROS, singlet oxygen, is continuously produced by PSII through energy transfer from excited chlorophyll to oxygen (Gollnick 1968; Krieger-Liszkay 2005). The quenching of this singlet oxygen has been linked to the turnover of the D1 protein of the PSII reaction center (Telfer et al. 1994; Trebst 2003). The enhanced production of H_2O_2, superoxide radical and singlet oxygen in chloroplasts and peroxisomes leads to various stress responses of the plant. If they act as signals, their biological activities should exhibit a high degree of specificity and selectivity that may result from the intracellular sites at which they were produced and/or their chemical identity. In prokaryotes, different biological activities of chemically distinct ROS have been well documented (Toledano et al. 2004). Interactions of superoxide and hydrogen peroxide with SoxR and OxyR proteins, respectively, have been shown to trigger the activation of distinct sets of genes (Zheng et al. 1998). Similar specific biological activities of ROS have been documented also in eucaryotic organisms (Jabs et al. 1996; Leisinger et al. 2001; Delaunay et al. 2002; Mou et al. 2003; op den Camp et al. 2003; Gadjev et al. 2006).

In plants, one of the difficulties in elucidating the biological activities of ROS generated in chloroplasts and peroxisomes during light stress stems from the fact that normally they are generated simultaneously, thus making it difficult to link a particular stress response to a specific ROS (Fryer et al. 2002; Hideg et al. 2002; Gadjev et al. 2006). This problem has been alleviated by using the conditional *flu* mutant of Arabidopsis that allows inducing the production of only one ROS, singlet oxygen ($^1O_2$), within plastids in a non-invasive, controlled manner (Meskauskiene et al. 2001; op den Camp et al. 2003).

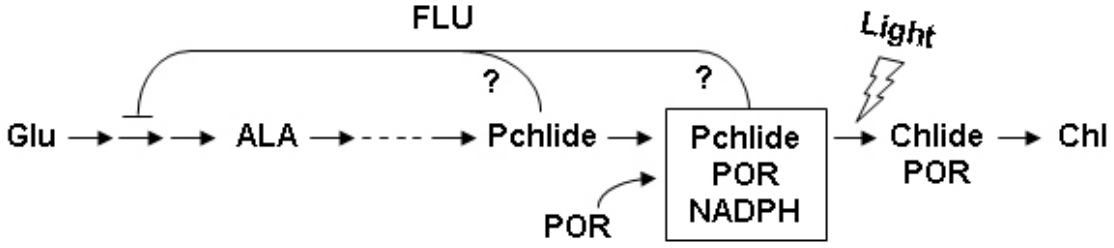

Fig 1.1. FLU-Dependent Regulation of Pchlide Synthesis in Arabidopsis. FLU has been identified as a membrane-bound plastid protein that mediates the feedback control of chlorophyll synthesis (Meskauskiene et al., 2001). As indicated by the question marks, it is not known whether Pchlide acts in its free form or as part of the ternary POR-Pchlide-NADPH complex as an effector of feedback inhibition. Glu, glutamate; ALA, δ-aminolevulinic acid; Chlide, chlorophyllide; Chl, chlorophyll

FLU is a nuclear-encoded protein that, after import and processing, becomes tightly associated with plastid membranes. It affects the Mg^{2+} branch of tetrapyrrole biosynthesis by directly interacting with Glu-tRNA reductase (Meskauskiene and Apel 2002; Goslings et al. 2004) (Fig. 1.1).

In contrast to etiolated wild-type seedlings, etiolated *flu* seedlings are no longer able to restrict the accumulation of Pchlide (Meskauskiene et al. 2001) (Fig. 1.2, DD). When these seedlings are transferred from the dark to the light, they rapidly bleach and die because of the photosensitizing activity of excess amounts of free Pchlide and the sudden release of $^1O_2$ (op den Camp et al. 2003) (Fig. 1.2, D→L). The *flu* mutant remains viable, however, when it is kept from the very beginning under continuous light (Fig. 1.2, LL).

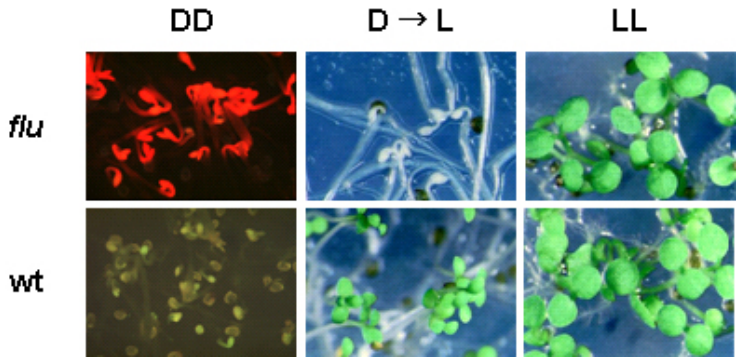

Fig 1.2. Phenotype of conditional *flu* mutant in seedling stage. *flu* and wt seedlings were grown in the dark and fluorescence was recorded after exposure to blue light (DD). Etiolated seedlings were transferred to white light for 12 hours (D→L). Seedlings were grown under permissive continuous light (LL).

Under these conditions, Pchlide in the *flu* mutant is immediately photoreduced to chlorophyllide (Chlide) and in this way does not reach critical levels that might lead to the production of $^1O_2$ and cause photooxidative damage (Rebeiz et al. 1988). As long as *flu* plants are kept under continuous light, no obvious difference between mutant and wild type can be observed (Meskauskiene et al. 2001; op den Camp et al. 2003). These properties of the *flu* mutant have been exploited to study the physiological role of $^1O_2$ by growing *flu* plants initially under continuous light, until they reach a developmental stage of interest, and then transferring them to the dark and re-exposing them to light. The release of $^1O_2$ in the *flu* mutant has been determined directly by using two $^1O_2$-specific probes, DanePy and $^1O_2$-Sensor Green (Hideg et al. 1998; op den Camp et al. 2003; Flors et al. 2006). With both probes, however, $^1O_2$ measurements are at best semi-quantitative. A more accurate way to estimate the extent of $^1O_2$ production has been the determination of the photosensitizer Pchlide by HPLC (Laloi et al. 2007; Lee et al. 2007).

The response of the *flu* mutant to $^1O_2$ has been analyzed in seedlings and in mature plants that are ready to bolt. Seedlings of *flu* bleach and die, when they are kept under repeated 16 h light / 8 h dark cycles, whereas mature plants grown initially under continuous light develop necrotic lesions on their leaves and stop their growth immediately after being shifted to daily dark/light cycles (op den Camp et al. 2003). An extensive second-site mutant screen of the *flu* mutant was undertaken to identify suppressor mutants that in the dark accumulate similar excess amounts of free Pchlide as the original *flu* line, but upon re-illumination suppress $^1O_2$-mediated growth inhibition and lesion formation of mature *flu* plants and/or the bleaching of *flu* seedlings. Thus far, studies have been focused on analyzing one particular group of 15 suppressor mutants, dubbed *executer (ex)* (Wagner et al. 2004). Allelism tests and mapping of these mutated genes revealed that they represent only a single locus, *EXECUTER1 (EX1)*. Under non-permissive dark/light conditions the *executer1* (*ex1*)/*flu* double mutant generates similar amounts of $^1O_2$ as the parental *flu* line (Wagner et al. 2004), but in contrast to *flu* behaves like wild type in that seedlings remain viable and do not bleach and mature plants continue to grow (Fig. 1.3). It seems, as if *flu* plants, because of the *ex1* mutation, have lost the ability to perceive the presence of $^1O_2$ within their chloroplasts and to activate $^1O_2$-mediated response programs.

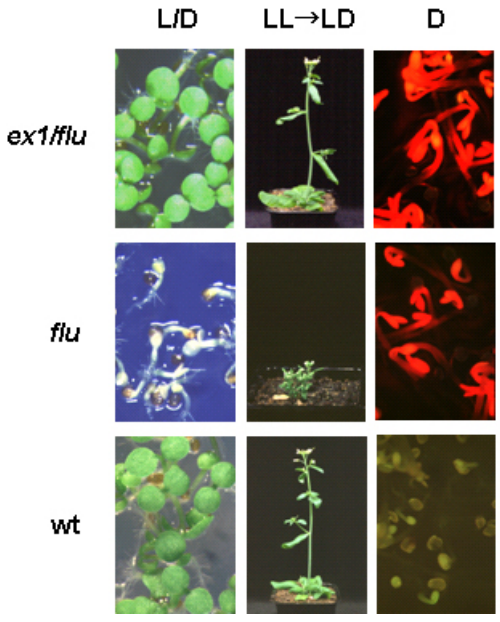

Fig 1.3. The phenotypic differences between *ex1/flu*, *flu* and wild-type seedlings grown under 16 h light/8 h dark cycles (L/D) or in the dark (D) and mature plants initially grown under continuous light until they were ready to bolt and then shifted to 16 h light/8 h dark cycles (LL → L/D). Free Pchlide accumulates in etiolated seedlings of *flu* and *ex1/flu* that upon excitation with blue light emits a strong red fluorescence, whereas in wild-type seedlings Pchlide forms part of the photoactive ternary NADPH-Pchlide-POR complex. The release of singlet oxygen in *flu* following a dark/light transition triggers two major stress responses, growth inhibition of mature plants and seedling lethality. In *ex1/flu* mutants the both lethality of seedlings and growth inhibition of mature plants are blocked.

The present Ph.D. work has been aimed at addressing three major problems linked to the biological activity of singlet oxygen. Firstly, enhanced levels of $^1O_2$ within plastids of the *flu* mutant do not only induce phenotypic changes but also affect greatly the expression of nuclear genes (op den Camp et al. 2003). Inactivation of EXECUTER1 (EX1) attenuates the up-regulation of $^1O_2$-responsive nuclear genes, but does not fully eliminate these changes. In the present work a second related nuclear-encoded protein, dubbed EXECUTER2 (EX2), has been identified that is also involved in signaling of $^1O_2$-dependent nuclear gene expression changes **(Chapter 2)**. Like EX1, EX2 is confined to the plastid. Inactivation of both EXECUTER proteins in the *ex1/ex2/flu* triple mutant is sufficient to suppress the up-regulation of almost all $^1O_2$-responsive genes.

Secondly, in previous work of our laboratory a signaling role of $^1O_2$ has been documented only in the *flu* mutant but not in wild type. This raises the questions whether $^1O_2$-mediated responses in the mutant may also occur in wild-type plants. In the present work **(Chapter3)** $^1O_2$-mediated signaling in embryos of wild-type plants has been shown to predetermine the fate of plastid differentiation during seedling development.

Finally, a novel $^1O_2$-specific genetically controlled programmed cell death response has been identified that requires the activities of both EXECUTER1 and EXECUTER2 **(Chapter 4)**.

1.1 References

Apel, K. and Hirt, H. 2004. Reactive oxygen species: metabolism, oxidative stress, and signal transduction. *Annu Rev Plant Biol* 55: 373-399.

Asada, K. 1999. The water-water cycle in chloroplasts: scavenging of active oxygens and dissipation of excess photons. *Annu Rev Plant Physiol Plant Mol Biol* 50: 601-639.

Delaunay, A., Pflieger, D., Barrault, M.B., Vinh, J., and Toledano, M.B. 2002. A thiol peroxidase is an H_2O_2 receptor and redox-transducer in gene activation. *Cell* 111(4): 471-481.

Flors, C., Fryer, M.J., Waring, J., Reeder, B., Bechtold, U., Mullineaux, P.M., Nonell, S., Wilson, M.T., and Baker, N.R. 2006. Imaging the production of singlet oxygen in vivo using a new fluorescent sensor, Singlet Oxygen Sensor Green. *J Exp Bot* 57(8): 1725-1734.

Foote, C.S. 1968. Mechanisms of photosensitized oxidation. There are several different types of photosensitized oxidation which may be important in biological systems. *Science* 162(857): 963-970.

Foyer, C.H. and Noctor, G. 2000. Oxygen processing in photosynthesis: regulation and signalling. *New Phytol* 146(3): 359-388.

Fryer, M.J., Oxborough, K., Mullineaux, P.M., and Baker, N.R. 2002. Imaging of photo-oxidative stress responses in leaves. *J Exp Bot* 53(372): 1249-1254.

Fujita, M., Fujita, Y., Noutoshi, Y., Takahashi, F., Narusaka, Y., Yamaguchi-Shinozaki, K., and Shinozaki, K. 2006. Crosstalk between abiotic and biotic stress responses: a current view from the points of convergence in the stress signaling networks. *Curr Opin Plant Biol* 9(4): 436-442.

Gadjev, I., Vanderauwera, S., Gechev, T.S., Laloi, C., Minkov, I.N., Shulaev, V., Apel, K., Inze, D., Mittler, R., and Van Breusegem, F. 2006. Transcriptomic footprints disclose specificity of reactive oxygen species signaling in Arabidopsis. *Plant Physiol* 141(2): 436-445.

Gechev, T.S. and Hille, J. 2005. Hydrogen peroxide as a signal controlling plant programmed cell death. *J Cell Biol* 168(1): 17-20.

Girotti, A.W. 2001. Photosensitized oxidation of membrane lipids: reaction pathways, cytotoxic effects, and cytoprotective mechanisms. *J Photochem Photobiol B* 63(1-3): 103-113.

Gollnick, K. 1968. Type 2 photosensitized oxygenation reactions. *Adv Chem Ser* 77: 78-101.

Goslings, D., Meskauskiene, R., Kim, C., Lee, K.P., Nater, M., and Apel, K. 2004. Concurrent interactions of heme and FLU with Glu-tRNA reductase (HEMA1), the target of metabolic feedback inhibition of tetrapyrrole biosynthesis, in dark- and light-grown Arabidopsis plants. *Plant J* 40(6): 957-967.

Halliwell, B. 2006. Reactive species and antioxidants. Redox biology is a fundamental theme of aerobic life. *Plant Physiol* 141(2): 312-322.

Hideg, E., Barta, C., Kalai, T., Vass, I., Hideg, K., and Asada, K. 2002. Detection of singlet oxygen and superoxide with fluorescent sensors in leaves under stress by photoinhibition or UV radiation. *Plant Cell Physiol* 43(10): 1154-1164.

Hideg, E., Kalai, T., Hideg, K., and Vass, I. 1998. Photoinhibition of photosynthesis in vivo results in singlet oxygen production detection via nitroxide-induced fluorescence quenching in broad bean leaves. *Biochemistry* 37(33): 11405-11411.

Jabs, T., Dietrich, R.A., and Dangl, J.L. 1996. Initiation of runaway cell death in an Arabidopsis mutant by extracellular superoxide. *Science* 273(5283): 1853-1856.

Kozaki, A. and Takeba, G. 1996. Photorespiration protects C3 plants from photooxidation. *Nature* 384: 557-560

Krieger-Liszkay, A. 2005. Singlet oxygen production in photosynthesis. *J Exp Bot* 56(411): 337-346.

Laloi, C., Stachowiak, M., Pers-Kamczyc, E., Warzych, E., Murgia, I., and Apel, K. 2007. Cross-talk between singlet oxygen- and hydrogen peroxide-dependent signaling of stress responses in *Arabidopsis thaliana*. *Proc Natl Acad Sci U S A* 104(2): 672-677.

Lee, K.P., Kim, C., Landgraf, F., and Apel, K. 2007. EXECUTER1- and EXECUTER2-dependent transfer of stress-related signals from the plastid to the nucleus of *Arabidopsis thaliana*. *Proc Natl Acad Sci U S A* 104(24): 10270-10275.

Leisinger, U., Rufenacht, K., Fischer, B., Pesaro, M., Spengler, A., Zehnder, A.J., and Eggen, R.I. 2001. The glutathione peroxidase homologous gene from *Chlamydomonas reinhardtii* is transcriptionally up-regulated by singlet oxygen. *Plant Mol Biol* 46(4): 395-408.

Meskauskiene, R. and Apel, K. 2002. Interaction of FLU, a negative regulator of tetrapyrrole biosynthesis, with the glutamyl-tRNA reductase requires the tetratricopeptide repeat domain of FLU. *FEBS Lett* 532(1-2): 27-30.

Meskauskiene, R., Nater, M., Goslings, D., Kessler, F., op den Camp, R., and Apel, K. 2001. FLU: a negative regulator of chlorophyll biosynthesis in Arabidopsis thaliana. *Proc Natl Acad Sci U S A* 98(22): 12826-12831.

Mou, Z., Fan, W., and Dong, X. 2003. Inducers of plant systemic acquired resistance regulate NPR1 function through redox changes. *Cell* 113(7): 935-944.

Muller, P., Li, X.P., and Niyogi, K.K. 2001. Non-photochemical quenching. A response to excess light energy. *Plant Physiol* 125(4): 1558-1566.

Neill, S.J., Desikan, R., Clarke, A., Hurst, R.D., and Hancock, J.T. 2002. Hydrogen peroxide and nitric oxide as signalling molecules in plants. *J Exp Bot* 53(372): 1237-1247.

Niyogi, K.K. 1999. Photoprotection revisited: Genetic and molecular approaches. *Annu Rev Plant Physiol Plant Mol Biol* 50: 333-359.

op den Camp, R.G., Przybyla, D., Ochsenbein, C., Laloi, C., Kim, C., Danon, A., Wagner, D., Hideg, E., Gobel, C., Feussner, I., Nater, M., and Apel, K. 2003. Rapid induction of distinct stress responses after the release of singlet oxygen in Arabidopsis. *Plant Cell* 15(10): 2320-2332.

Rebeiz, C.A., Montazer-Zouhoor, A., Mayasich, J.M., Tripathy, B.C., Wu, S.M., and Rebeiz, C. 1988. Photodynamic herbicides. Recent developments and molecular basis of selectivity. *CRC Crit Rev Plant Sci* 6: 385–436

Rizhsky, L., Liang, H., and Mittler, R. 2003. The water-water cycle is essential for chloroplast protection in the absence of stress. *J Biol Chem* 278(40): 38921-38925.

Telfer, A., Bishop, S.M., Phillips, D., and Barber, J. 1994. Isolated photosynthetic reaction center of photosystem II as a sensitizer for the formation of singlet oxygen. Detection and quantum yield determination using a chemical trapping technique. *J Biol Chem* 269(18): 13244-13253.

Toledano, M.B., Delaunay, A., Monceau, L., and Tacnet, F. 2004. Microbial H_2O_2 sensors as archetypical redox signaling modules. *Trends Biochem Sci* 29(7): 351-357.

Trebst, A. 2003. Function of beta-carotene and tocopherol in photosystem II. *Z Naturforsch [C]* 58(9-10): 609-620.

Wagner, D., Przybyla, D., Op den Camp, R., Kim, C., Landgraf, F., Lee, K.P., Wursch, M., Laloi, C., Nater, M., Hideg, E., and Apel, K. 2004. The genetic basis of singlet oxygen-induced stress responses of *Arabidopsis thaliana*. *Science* 306(5699): 1183-1185.

Zheng, M., Aslund, F., and Storz, G. 1998. Activation of the OxyR transcription factor by reversible disulfide bond formation. *Science* 279(5357): 1718-1721.

2. EXECUTER1- and EXECUTER2-dependent transfer of stress-related signals from the plastid to the nucleus of *Arabidopsis thaliana*

Keun Pyo Lee[1], Chanhong Kim[1], Frank Landgraf and Klaus Apel[2]

Institute of Plant Sciences, Plant Genetics, Swiss Federal Institute of Technology (ETH), CH–8092, Zurich, Switzerland

[1] These authors contributed equally to this work

[2] Correspondance, E-mail: kapel@ethz.ch

***Proc Natl Acad Sci USA* (2007), 104(24), 10270-10275**

2.1 Abstract

Shortly after the release of singlet oxygen ($^1O_2$) within the plastid of the conditional *flu* mutant of Arabidopsis drastic changes in nuclear gene expression occur that reveal a rapid transfer of signals from the plastid to the nucleus. In contrast to retrograde control of nuclear gene expression by plastid signals described earlier, the primary effect of $^1O_2$ generation in the *flu* mutant is not the control of chloroplast biogenesis but the activation of a broad range of signaling pathways known to be involved in numerous biotic and abiotic stress responses. This novel and distinct activity of a plastid-derived signal suggests a new function of the chloroplast, namely that of a sensor of environmental changes that activates a broad range of stress responses. Inactivation of the plastid protein EXECUTER1 attenuates the extent of $^1O_2$-induced upregulation of nuclear gene expression, but it does not fully eliminate these changes. A second related nuclear-encoded protein, dubbed EXECUTER2, has also been implicated with the signaling of $^1O_2$-dependent nuclear gene expression changes. Like EXECUTER1, EXECUTER2 is confined to the plastid. In contrast to EXECUTER1, however, inactivation of EXECUTER2 further enhances the intensity of $^1O_2$–mediated changes of nuclear gene expression. Inactivation of both EXECUTER proteins in the *ex1/ex2/flu* triple mutant is sufficient to suppress the up- and downregulation of almost all $^1O_2$-responsive genes and to adjust their transcripts to the wild-type level. Retrograde control of $^1O_2$-responsive genes seems to require the concerted action of both EXECUTER proteins within the plastid compartment

2.2 Introduction

In plants, continuous generation of reactive oxygen species (ROS) is an unavoidable consequence of aerobic metabolic processes such as photosynthesis and respiration that has necessitated the evolution of various scavengers to minimize the cytotoxic impact of ROS on cells. Sensing changes of ROS concentrations that result from metabolic disturbances is being used by plants to evoke stress responses that support plants to cope with environmental variation (Elstner and Osswald 1994; Neill et al. 2002; Apel and Hirt 2004). Plants may also produce ROS in a genetically controlled way (e.g., by NADPH oxidases) and use these molecules as signals to control a broad range of processes that comprise defense reactions against pathogens (Torres et al. 2002), the closure of stomata (Kwak et al. 2003), the regulation of cell expansion and plant development (Foreman et al. 2003), and the control of plant–fungus interactions (Tanaka et al. 2006). Chloroplasts and peroxisomes have been shown to be major sites of ROS production (Niyogi 1999; Apel and Hirt 2004). The enhanced generation of ROS in these cellular compartments has been attributed to the disturbance of photosynthetic electron transport by a variety of environmental factors (such as high light, high or low temperatures, salt, and drought) that trigger various stress responses (Niyogi 1999; Apel and Hirt 2004). One of the difficulties in elucidating the biological activities of ROS during these processes stems from the fact that, in plants under stress, several chemically distinct ROS are generated simultaneously within different intracellular compartments, thus making it very difficult to link a particular stress response to a specific ROS (op den Camp et al. 2003; Apel and Hirt 2004). This problem has been alleviated by using the conditional *flu* mutant of *Arabidopsis* to study the biological activity of only one of these ROS at a given time (op den Camp et al. 2003).

In the dark, the *flu* mutant accumulates protochlorophyllide (Pchlide), a potent photosensitizer that upon illumination generates singlet oxygen ($^1O_2$) (Gollnick 1968; Meskauskiene et al. 2001; op den Camp et al. 2003). Immediately after a dark-to-light shift, mature *flu* plants stop growing, whereas *flu* seedlings bleach and die. By varying the length of the dark period, one can modulate noninvasively the level of the photosensitizer Pchlide and define conditions that minimize the cytotoxicity of $^1O_2$ and reveal the genetic basis of $^1O_2$-mediated signaling as indicated by the inactivation of the *EXECUTER1* gene that is sufficient to abrogate $^1O_2$–dependent stress responses (Wagner et al. 2004). The enhanced generation of $^1O_2$ within plastids that triggers drastic phenotypic changes would be expected to modulate nuclear gene expression as well. Indeed, 2 h after the release of $^1O_2$, rapid changes in the expression of nuclear genes have been shown to affect ≈5% of the total genome of *Arabidopsis* (op den Camp

et al. 2003). However, as reported in the present work, inactivation of the *EXECUTER1* gene of the *flu* mutant is not sufficient to fully suppress $^1O_2$-induced changes in nuclear gene expression, suggesting that a residual $^1O_2$-induced transduction of signals from the plastid to the nucleus still operates in the absence of EXECUTER1. We have identified a second signaling component closely related to EXECUTER1 that is also present inside the plastid compartment and, together with EXECUTER1, is required for $^1O_2$-dependent signaling of nuclear gene activities. This protein has been dubbed EXECUTER2. The *EXECUTER1* and *EXECUTER2* genes are highly conserved among higher plants and thus seem to play an important but hitherto unknown role during the transfer of stress-related signals from the plastid to the nucleus.

2.3 Results

2.3.1 Identification and localization of EXECUTER2

During an extensive second-site-mutant screen of the *flu* mutant, 15 different allelic lines of *executer1* (*ex1*) were identified. In three of these mutant lines, the mutations led to an amino acid exchange (Wagner et al. 2004). These amino acid residues are conserved among all EXECUTER1 proteins of higher plants for which sequence data are available (Wagner et al. 2004). A second *EXECUTER1*-like gene was found in *Arabidopsis* that was dubbed *EXECUTER2* and that was considered to be a candidate gene for a second putative signal component involved in $^1O_2$-dependent signaling. The predicted overall amino acid sequence identity between EXECUTER1 and EXECUTER2 is 38%, but the sequence identity increases to 42%, if only sequences of mature proteins without the signal sequences are compared (Fig. 2.1).

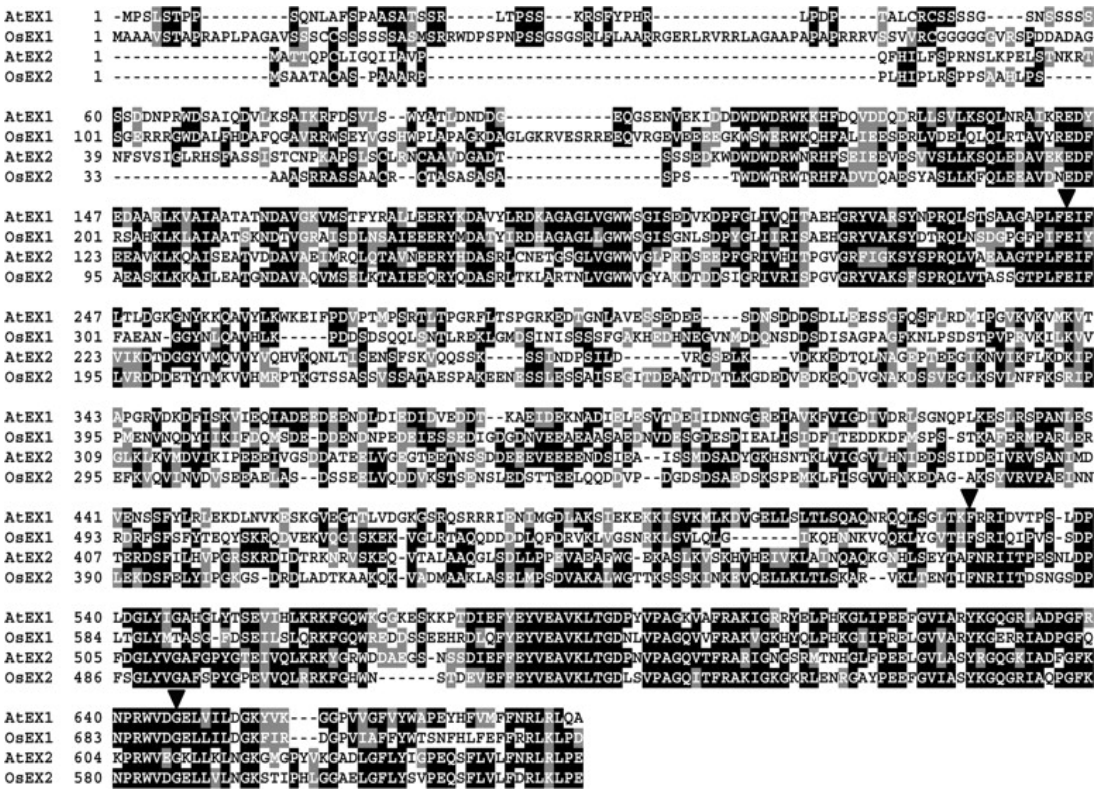

Fig. 2.1. Multiple alignments of deduced amino acid sequences of full-length cDNAs of *EXECUTER1* and *EXECUTER2* from *Arabidopsis* and rice. The three highly conserved amino acid residues of EXECUTER1 that were identified in a previous suppressor mutant screen of *flu* (12) are indicated by arrow heads. The amino acid sequences were aligned by using the ClustalW program. Gaps, which were introduced to maximize the alignment, are indicated by dashes. AtEX1(NP_567929) and AtEX2(NP_564287) from Arabidopsis *thaliana*, OsEX1(AAL59023) and OsEX2 (BAD44852) from rice.

EXECUTER1 and EXECUTER2 of *Arabidopsis* are closely related to the corresponding proteins of the monocotyledonean plant rice (Fig. 2.1). In particular the C termini of the EXECUTER proteins are highly conserved (Fig. 2.1). The three highly conserved amino acid residues of EXECUTER1 that seem to be essential for its activity are also conserved in all EXECUTER2 proteins of higher plants for which sequence data are available (Fig. 2.1; unpublished data).

The ORF of EXECUTER2 predicts a protein of 652 aa with a molecular mass of 72 kDa. Like EXECUTER1, it is unrelated to known proteins, except that its N-terminal part resembles import signal sequences of nuclear-encoded plastid proteins. This prediction was confirmed experimentally by expressing EXECUTER1- and EXECUTER2-GFP fusion proteins in stably transformed Arabidopsis plants and determining their intracellular localization under the confocal microscope (Fig. 2.2). As controls also plants expressing the small subunit (SSU) of the ribulose-1,5-bisphosphate carboxylase-GFP fusion protein and the NADPH protochlorophyllide oxidoreductase (POR)B-GFP fusion protein were analyzed (Fig. 2.2). The former accumulates within the stroma of plastids, whereas PORB is part of the chloroplast membranes (Griffiths 1978; Kim and Apel 2004). Both EXECUTER1 and EXECUTER2 accumulate within chloroplasts and seem to be associated with thylakoid membranes (Fig. 2.2).

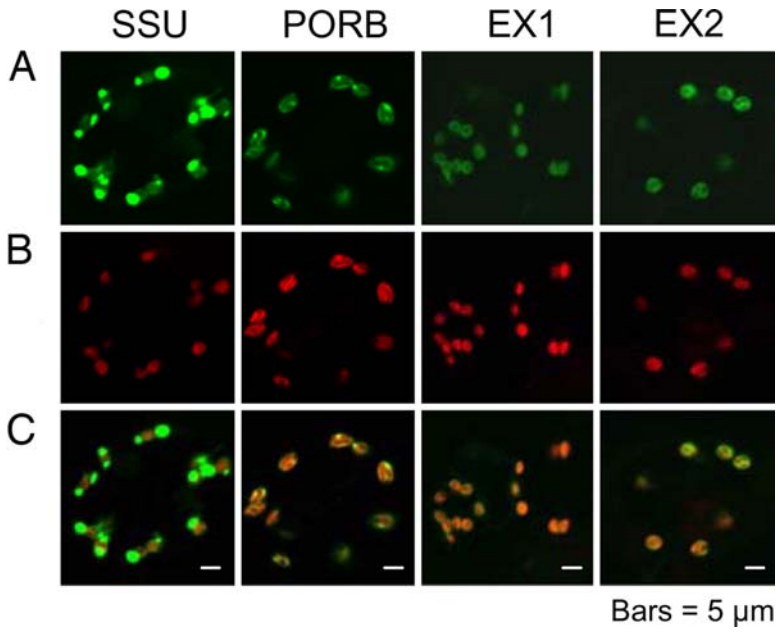

Fig. 2.2. Intracellular accumulation of GFP fusions with the small subunit of ribulose-1,5-bisphosphate carboxylase (SSU), the NADPH-Pchlide oxidoreductase B (PORB), EXECUTER1 (EX1), and EXECUTER2 (EX2) in cotyledons of transgenic seedlings grown for 5 days under continuous light. The green fluorescence of GFP fusion proteins (*A*) and the red fluorescence of chlorophyll (*B*) were monitored separately by using a confocal laser scanning microscope,and the the two fluorescence images were merged (*C*).

2.3.2 Functional characterization of EXECUTER2

During the second-site mutant screen of *flu* a large number of allelic *ex1* mutant lines, but no *executer2* (*ex2*) mutants have been found (Wagner et al. 2004). These results suggest that the EXECUTER2 protein is not essential for mediating the visible stress responses that have been used for the selection of second-site mutants (Wagner et al. 2004). However, this conclusion does not preclude the possibility that EXECUTER2 is involved in mediating other $^1O_2$-dependent stress responses. These predictions were tested experimentally by first identifying an *EXECUTER2* mutant line and crossing it with *flu* and then studying the effect of *EXECUTER2* inactivation on $^1O_2$-mediated stress responses in the *flu* background.

We have identified an *Arabidopsis* T-DNA [portion of the Ti (tumor-inducing) plasmid that is transferred to plant cells] insertion line from the SALK collection with a predicted insertion of the T-DNA in the *EXECUTER2* gene. The genetic background of this line was Columbia (Col-0). Because the *ex1* mutation had been found originally in Ler we searched for and identified a Col-0 line with the insertion of the T-DNA also predicted to be in the *EXECUTER1* gene. This prediction could be confirmed by PCR (data not shown). Both T-DNA-insertion lines were crossed with each other and a *flu* Col-0 line. Mature plants of the resulting *ex1*/*flu*, *ex2*/*flu* and *ex1*/*ex2*/*flu* mutant lines, *flu*, and wild type, all in Col-0, were subjected to the same dark/light shift experiment used previously to characterize the *flu* and *ex1* mutations in the Ler lines (Wagner et al. 2004). Mutant and wild-type plants were grown under continuous light until they reached the rosette leaf stage and were ready to bolt. Plants were then shifted from continuous light to a 16 h light/8 h dark program for the next 30 days. Once they were transferred to the long day conditions, *flu* and *ex2*/*flu* plants stopped growing, whereas *ex1*/*flu* and *ex1*/*ex2*/*flu* plants continued to grow similar to wild type except that their growth was slightly reduced and their final height was ≈80% of that of wild type. Under continuous light all five lines grew equally well and finally reached the same height (Fig. 2.3). When mature plants grown under continuous light were shifted to the dark for 8 h free Pchlide accumulated in all four mutant lines to similar levels in rosette leaves and were 3- to 4-fold higher than in wild-type controls.

Collectively, these results demonstrate that in the Col-0 background the effect of the *flu* mutation is similar to that in Ler (op den Camp et al. 2003; Wagner et al. 2004). Furthermore, also in Col-0 the *ex1* mutation in the *flu* background suppresses singlet oxygen-mediated growth inhibition of mature plants, whereas inactivation of the *EXECUTER2* gene of the *flu* mutant has only a minor effect on this $^1O_2$-mediated stress response, as one would expect based on our previous failure to isolate *ex2*/*flu* double mutants during an extensive second-site mutant screen of *flu*

(Wagner et al. 2004). Mature *ex1*/*ex2* mutant plants without the *flu* mutation are phenotypically similar to wild type (data not shown).

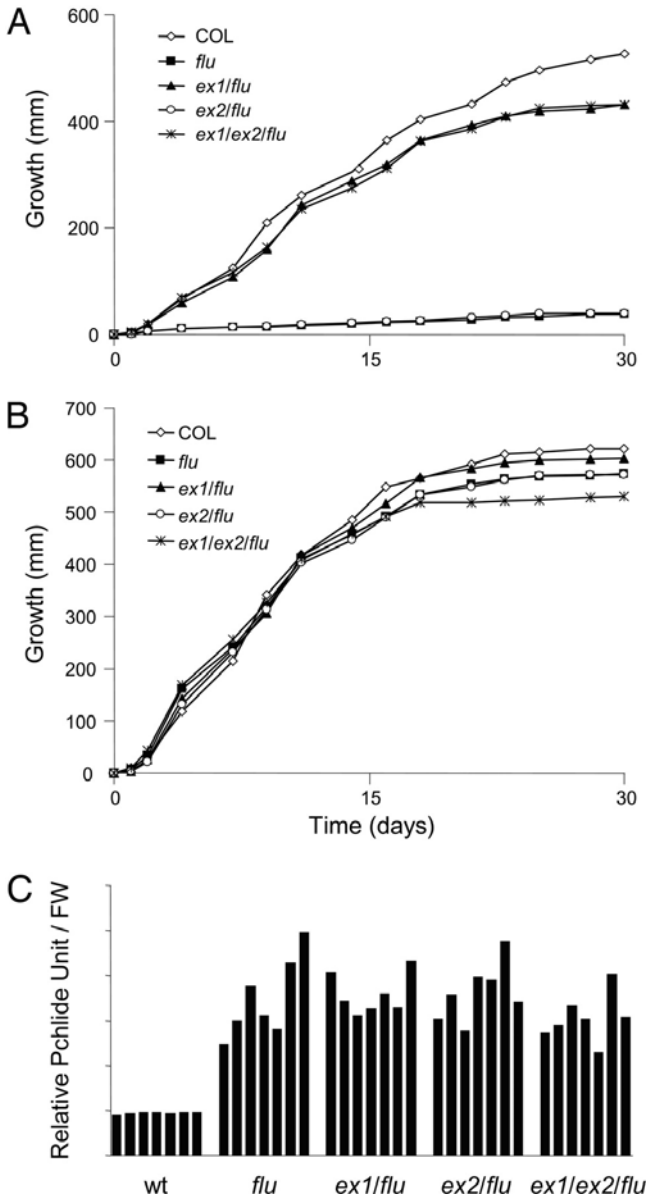

Fig. 2.3. $^1O_2$-mediated growth inhibition of mature ex1/flu, ex2/flu, ex1/ex2/flu, flu, and wild-type (wt) plants. Plants were grown for 21 days under continuous light until they were ready to bolt. Plants were then either shifted to a 16 h light/8 h dark program (*A*) or kept under continuous light (*B*), and the elongation of the inflorescence was followed over the next 30 days. Long-day conditions were used instead of short-day conditions to avoid the overaccumulation of excess amounts of Pchlide during an extended dark period. Under these light conditions, toxic effects of $^1O_2$ could be minimized. In contrast to Ler plants used previously (9, 12), the onset of bolting of Col-0 varied greatly between different plants. Growth curves of individual plants were corrected for these differences. Each value represents the average growth measurements of 10 different plants. (*C*) The accumulation of Pchlide in 21-day-old plants grown under continuous light and transferred to the dark for 8 h. Total Pchlide was extracted from aerial parts of single plants and analyzed by HPLC. For each genotype, seven independent Pchlide measurements are shown.

2.3.3 The effects of EXECUTER1 and EXECUTER2 inactivation on $^1O_2$-dependent signaling of nuclear gene expression

The impact of the *ex1* and *ex2* mutations on rapid $^1O_2$-mediated changes in nuclear gene expression was analyzed by growing plants for 3 weeks under continuous light, until they were ready to bolt. Plants at the rosette leaf stage were transferred to the dark for 8 h and reexposed to light for 30 min. Total RNA was extracted from the leaves and was first transcribed into cDNAs and then into biotinylated complementary RNAs that were hybridized to Affymetrix gene chips. Genes with a 2-fold or greater transcript level than the control were considered to be significantly upregulated. After 30 min of reillumination, a total of 245 genes had been up-regulated in *flu* relative to wild type (Figs. 2.4 and 2.5). This number in ecotype Col-0 was lower than that in *flu* Ler reported earlier (op den Camp et al. 2003). Inactivation of EXECUTER1 led to a dramatic drop in the number of up-regulated genes from 245 in *flu* down to 54 in *ex1*/*flu* (Fig. 2.5). This suppressive effect of *EXECUTER1* inactivation in *flu* can also be seen by comparing scatter plots of nuclear transcripts of genes significantly upregulated in *flu* and suppressed in *ex1*/*flu* (Fig. 2.4). EXECUTER1 seems to play a major role during the up-regulation of nuclear genes in the *flu* mutant, but its absence in *ex1*/*flu* double mutants does not completely eliminate activation of $^1O_2$-responsive genes. Therefore, additional components must be implicated with the $^1O_2$-induced transduction of signals from the plastid to the nucleus.

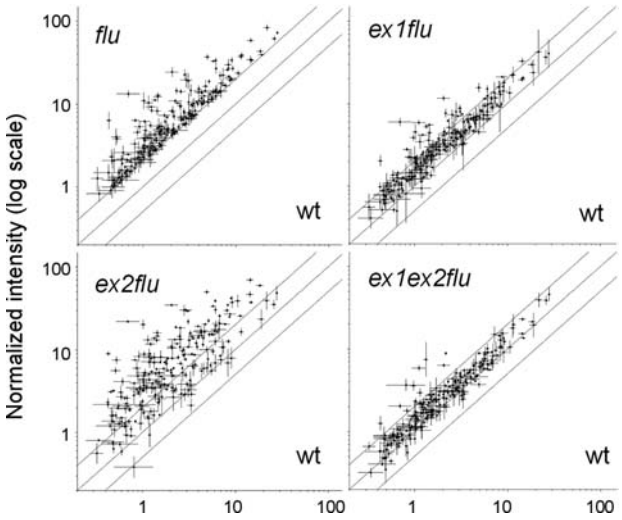

Fig. 2.4. The impact of *EXECUTER1* and *EXECUTER2* mutations on the upregulation of $^1O_2$-responsive nuclear genes in the *flu* mutant. Plants (Col-0) were grown for 21 days under continuous light, shifted to the dark for 8 h, and re-exposed to light for30min.Globalchangesin transcript levels were determined by using Affymetrix gene chips. Among 13,600 genes that were selected as present in all replicas, 245 were up-regulated at least 2-fold in *flu* relative to wild type. Transcript levels of these selected genes are shown in scatter plots of *flu* versus wild type, *ex1*/*flu*versus wild type, *ex2*/*flu*versus wild type, and *ex1*/*ex2*/*flu* versus wild type. The individual dots shown on the scatter plots were derived as average expression values from both replicate experiments.

EXECUTER2 may play a supplementary role during $^1O_2$- mediated signaling that may account for the residual activation of $^1O_2$-responsive genes in *ex1*/*flu* after a dark-to-light shift. This proposition was tested experimentally first by analyzing in *ex2*/*flu* the transcript profiles of those genes that in *flu* were at least 2-fold up-regulated relative to wild type. The scatter plot analysis of these transcripts in *ex2*/*flu* revealed that inactivation of EXECUTER2 modified drastically the up-regulation of $^1O_2$-responsive genes in the *flu* mutant by further enhancing or reducing the transcript levels of these genes (Fig. 2.4). In a subsequent step, additional genes were included in this analysis that were up-regulated in the *ex1*/*flu*, *ex2*/*flu* and *ex1*/*ex2*/*flu* mutant lines relative to wild type (Fig. 2.5 and Table 2.1). The majority of $^1O_2$-up-regulated genes in the *flu* mutant are found in a cluster of 178 genes that are up-regulated both in *flu* as well as in *ex2*/*flu* (Fig. 2.5, groups A, I, and M). Unexpectedly, in *ex2*/*flu* the up-regulation of a larger part of these genes is significantly higher than in *flu* (Fig. 2.4). Half of the genes with an assigned function have been associated with signaling, gene transcription and stress responses. Among the genes predicted to encode transcription factors and DNA binding proteins, nine belong to the large gene family of WRKY transcription factors that have been associated with various disorders such as stress, aging, senescence and diseases (Eulgem et al. 2000). The enhanced expression of $^1O_2$-responsive genes caused by the inactivation of EXECUTER2 is also reflected in the appearance of additional $^1O_2$-responsive genes that are significantly upregulated in *ex2*/*flu* but not in *flu* (Fig. 2.5, groups L and G). Approximately half of these genes are of unknown function. Similar to the gene groups A, I, and M, also in groups L and G >50% of the remaining genes encode proteins predicted to be involved in transcription, signaling or stress-related responses (Table 2.1).

Inactivation of EXECUTER2 does not only accelerate the expression of a large number of $^1O_2$-responsive genes, but at the same time also evokes the down-regulation of a subset of 62 $^1O_2$-responsive genes (Fig. 2.5, groups E, B, and J). Up-regulation of 59 of these genes in response to $^1O_2$ generated in chloroplasts of the *flu* mutant depends on the combined activities of EXECUTER1 and EXECUTER2 (Fig. 2.5, group E). In *ex1*/*flu* and *ex2*/*flu*, but also in the *ex1*/*ex2*/*flu* triple mutant the $^1O_2$-induced enhanced expression of these genes is suppressed. Several of these genes have been associated with various stress-related responses such as two trehalose 6-phosphate synthetase genes which have been implicated in conferring desiccation tolerance to plants (Muller et al. 1995; Leyman et al. 2001). Collectively, these results reemphasize a key role of EXECUTER1 in stimulating the up-regulation of a larger number of nuclear genes that comprise the majority of $^1O_2$-responsive genes in the *flu* mutant. At the same time, they reveal a striking regulatory role of EXECUTER2 that seems to attenuate and antagonize the activity of EXECUTER1. However, EXECUTER2 alone in the absence of active

EXECUTER1 has only a limited effect on the expression of $^1O_2$-responsive genes. Because of the reciprocal activities of the two EXECUTER proteins in the *flu* mutant that impact each other during the $^1O_2$-induced transfer from the plastid to the nucleus, it was of interest to see whether inactivation of both these proteins in the *ex1*/*ex2*/*flu* triple mutant would completely abrogate the singlet oxygen-mediated up-regulation of nuclear genes. Almost all of the transcripts that in *flu* had been upregulated at least twofold remained in the triple mutant below the 2-fold threshold value, but were still slightly higher than in the wild-type control. Six of the $^1O_2$-responsive genes were significantly up-regulated only in the triple mutant relative to wild type (Fig. 2.5, group H). Two of these genes encode proteins of unknown function. One of the four genes with an assigned function is predicted to encode an auxin-responsive transcription factor. At the same time two of seven genes that are significantly up-regulated in *ex1*/*flu* are also involved in auxin-dependent responses (Fig. 2.5, group F; Table 2.1).

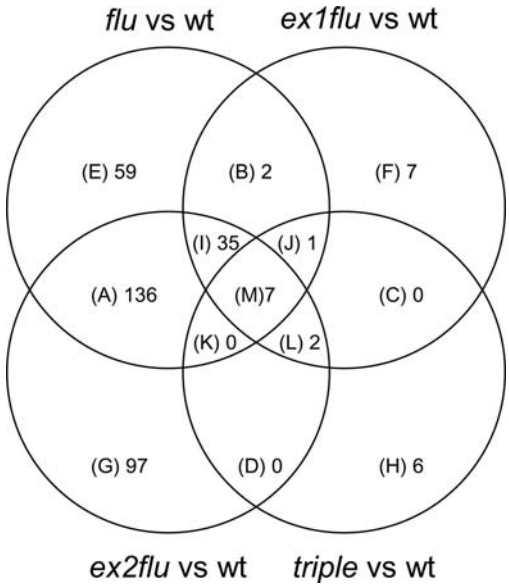

Fig. 2.5. The impact of *EXECUTER1* and *EXECUTER2* mutations on $^1O_2$-mediated changes in nuclear gene expression. The relationships of four selected groups of genes up-regulated at least 2-fold in *flu* versus wild type, *ex1*/*flu* versus wild type, *ex2*/*flu* versus wild type, and *ex1*/*ex2*/*flu* versus wild type were analyzed by using a Venn diagram. A subset of five genes up-regulated only in *flu* and *ex1*/*ex2*/*flu* relative to wild type is not shown in the Venn diagram, but has been included in Table 2.1. Plants were grown and treated as described under Fig. 2.4.

Among the genes that had been shown by the Affymetrix chip analysis to be induced stronger in *ex2*/*flu* than in *flu*, four were selected and changes in their transcript levels were quantified independently by using real-time PCR to test the reliability of the Affymetrix chip analysis (Fig. 2.6). The expression of genes that encode the WRKY33 (*At2g38470*) and WRKY46 (*At2g46400*)

transcription factors (Eulgem et al. 2000), a disease resistance protein (*At1g66090*) and the 1-amino-cyclopropane-1 carboxylic acid (ACC) synthase 6 (*At1g11280*) (Liu and Zhang 2004) were up-regulated in *flu* during the first 30 min of reillumination. For each gene the transcript level was 2- to 3-fold higher in *ex2*/*flu* than in *flu*, whereas in *ex1*/*flu* and the triple mutant these levels were down-regulated and similar to those of wild type.

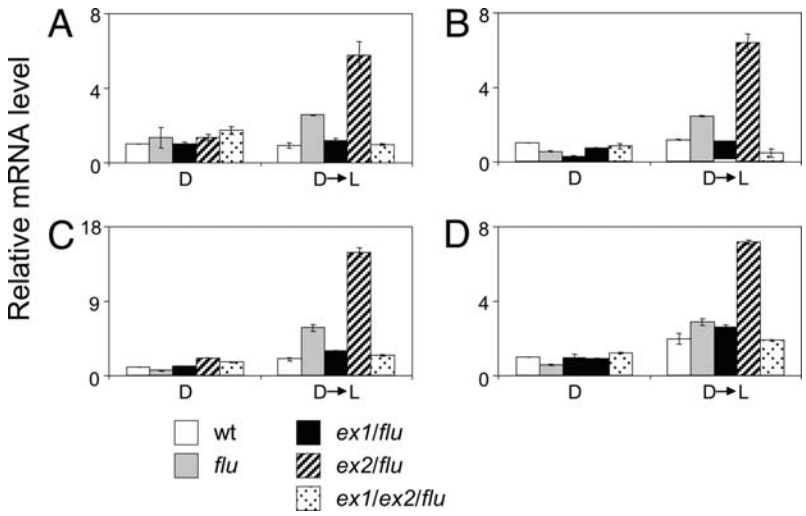

Fig. 2.6. Activation of four $^1O_2$-responsive genes in *flu* and *ex2*/*flu* and their suppression in *ex1*/*flu* and *ex1*/*ex2*/*flu* mutant plants. Plants were grown for 21 days under continuous light, transferred to the dark for 8 h, and in some cases reexposed to light for 30 min. Transcript levels of *WRKY33* (At2g38470) (*A*), *WRKY46* (At2g46400) (*B*), a putative disease resistance gene (At1g66090) (*C*), and the gene encoding the 1-amino-cyclopropane-1 carboxylic acid (ACC) synthase 6 (At1g11280) (*D*) were determined by Real-Time PCR. The results represent average values of measurements from three independent experiments ±SE. RNA was extracted at the end of the dark period (D) or after 30 min of reillumination (D →L).

2.4 Discussion

In our present work, we have used the conditional *flu* mutant to characterize the physiological role of $^1O_2$ that is generated within the plastid compartment after a dark-to-light shift. Shortly after the release of $^1O_2$ drastic changes in nuclear gene expression occur that reveal a rapid transfer of signals from the plastid to the nucleus. Because $^1O_2$ is very unstable and unlikely to leave the plastid compartment (Gorman and Rodgers 1992; Sies and Menck 1992), its physiological impact has been attributed to the generation of more stable second messengers within the plastid that are assumed to activate a signaling pathway and control the expression of a large number of nuclear genes (op den Camp et al. 2003). EXECUTER1 seems to play a key role during the transfer of signals from the plastid to the nucleus. Its biological activity, however, depends on its interaction with a second closely related protein, EXECUTER2. Even though it is not known yet whether EXECUTER1 and EXECUTER2 physically interact with each other, such a direct contact would be in line with some of the results of our present work. The two proteins localize in chloroplasts and seem to be both associated with thylakoid membranes. Upon inactivation of EXECUTER2 in the *flu* mutant, additional $^1O_2$-responsive genes emerge and genes that were already up-regulated in *flu* are either further stimulated or down-regulated. In the absence of EXECUTER1, EXECUTER2 has only a relatively minor effect on the expression of $^1O_2$-responsive genes (see e.g., Fig. 2.4). Thus, the primary function of EXECUTER2 seems to be that of a modulator attenuating and controlling the activity of EXECUTER1. Inactivation of EXECUTER1 greatly reduces but does not completely eliminate the up-regulation of nuclear $^1O_2$-responsive genes. Only when both EXECUTER proteins are inactive is the up-regulation of the vast majority of $^1O_2$-responsive genes abolished.

The EXECUTER1- and EXECUTER2-dependent signaling in the *flu* mutant bears a striking resemblance to retrograde signaling that has been shown to play a central role in controlling gene expression in the nucleus and the plastid (Rodermel 2001; Beck 2005). Chloroplast proteins are encoded by both nuclear and plastid genomes (Bogorad 1975). Because of this separation of the genetic information, the expression of these two genomes needs to be coordinated. It is well established that the development and activity of chloroplasts depend on the synthesis and import of a large number of nuclear encoded plastid proteins (Kirk and Tilney-Bassett 1978). On the other hand, the expression of at least some of the nuclear genes depends on the functional state of the plastid by means of a process known as retrograde signaling (Mayfield and Taylor 1984; Kropat et al. 1997; Strand et al. 2003).

Initially the biological impact of plastid-derived signals had been considered to be confined to the fine-tuning and coordination of nuclear and chloroplast gene activities that are required for the optimization and protection of chloroplast-specific functions such as e.g., photosynthesis (Mayfield and Taylor 1984; Rodermel 2001; Beck 2005). The results of our work demonstrate that the primary function of singlet oxygen in the *flu* mutant does not seem to be the control of chloroplast performance but the activation of a stress-related signaling cascade that encompasses numerous signaling pathways known to be activated by pathogen attack, wounding, light and drought stress (Danon et al. 2005; Danon et al. 2006; Ochsenbein et al. 2006). Less than 15% of the $^1O_2$-responsive genes of the *flu* mutant are predicted to encode plastid proteins and none of these genes can be linked to photosynthesis or the control of chloroplast development, whereas a large fraction of $^1O_2$-responsive genes are known to be involved in different stress responses. The $^1O_2$-activated cell death program and growth inhibition resemble stress-related resistance strategies of higher plants (Netting 2000; Bray et al. 2002). These $^1O_2$-dependent stress responses of the *flu* mutant were suppressed after the inactivation of EXECUTER1 and EXECUTER2. Both the generation of $^1O_2$ within plastids and the plastid-specific localization of the EXECUTER1 and 2 proteins reiterate the importance of chloroplasts as a major source of stress-related signals.

The activation of a suicidal program in seedlings and the block of growth in mature plants of *flu* has not been reported to occur in wild-type plants even under conditions that would be expected to stimulate the release of $^1O_2$. This apparent difference between *flu* and wild type may question the physiological relevance of $^1O_2$-mediated stress responses of the *flu* mutant. EXECUTER1 and EXECUTER2 are highly conserved among all higher plants for which sequence data are available. This conservation is consistent with EXECUTER1 and EXECUTER2 being involved in processes that are both beneficial and common to higher plants. The overaccumulation of the photosensitizer Pchlide and the sudden shift from the dark to the light that in the *flu* mutant evokes the instantaneous release of $^1O_2$ does normally not occur in wild-type plants. Conditions to which wild-type plants are genetically adapted and that endorse the enhanced production of $^1O_2$ would thus be expected to induce the release of modulating factors that control and subdue the extreme $^1O_2$-mediated stress responses as seen in *flu*. Two such modulating activities have recently been identified. Various stress conditions may lead to the hyperreduction of the photosynthetic electron transfer chain that blocks electron transfer by PSII and enhances the production of $^1O_2$ (Fryer et al. 2002; Hideg et al. 2002). Plants may use additional electron sinks to maintain the acceptor site of PSII in a partially oxidized state (Niyogi 1999). One of these additional electron acceptors is molecular oxygen. It can be reduced by PSI to superoxide that is

rapidly converted to hydrogen peroxide (Asada 1999). Hydrogen peroxide has been shown recently to antagonize the biological activity of $^1O_2$ and to suppress $^1O_2$-mediated cell death and growth inhibition (Laloi et al. 2007). Another modulation of $^1O_2$-dependent stress responses has been attributed to acclimation activated by minor stress conditions that precede the release of $^1O_2$ (M. Würsch and K. Apel, unpublished results). Therefore, EXECUTER1- and EXECUTER2-dependent signaling of stress responses in wild-type plants seems to form an integral part of a complex signaling network and is subject to the control by various modulators that weaken the extreme consequences of this signaling as seen in the *flu* mutant. As shown in the present work, the *flu* mutant offers a way of how to penetrate and dissect this complexity and identify individual signaling pathways.

2.5 Materials and Methods

2.5.1 Plant Material

The *EX1* (At4g33630) T-DNA insertion line SALK_002088 and *EX2* (At1g27510) T-DNA insertion line SALK_012127 were obtained from the European Arabidopsis Stock Centre (NASC). Homozygous mutant lines were identified by PCR analysis using T-DNA-, *EX1*- and *EX2*-specific primers. Both T-DNA-lines were crossed with a *flu* Col-0 line that had been obtained by 5 backcrosses of *flu1-1* in Landsberg erecta with wild-type Columbia. The *ex1*/*flu* and *ex2*/*flu* mutant lines were crossed and within the segregating F2 population triple mutants were identified by PCR-based genotyping. For the cultivation of mature plants, seeds of wild type, *flu*, *ex1/flu*, *ex2/flu* and *ex1/ex2/flu*, all in Col-0 ecotype, were sown on soil and plants were grown under continuous light (100μmol·m^{-2}·s^{-1}).

2.5.2 Extraction and Measurement of Protochlorophyllide

Pchlide was extracted separately from seven biological samples of each of the 5 genotypes (wild type, *flu*, *ex1/flu*, *ex2/flu* and *ex1/ex2/flu*) growing under continuous light (100μmol·m^{-2}·s^{-1}) for 21days and then transferred to the dark for 8 h. After the end of dark periods, samples were harvested and homogenized with liquid nitrogen under green safety light. About 0.1g of the powdered samples were suspended in 1 ml of cold 90 % acetone, and centrifuged for 5min at 10,000rpm. The supernatants were used to determine the level of Pchlide by HPLC according to Kim and Apel (2004).

2.5.3 RNA extraction and Real-Time PCR

Total RNA was extracted by using an RNeasy plant mini kit (Qiagen, Hilden, Germany) and quantified spectrophotometrically at 260 nm. For the real-time PCR, RNAs were treated with RQ1 RNase-Free DNase (Promega, Madison, WI, USA) and reverse-transcribed using oligo$(dT)^{15}$ primer(Promega) and and Improm II reverse transcriptase (Promega) according to the manufacturer's recommendations. Real-time PCR was performed with equal amounts of cDNAs by using the ABI PRISM 7700 Sequence Detection System (Applied Biosystems, Foster City, CA, USA), a SYBR Green PCR kit from Applied Biosystems, and gene-specific primers. Relative mRNA abundance was calculated by using the comparative delta-Ct method and normalized to the *ACT2* (At3g18780) gene levels. The sequences of the primers for the selected genes are:

At2g38470, 5'-GAAACAAATGGTGGGAATGG-3' and 5'-TGTCGTGTGATGCTCTCTCC-3';
At2g46400, 5'-GATCCTTAAGCGAAGCCTTG-3' and 5'-TCGATGCGTGCATCTGTAAT-3';
At4g11280, 5'-GACGAGTTTATCCGCGAGAG-3' and 5'-ACACGCCATAGTTCGGTTTC-3';
At1g66090, 5'-AACCGGAGTACACGTCCAAG-3' and 5'-CGGAGATCCCAACGATCTTA-3'

2.5.4 Microarray Hybridization and Analysis

Two individual biological replicates, each containing material of five mature plants of wild type, *flu*, *ex1flu*, *ex2flu* and *ex1ex2flu*, respectively, were used for the microarray analysis. Plants were germinated on soil and kept under continuous light until the beginning of bolting and then transferred to the dark for 8 h. Dark-incubated mature plants were re-illuminated for 30 min and subsequently harvested for RNA extraction. Total RNA was prepared as follow.

2.5.4.1 cRNA preparation

Total RNAs from the different samples were extracted. The quality of the isolated RNA was determined with a NanoDrop ND 1000 (NanoDrop Technologies, Wilmington, DE) and a Bioanalyzer 2100 (Agilent, Waldbronn, Germany). Only those samples with a 260/280 nm ratio between 1.8-2.1 and a 28S/18S ratio within 1.5-2 were further processed. Total RNA samples (5 mg) were reverse-transcribed into double-stranded cDNA with a One-Cycle cDNA synthesis kit (P/N 900431; Affymetrix, Santa Clara, CA). The double-stranded cDNA was purified using a Sample Cleanup Module (P/N 900371; Affymetrix). The purified double-stranded cDNAs were *in vitro*-transcribed in the presence of biotin-labeled nucleotides using a IVT labeling kit (P/N 900449; Affymetrix). The biotinylated c RNA was purified by using a Sample Cleanup Module (P/N 900371; Affymetrix), and its quality and quantity were determined with a NanoDrop ND 1000 and Bioanalyzer 2100.

2.5.4.2 Array Hybridization

Biotin-labeled cRNA samples (15 mg) were fragmented randomly to 35-200 bp at 94°C in fragmentation buffer (P/N 900371; Affymetrix) and were mixed in 300 ml of hybridization buffer containing a hybridization control cRNA and control oligo B2 control (P/N 900454; Affymetrix), 0.1 mg/ml herring sperm DNA, and 0.5 mg/ml acetylated BSA in 2-(4-morpholino)-ethane sulfonic acid (Mes) buffer, pH 6.7, before hybridization to GeneChip *Arabidopsis* ATH1 genome arrays for 16 h at 45°C. Arrays were then washed using an Affymetrix Fluidics Station 450 EukGE-WS2v4_450 protocol. An Affymetrix GeneChip Scanner 3000 was used to measure the fluorescence intensity emitted by the labeled target.

2.5.4.3 Statistical Analysis

Raw data processing was performed by using the Affymetrix GCOS 1.2 software. After hybridization and scanning, probe cell intensities were calculated and summarized for the respective probe sets by means of the MAS5 algorithm (Hubbell et al. 2002). To compare the expression values of the genes from chip to chip, global scaling was performed, which resulted in the normalization of the trimmed mean of each chip to a target intensity (TGT value) of 500 as detailed by Affymetrix. Quality control measures were considered before performing the statistical analysis. These included adequate scaling factors (between 1 and 3 for all samples), and appropriate numbers of present calls were calculated by application of a signedrank call algorithm (Liu et al. 2002). The efficiency of the labeling reaction and the hybridization performance were controlled with the following parameters: Present calls and optimal 3'/5' hybridization ratios (≈1) for the housekeeping genes (GAPDH and ACO7), for the poly(A) spike in controls and the prokaryotic control (BIOB, BIOC, CREX, BIODN). After normalization, "baseline" samples were compared (i.e., wild type after a dark/light shift versus either *flu* or *ex1/flu* or *ex2/flu* or *ex1/ex2/flu*) and for the comparative analysis of changes in gene expression between wild type and others, only the genes that met the following criteria were considered: (*i*) The genes should show a reliable level of RNA giving a detection call of P (present in the Affymetrix nomenclature), and (*ii*) the signals should be changed by at least 2-fold or greater ("difference" call) relative to the baseline sample. Based on these criteria, the remaining genes were selected for analysis using Genespring 7.2 package. The microarray analyses were performed in duplicate using independent samples for wild type, *flu*, *ex1/flu*, *ex2/flu*, and *ex1/ex2/flu* plants.

2.5.5 Growth Measurements.

Growth of the primary stem was determined by measuring its length daily for 30 days with wild type, *flu*, *ex1/flu*, *ex2/flu* and *ex1/ex2/flu* growing under continuous light (100µmol·m^{-2}·s^{-1}) or under long day conditions (16 h light/8 h dark).

2.5.6 Construction and Detection of the GFP Fusion Proteins *in vivo*

A modified pCAMBIA 3300 binary vector containing the CaMV 35S promoter, a Nco1 cloning site, the *EGFP*-sequence and the terminal polyadenylation site was used as a basis for all subsequent constructions (Kim and Apel 2004). For the *in vivo* localization of the fusion protein, full-length *EXECUTER1* and *EXECUTER2* without their stop codons were amplified from the cDNA of *Arabidopsis thaliana* (Col-0) and subcloned between the promoter and *EGFP* of the

modified pCAMBIA 3300 vector. To amplify this plasmid, competent *Escherichia coli* cells (DH5α) were used. Competent cells of *Agrobacterium tumefaciens* C58 were transformed with the plasmid and then used for stable *in planta* transformation of Arabidopsis Col-0. The primary transgenic plants were selected on MS agar plates containing phosphinothricin (25 mg/l) and transferred to soil to harvest seeds. The green fluorescence of GFP and the red fluorescence of chlorophyll were monitored using a Confocal Laser Scanning Microscope (TCS-NT; Leica Microsystems, Heidelberg, Germany) according to Kim and Apel (2004).

2.5.7 Other Methods

For homology searches and protein structure predictions, NCBI (http://www.ncbi.nlm.nik.gov /BLAST/) and ExPASy Molecular Biology Server (http://www.expasy.ch) were used.
For multiple sequence alignment, ClustalW (http://www.ebi.ac.uk/clustalw/) and Boxshade 3.21 (http://www.ch.embnet.org/software/BOX_form.html) were used.

2.6 Acknowledgments

We thank André Imboden for taking care of plants and measuring growth, Mena Nater for doing numerous crosses and identifying mutant lines, Jean-Charles Isner for help with the HPLC measurements, and Dr. Dieter Rubli for photographs. We thank members of our group, in particular Drs. Rasa Meskauskiene and Christophe Laloi for critical comments. We acknowledge the editorial work of Ursula Baldenweg. This work was supported by grants from the Swiss National Science Foundation (NSF), the Functional Genomic Center Zurich (FGCZ), and the ETH-Zurich.

2.7 References

Apel, K. and Hirt, H. 2004. Reactive oxygen species: metabolism, oxidative stress, and signal transduction. *Annu Rev Plant Biol* 55: 373-399.

Asada, K. 1999. The water-water cycle in chloroplasts: Scavenging of active oxygens and dissipation of excess photons. *Annu Rev Plant Physiol Plant Mol Biol* 50: 601-639.

Beck, C.F. 2005. Signaling pathways from the chloroplast to the nucleus. *Planta* 222(5): 743-756.

Bogorad, L. 1975. Evolution of organelles and eukaryotic genomes. *Science* 188(4191): 891-898.

Bray, E.A., Bailey-Serres, J., and Weretilnyk, E. 2002. *in Biochemistry and Molecular Biology of Plants*, eds Buchanan BB, Gruissem W, Jones RL. (Am Soc Plant Physiol, Rockville, MD): 1158-1203.

Danon, A., Coll, N.S., and Apel, K. 2006. Cryptochrome-1-dependent execution of programmed cell death induced by singlet oxygen in *Arabidopsis thaliana*. *Proc Natl Acad Sci U S A* 103(45): 17036-17041.

Danon, A., Miersch, O., Felix, G., Camp, R.G., and Apel, K. 2005. Concurrent activation of cell death-regulating signaling pathways by singlet oxygen in *Arabidopsis thaliana*. *Plant J* 41(1): 68-80.

Elstner, E.F. and Osswald, K. 1994. Mechanism of oxygen activation during plant stress. *Proc R Soc Edinburgh* 102B: 131-154.

Eulgem, T., Rushton, P.J., Robatzek, S., and Somssich, I.E. 2000. The WRKY superfamily of plant transcription factors. *Trends Plant Sci* 5(5): 199-206.

Foreman, J., Demidchik, V., Bothwell, J.H., Mylona, P., Miedema, H., Torres, M.A., Linstead, P., Costa, S., Brownlee, C., Jones, J.D., Davies, J.M., and Dolan, L. 2003. Reactive oxygen species produced by NADPH oxidase regulate plant cell growth. *Nature* 422: 442-446.

Fryer, M.J., Oxborough, K., Mullineaux, P.M., and Baker, N.R. 2002. Imaging of photo-oxidative stress responses in leaves. *J Exp Bot* 53(372): 1249-1254.

Gollnick, K. 1968. Type II photooxygenation reactions in solution. *Adv Photochem* 6: 1-122.

Gorman, A.A. and Rodgers, M.A. 1992. Current perspectives of singlet oxygen detection in biological environments. *J Photochem Photobiol B* 14(3): 159-176.

Griffiths, W.T. 1978. Reconstitution of chlorophyllide formation by isolated etioplast membranes. *Biochem J* 174(3): 681-692.

Hideg, E., Barta, C., Kalai, T., Vass, I., Hideg, K., and Asada, K. 2002. Detection of singlet oxygen and superoxide with fluorescent sensors in leaves under stress by photoinhibition or UV radiation. *Plant Cell Physiol* 43(10): 1154-1164.

Hubbell, E., Liu, W.M., and Mei, R. 2002. Robust estimators for expression analysis. *Bioinformatics* 18(12): 1585-1592.

Kim, C. and Apel, K. 2004. Substrate-dependent and organ-specific chloroplast protein import in planta. *Plant Cell* 16(1): 88-98.

Kirk, J. and Tilney-Bassett, R. 1978. *The plastids: Their chemisty, Structure, Growth and Inheritance* (Elsevier, New York) 2nd Ed.

Kropat, J., Oster, U., Rudiger, W., and Beck, C.F. 1997. Chlorophyll precursors are signals of chloroplast origin involved in light induction of nuclear heat-shock genes. *Proc Natl Acad Sci U S A* 94(25): 14168-14172.

Kwak, J.M., Mori, I.C., Pei, Z.M., Leonhardt, N., Torres, M.A., Dangl, J.L., Bloom, R.E., Bodde, S., Jones, J.D., and Schroeder, J.I. 2003. NADPH oxidase AtrbohD and AtrbohF genes function in ROS-dependent ABA signaling in Arabidopsis. *EMBO J* 22(11): 2623-2633.

Laloi, C., Stachowiak, M., Pers-Kamczyc, E., Warzych, E., Murgia, I., and Apel, K. 2007. Cross-talk between singlet oxygen- and hydrogen peroxide-dependent signaling of stress responses in *Arabidopsis thaliana*. *Proc Natl Acad Sci U S A* 104(2): 672-677.

Leyman, B., Van Dijck, P., and Thevelein, J.M. 2001. An unexpected plethora of trehalose biosynthesis genes in *Arabidopsis thaliana*. *Trends Plant Sci* 6(11): 510-513.

Liu, W.M., Mei, R., Di, X., Ryder, T.B., Hubbell, E., Dee, S., Webster, T.A., Harrington, C.A., Ho, M.H., Baid, J., and Smeekens, S.P. 2002. Analysis of high density expression microarrays with signed-rank call algorithms. *Bioinformatics* 18(12): 1593-1599.

Liu, Y. and Zhang, S. 2004. Phosphorylation of 1-aminocyclopropane-1-carboxylic acid synthase by MPK6, a stress-responsive mitogen-activated protein kinase, induces ethylene biosynthesis in Arabidopsis. *Plant Cell* 16(12): 3386-3399.

Mayfield, S.P. and Taylor, W.C. 1984. Carotenoid-deficient maize seedlings fail to accumulate light-harvesting chlorophyll a/b binding protein (LHCP) mRNA. *Eur J Biochem* 144(1): 79-84.

Meskauskiene, R., Nater, M., Goslings, D., Kessler, F., op den Camp, R., and Apel, K. 2001. FLU: a negative regulator of chlorophyll biosynthesis in Arabidopsis thaliana. *Proc Natl Acad Sci U S A* 98(22): 12826-12831.

Muller, J., Boller, T., and Wiemken, A. 1995. Trehalose and trehalase in plants: recent developments. *Plant Sci* 112(11): 1-9.

Neill, S., Desikan, R., and Hancock, J. 2002. Hydrogen peroxide signalling. *Curr Opin Plant Biol* 5(5): 388-395.

Netting, A.G. 2000. pH, abscisic acid and the integration of metabolism in plants under stressed and non-stressed conditions: cellular responses to stress and their implication for plant water relations. *J Exp Bot* 51(343): 147-158.

Niyogi, K.K. 1999. Photoprotection revisited: Genetic and molecular approaches. *Annu Rev Plant Physiol Plant Mol Biol* 50: 333-359.

Ochsenbein, C., Przybyla, D., Danon, A., Landgraf, F., Gobel, C., Imboden, A., Feussner, I., and Apel, K. 2006. The role of EDS1 (enhanced disease susceptibility) during singlet oxygen-mediated stress responses of Arabidopsis. *Plant J* 47(3): 445-456.

op den Camp, R.G., Przybyla, D., Ochsenbein, C., Laloi, C., Kim, C., Danon, A., Wagner, D., Hideg, E., Gobel, C., Feussner, I., Nater, M., and Apel, K. 2003. Rapid induction of distinct stress responses after the release of singlet oxygen in Arabidopsis. *Plant Cell* 15(10): 2320-2332.

Rodermel, S. 2001. Pathways of plastid-to-nucleus signaling. *Trends Plant Sci* 6(10): 471-478.

Sies, H. and Menck, C.F. 1992. Singlet oxygen induced DNA damage. *Mutat Res* 275(3-6): 367-375.

Strand, A., Asami, T., Alonso, J., Ecker, J.R., and Chory, J. 2003. Chloroplast to nucleus communication triggered by accumulation of Mg-protoporphyrinIX. *Nature* 421(6918): 79-83.

Tanaka, A., Christensen, M.J., Takemoto, D., Park, P., and Scott, B. 2006. Reactive oxygen species play a role in regulating a fungus-perennial ryegrass mutualistic interaction. *Plant Cell* 18(4): 1052-1066.

Torres, M.A., Dangl, J.L., and Jones, J.D. 2002. Arabidopsis gp91phox homologues AtrbohD and AtrbohF are required for accumulation of reactive oxygen intermediates in the plant defense response. *Proc Natl Acad Sci U S A* 99(1): 517-522.

Wagner, D., Przybyla, D., Op den Camp, R., Kim, C., Landgraf, F., Lee, K.P., Wursch, M., Laloi, C., Nater, M., Hideg, E., and Apel, K. 2004. The genetic basis of singlet oxygen-induced stress responses of *Arabidopsis thaliana*. *Science* 306(5699): 1183-1185.

Supplementary Materials

Supplemental table 2.1 List of genes in the Venn diagram as described under Fig 2.5.

Group A (136)

Gene ID	Common	Description	Localization
At2g26190		calmodulin-binding family protein	chloroplast
At2g40000		putative nematode-resistance protein	Unknown
At2g44080		unknown protein	Unknown
At2g41010		Encodes a novel calmodulin binding protein	Nucleus
At2g38470	WRKY33	putative WRKY-type DNA binding protein	Nucleus
At2g30040	MAPKKK14	putative protein kinase	chloroplast
At2g25735		Expressed protein	chloroplast
At2g25900	ATCTH	putative CCCH-type zinc finger protein	Unknown
At2g29420	ATGSTU7	putative glutathione S-transferase	cytoplasm
At2g27830		unknown protein	chloroplast
At2g35710		putative glycogenin	chloroplast
At2g01180	ATPAP1	putative phosphatidic acid phosphatase	plasma membrane
At2g32020		putative alanine acetyl transferase	Unknown
At2g28400		hypothetical protein	mitochondrion
At2g36790		putative glucosyl transferase an EST	Unknown
At1g23710		unknown protein	Unknown
At1g24140		putative metalloproteinase	extracellular
At2g17880		putative DnaJ protein	chloroplast
At1g61340		late embryogenesis abundant protein	mitochondrion
At1g62300	WRKY6	WRKY-type DNA-binding protein	Nucleus
At1g65390		disease resistance protein RPS4, TIR group	chloroplast
At2g35930		U-box domain-containing protein, similar to CMPG1	Unknown
At2g36220		unknown protein	Unknown
At2g46400	WRKY46	putative WRKY-type DNA binding protein	nucleus
At2g40140		putative CCCH-type zinc finger protein	Unknown
At1g05560	UGT1	indole-3-acetate beta-D-glucosyltransferase	chloroplast
At1g16420	AMC8	latex-abundant protein, putative (AMC8)	Unknown
At1g72900		disease resistance protein (TIR-NBS class)	membrane
At1g01720	ATAF1	NAC domain protein	Unknown
At1g21110		O-methyltransferase	cytosol
At1g21120		O-methyltransferase	cytosol
At1g28480		glutaredoxin	Unknown
At1g32920		unknown protein	endomembrane
At1g19770	ATPUP14	Member of a family of proteins related to PUP1, a purine transporter	membrane
At1g21910		encodes a member of the DREB subfamily	nucleus
At1g78410		VQ motif-containing protein	Unknown
At1g19380		hypothetical protein	Unknown
At1g55920	ATSERAT	serine acetyltransferase	chloroplast/cytosol
At1g11050		Ser/Thr protein kinase isolog	endomembrane
At1g72520	LOX	putative lipoxygenase	chloroplast
At1g63750		putative disease resistance protein	chloroplast
At1g30040	ATGA2OX2	gibberellin 2-oxidase	Unknown
At1g76360		putative protein kinase	chloroplast

At1g76650		putative calmodulin similar to calmodulin	chloroplast
At1g76690	OPR2	12-oxophytodienoate reductase (OPR2)	Unknown
At1g29690		Encodes a protein containing a domain with homology to the MACPF	Unknown
At1g77450		no apical meristem (NAM) family protein	Unknown
At1g13260		DNA-binding protein RAV1 identical to RAV1	Unknown
At3g05200	ATL6	putative RING-H2 zinc finger protein ATL6	endomembrane
At3g01830		calmodulin-related protein	Unknown
At3g04640		glycine-rich protein	endomembrane
At3g08720	ATPK19	putative ribosomal-protein S6 kinase (ATPK19)	chloroplast
At3g02840		immediate-early fungal elicitor family protein	mitochondrion
At3g16720	ATL2	putative RING zinc finger protein (defense response)	Unknown
At3g23230		ethylene responsive element binding protein	chloroplast
At3g18690	MKS1	VQ motif-containing protein	nucleus
At3g18710		U-box domain-containing protein	Unknown
At3g02800		similar to tyrosine specific protein phosphatase family protein	Unknown
At3g19580	AZF2	zinc finger protein	nucleus
At3g25600		calmodulin	Unknown
At3g28340		Encodes a protein with putative galacturonosyltransferase activity.	endomembrane
At1g66090		TIR-NBS, AAA ATPase	chloroplast
At1g66160		U-box domain-containing protein	mitochondrion
At3g10930		hypothetical protein	mitochondrion
At1g20823		zinc finger (C3HC4-type RING finger) family protein	Unknown
At1g17860		trypsin and protease inhibitor family protein	endomembrane
At2g33580		kinase activity, cell wall catabolism	endomembrane
At4g01250	WRKY22	putative DNA-binding protein	nucleus
At4g01870		tolB protein-related, contains weak similarity to TolB protein precursor	Unknown
At4g02200		drought-induced-19-like 1	Unknown
At4g02410		contains similarity to a protein kinase domain	endomembrane
At4g11280	ACS6	ACC synthase (AtACS-6)	Unknown
At4g13180		short-chain alcohol dehydrogenase like protein	mitochondrion
At4g18880	HSF21	heat shock transcription factor - like protein	nucleus
At4g21510		F-box family protein	Unknown
At4g21990	APR3	disulfide isomerase-like (PDIL) protein	chloroplast
At4g23190	CRK1	serine/threonine kinase - like protein	endomembrane
At4g23810	WRKY53	WRKY family transcription factor	nucleus
At4g24160		hydrolase, alpha/beta fold family protein	chloroplast
At4g26400		zinc finger (C3HC4-type RING finger) family protein	endomembrane
At4g30280		xyloglucan endo-1,4-beta-D-glucanase-like protein	endomembrane
At4g31550	WRKY11	DNA-binding protein DNA-binding protein	nucleus
At4g31800	WRKY18	similar to WRKY family transcription factor	nucleus
At4g34138		UDP-glucoronosyl/UDP-glucosyl transferase family protein	endomembrane
At4g37610		TAZ zinc finger family protein / BTB/POZ domain-containing protein	nucleus
At3g44190		pyridine nucleotide-disulphide oxidoreductase family protein	cytoplasm
At3g45640	MPK3	mitogen-activated protein kinase 3	Unknown
At3g46110		putative protein predicted proteins	mitochondrion
At3g46600		scarecrow-like protein scarecrow-like 11	Unknown
At3g48650		hypothetical protein	Unknown
At3g49530		NAC2-like protein NAC2	Unknown
At3g50930		AAA-type ATPase family protein	mitochondrion
At3g55840		nematode resistance protein-like protein Hs1pro-1	Unknown

At3g57450		putative protein	mitochondrion
At3g57530	CPK32	calcium-dependent protein kinase	Unknown
At5g01540		lectin protein kinase	endomembrane
At5g05300		putative protein	endomembrane
At5g05410	DREB2A	DREB2A (dbj|BAA33794.1)	nucleus
At5g09800		U-box domain-containing protein	Unknown
At5g22920		zinc finger (C3HC4-type RING finger) family protein	Unknown
At5g24110	WRKY30	WRKY family transcription factor	Unknown
At5g41740		TIR-NBS-LRR, AAA ATPase	chloroplast
At5g42380		calmodulin-related protein	chloroplast
At5g43170	AZF3	Cys2/His2-type zinc finger protein 3	nucleus
At5g44070	CAD1	phytochelatin synthase	Unknown
At5g46710		zinc-binding family protein	Unknown
At5g47220	ERF2	ethylene responsive element binding factor 2	nucleus
At5g47910	RbohD	respiratory burst oxidase protein	Unknown
At5g48540		33 kDa secretory protein-like	endomembrane
At5g49520	WRKY48	WRKY-type DNA-binding protein	nucleus
At5g52750		heavy-metal-associated domain-containing protein	Unknown
At5g54720		ankyrin repeat family protein	Unknown
At5g57220		cytochrome P450	endomembrane
At5g57560	TCH4	xyloglucan:xyloglucosyl transferase	endomembrane
At5g58430		A member of EXO70 gene family	exocyst
At5g59550		zinc finger (C3HC4-type RING finger) family protein	Unknown
At5g59730		A member of EXO70 gene family	exocyst
At5g61590	ERF5	ethylene responsive element binding factor	Unknown
At5g61440		thioredoxin-like 3	chloroplast
At5g61900	BON1	copine - like protein copine I	plasma membrane
At5g62570		similarity to calmodulin-binding protein	Unknown
At5g64870		expressed protein	Unknown
At5g65300		unknown protein	chloroplast
At5g66210	CPK28	calcium-dependent protein kinase	chloroplast
At5g26920		calmodulin-binding - like protein	chloroplast
At5g27420		RING-H2 zinc finger protein-like RING-H2	endomembrane
At5g14730		putative protein predicted protein	Unknown
At3g56710	SIB1	SigA binding protein	chloroplast
At3g56880		VQ motif-containing protein	Unknown
At4g36500		putative protein	mitochondrion
At1g73540		MutT/nudix family protein	chloroplast
At1g35140	PHI	phosphate-induced (phi-1) protein	cell wall
At4g17460	HAT-1	homeobox-leucine zipper protein HAT1	nucleus
At4g15550	IAGLU	glucosyltransferase like protein	chloroplast
At4g17500	ERF1	ethylene responsive element binding factor 1	Unknown
At2g41640		unknown protein	Unknown

Group B (2)

Gene ID	Common	Description	Localization
At3g61060		Putative protein hypothetical proteins	Unknown
At5g62280		putative protein predicted proteins	Unknown

Group E (59)

Gene ID	Common	Description	Localization
At2g30610		unknown protein	Unknown
At2g39570		unknown protein	intracellular
At2g29670		unknown protein	chloroplast
At2g45170	APG8e	putative microtubule-associated protein	Unknown
At2g32150		putative hydrolase	Unknown
At2g05540		putative glycine-rich protein	endomembrane
At2g20670		unknown protein	Unknown
At1g60740		peroxiredoxin	Unknown
At1g10070	BCAT2	amino acid aminotransferase	mitochondrion
At1g70290		trehalose-6-phosphate synthase	endomembrane
At1g54740		hypothetical protein	Unknown
At1g03090	MCCA	3-methylcrotonyl-CoA carboxylase	mitochondrion
At1g23870		trehalose 6-phosphate synthase	endomembrane
At1g80920		J8-like protein similar to DnaJ homologue J8	chloroplast
At1g79700		putative AP2 domain transcription factor	chloroplast
At1g02660		hypothetical protein	Unknown
At1g06160		ethylene response factor	nucleus
At1g49170		hypothetical protein	chloroplast
At1g11080		Serine carboxypeptidase isolog	endomembrane
At1g69910		putative protein kinase	chloroplast
At1g71030		myb-related transcription factor	nucleus
At3g07590		putative small nuclear ribonucleoprotein(Sm-D1)	nucleus
At3g10020		unknown protein predicted	Unknown
At3g06850	din3	alpha-keto acid dehydrogenase E2 subunit	chloroplast
At3g15450		unknown protein_	Unknown
At3g30775	ERD5	proline oxidase, mitochondrial precursor	Unknown
At3g22060		hypothetical protein	endomembrane
At3g13450	din4	alpha-keto acid dehydrogenase E1 beta subunit	mitochondrion
At3g18560		unknown protein	chloroplast
At1g72060		unknown protein	endomembrane
At1g17990	OPR	12-oxophytodienoate reductase	Unknown
At1g25400		unknown protein	Unknown
At4g03510		RMA1 RING zinc finger protein	Unknown
At4g05070		coded for by A. thaliana cDNA T44741	chloroplast
At4g21480		glucose transporter	membrane
At4g35770	SEN1	senescence-associated protein	chloroplast
At3g45300	IVD	isovaleryl-CoA-dehydrogenase precursor (IVD)	mitochondrion
At3g47340	ASN1	glutamine-dependent asparagine synthetase	cytoplasm
At3g49160		pyruvate kinase -like protein	Unknown
At3g49790		putative protein predicted protein	mitochondrion
At3g54500		putative protein	Unknown
At3g57020		putative protein strictosidine synthase	endomembrane
At5g05440		putative protein	Unknown
At5g07100		SPF1-like protein SPF1 protein	mitochondrion
At5g12010		putative protein predicted proteins	Unknown
At5g19120		conglutin gamma - like protein	endomembrane
At5g49450		bZIP transcription factor	nucleus
At5g52250		similarity COP1	chloroplast

At5g56100		unknown protein	Unknown
At5g58650		putative protein	endomembrane
At5g67420	LBD37	putative protein	Unknown
At5g16110		putative protein	chloroplast
At4g36670		sugar transporter like protein	membrane
At5g20250		seed imbitition protein-like	chloroplast
At5g21170		AKIN beta1	chloroplast
At5g28770		bZIP transcription factor family protein	nucleus
At1g28330		dormancy-associated protein	Unknown
At2g23320	WRKY15	putative WRKY-type DNA-binding protein	nucleus
25SrRNA		Arabidopsis thaliana /REF=X52320 /DEF=25S rRNA /LEN=4310	Unknown

Group F (7)

Gene ID	Common	Description	Localization
At2g19440		putative beta-1,3-glucanase	endomembrane
At1g34310		auxin response factor 1	intracellular
At1g29440		auxin-induced protein	mitochondrion
At3g11210		unknown protein	Unknown
At5g08600		putative protein	nucleus
At5g23270		monosaccharide transporter	membrane
At5g35480		unknown protein	Unknown

Group G (97)

Gene ID	Common	Description	Localization
At2g41890		putative receptor-like protein kinase	endomembrane
At2g23810		hypothetical protein	endomembrane
At2g47060		putative protein kinase	Unknown
At2g29490		putative glutathione S-transferase	cytoplasm
At2g01150		RING-H2 finger protein RHA2b	Unknown
At2g32190		unknown protein	chloroplast
At2g32210		unknown protein	chloroplast
At2g15480		putative glucosyltransferase	Unknown
At2g07707		hypothetical protein	mitochondrion
At1g55450		similar to embryo-abundant protein	Unknown
At1g70420		unknown protein	Unknown
At2g22500		putative mitochondrial dicarboxylate carrier protein	mitochondrion
At2g36950		putative farnesylated protein	Unknown
At1g59910		hypothetical protein	etracellular
At1g64700		hypothetical protein	Unknown
At1g21820		unknown protein	Unknown
At1g59590		hypothetical protein	chloroplast
At1g63480		DNA-binding protein	chromatin
At1g14370		protein kinase	chloroplast
At1g44830		transcription factor, AP2 domain	chloroplast
At1g19970		ER lumen protein-retaining receptor	membrane
At1g07520		transcription factor scarecrow-like 14	Unknown
At1g17380		unknown protein	Unknown
At1g68330		hypothetical protein	Unknown
At1g69890		hypothetical protein	membrane
At1g69880		putative thioredoxin	Unknown

At1g63720		hypothetical protein	chloroplast
At1g67530		hypothetical protein	Unknown
At1g66400		calmodulin-related protein	Unknown
At1g68110		hypothetical protein	mitochondrion
At1g72260		thionin identical to GI:1181531	endomembrane
At1g42980		hypothetical protein	Unknown
At1g19020		Expressed protein	Unknown
At1g02400		dioxygenase	Unknown
At3g10720		putative pectinesterase	cell wall
At3g06890		hypothetical protein	Unknown
At3g16700		similar to 5-oxo-1,2,5-tricarboxilic-3-penten acid decarboxilase	Unknown
At3g21260		unknown protein	Unknown
At3g25780		unknown protein	chloroplast
At1g43000		hypothetical protein	Unknown
At2g26020		putative antifungal protein	endomembrane
At3g21070		unknown protein	Unknown
At3g19030		similarity to phosphoserine aminotransferase	endomembrane
At3g16860		unknown protein	endomembrane
At1g66080		hypothetical protein	Unknown
At1g66500		hypothetical protein	mitochondrion
At1g51700		dof zinc finger protein	Unknown
At1g19180		unknown protein	Unknown
At1g22190		AP2 domain containing protein RAP2	Unknown
At4g02330		hypothetical protein similar to pectinesterase	cell wall
At4g12720		growth factor like protein	Unknown
At4g23180		serine/threonine kinase -like protein	Unknown
At4g30290		xyloglucan endo-1,4-beta-D-glucanase-like protein	endomembrane
At4g33980		putative protein	Unknown
At4g33960		putative protein	endomembrane
At4g34150		hydroxyproline-rich glycoprotein precursor	membrane
At4g34135		glucosyltransferase -like protein	endomembrane
At4g34410		putative protein ethylene-responsive element binding protein	Unknown
At4g35480		RING-H2 finger protein RHA3b	Unknown
At4g38940		putative protein more than 30 predicted proteins	Unknown
At4g39670		putative protein	Unknown
At3g46020		COLD-INDUCIBLE RNA-BINDING PROTEIN	mitochondrion
At3g59080	CND41	chloroplast nucleoid DNA binding protein	endomembrane
At3g60290		SRG1 - like protein SRG1 protein	Unknown
At3g61640	AGP20	hypothetical protein	endomembrane
At5g03380		putative protein	Unknown
At5g12940		putative protein DRT100 protein precursor	endomembrane
At5g17350		putative protein	Unknown
At5g37770	TCH2	calmodulin-related protein 2, Touch-induced protein	Unknown
At5g39670		calcium-binding protein - like cbp1	Unknown
At5g40540		protein kinase	Unknown
At5g41100		putative protein	mitochondrion
At5g40920		disease resistance protein-like	mitochondrion
At5g42900		putative protein	Unknown
At5g44420		antifungal protein-like (PDF1.2)	endomembrane
At5g46910		putative protein similar to unknown protein	nucleus

At5g48655		Expressed protein	Unknown
At5g49480		NaCl-inducible Ca2+-binding protein-like	Unknown
At5g52760		putative protein	Unknown
At5g59450		scarecrow-like 11	Unknown
At5g59820	ZAT12	zinc finger protein Zat12	Unknown
At5g62020		heat shock factor 6	nucleus
At5g64310	AGP1	arabinogalactan-protein	endomembrane
At5g64660		unknown protein	Unknown
At5g66070		unknown protein	Unknown
At5g25170		apoptosis-related protein PNAS-4	mitochondrion
At5g26030		ferrochelatase-I	chloroplast
At5g16200		putative protein hypothetical protein	chloroplast
At5g17000		quinone oxidoreductase	Unknown
At1g57990		unknown protein	Unknown
At1g58420		hypothetical protein	mitochondrion
At1g44100	AAP5	amino acid permease	membrane
At1g73330	Dr4	Dr4(protease inhibitor)	endomembrane
At4g15680		glutaredoxin	endomembrane
At4g17250		hypothetical protein	Unknown
At4g17230		scarecrow-like 13 (SCL13)	mitochondrion
orf240a		hypothetical protein	Unknown

Group H (6)

Gene ID	Common	Description	Localization
At2g33860		auxin response transcription factor 3 (ETTIN/ARF3)	Unknown
At3g15400		anther development protein	endomembrane
At3g21560		UDP-glucose:indole-3-acetate beta-D-glucosyltransferase	Unknown
At3g49870		ADP-RIBOSYLATION FACTOR -like protein	endomembrane
At5g37300		putative protein predicted proteins	Unknown
At5g57880		unknown protein	chloroplast

Group I (35)

Gene ID	Common	Description	Localization
At2g39650		unknown protein	Unknown
At2g30020		putative protein phosphatase 2C	Unknown
At2g32030		putative alanine acetyl transferase	Unknown
At1g65400		hypothetical protein contains similarity to lectin polypeptide	Unknown
At2g24600		hypothetical protein predicted by genscan	Unknown
At1g72940		disease resistance protein	membrane
At1g72920		virus resistance protein	membrane
At1g80840	WRKY40	putative similar to WRKY transcription factor	Unknown
At1g27730		salt-tolerance zinc finger protein	Unknown
At1g68840		putative DNA-binding protein (RAV2-like)	nucleus
At1g76600		unknown protein	Unknown
At1g77640		hypothetical protein	chloroplast
At1g18570		myb factor	nucleus
At4g24380		putative protein dihydrofolate reductase	mitochondrion
At4g24570		putative mitochondrial uncoupling protein	mitochondrion
At4g27280		putative protein centrin	chloroplast
At4g29780		hypothetical protein	Unknown

At4g37290		hypothetical protein	endomembrane
At3g46620		putative protein several hypothetical proteins	Unknown
At3g48360		putative protein MEL-26, Caenorhabditis elegans	Unknown
At3g50060		R2R3-MYB transcription factor	nucleus
At3g55980		putative protein zinc finger transcription factor (PEI1)	Unknown
At3g61190	BAP1	putative protein hypothetical protein	Unknown
At3g62950		glutaredoxin -like protein glutaredoxin	endomembrane
At5g22250		CCR4-associated factor-like protein	Unknown
At5g45340	CYP707A3	cytochrome P450	endomembrane
At5g47960		RAS superfamily GTP-binding protein-like	endomembrane
At5g53830		unknown protein	chloroplast
At5g54490		unknown protein	Unknown
At5g63790		putative protein contains similarity to NAC-domain protein	chloroplast
At5g28630		putative protein retinal glutamic acid-rich protein	Unknown
At1g35210		hypothetical protein	chloroplast
At1g73500		MAP kinase, putative similar to MAP kinase kinase 5	mitochondrion
At5g04340		putative c2h2 zinc finger transcription factor	Unknown
At2g26530		AR781, similar to yeast pheromone receptor	chloroplast

Group J (1)

Gene ID	Common	Description	Localization
At3g09540		putative pectate lyase	chloroplast

Group L (2)

Gene ID	Common	Description	Localization
At3g16175		Expressed protein	Unknown
At5g24780	VSP1	vegetative storage protein Vsp1	endomembrane

Group M (7)

Gene ID	Common	Description	Localization
At2g20870		unknown protein	endomembrane
At1g05575		Expressed protein	endomembrane
At3g28500		acidic ribosomal protein P2b (rpp2b)	Unknown
At3g44260		CCR4-associated factor 1-like protein CAF1	Unknown
At5g51190		ethylene responsive element binding factor	Unknown
At5g61600		DNA binding protein EREBP-4	Unknown
At5g66650		unknown protein	mitochondrion

Upregulated genes only in *flu* and *ex1ex2flu* vs wt (5)

Gene ID	Common	Description	Localization
At2g19800		unknown protein	Unknown
At3g57520		imbibition protein homolog probable imbibition protein	Unknown
At5g41080		unknown protein	Unknown
At5g59310	LTP4	nonspecific lipid-transfer protein precursor - like	endomembrane
At5g60910		MAD box containing protein NAP1-1 - like NAP1-1	nucleus

3. Singlet oxygen-mediated signaling during late embryogenesis of Arabidopsis primes the fate of plastid differentiation during seedling development.

Keun Pyo Lee[1,5], Chanhong Kim[1,3,5], Aiswarya Baruah[1,3], Christophe Laloi[1], Mena Nater[1], Ivo Feussner[2] and Klaus Apel[1,3,4]

[1] Institute of Plant Sciences, Plant Genetics, Swiss Federal Institute of Technology (ETH), CH–8092, Zurich, Switzerland

[2] Albrecht-von-Haller-Institute for Plant Sciences, Georg-August-Universität Göttingen, Germany

Present address

[3] Boyce Thompson Institute Plant Research, Ithaca, USA

[4] To whom correspondence should be addressed

[5] These authors contributed equally to this work

In preparation

3.1 Abstract

Singlet oxygen ($^1O_2$) has been considered to be detrimental to cells due to its high reactivity and potential toxicity. Contrary to this view, $^1O_2$ acts as a signal during late embryogenesis in wild type Arabidopsis and predetermines plastid differentiation in seedlings. Inactivation of the two nuclear-encoded plastid proteins EXECUTER1 and EXECUTER2 blocks $^1O_2$ signaling and impairs normal plastid formation. Plastid formation at the beginning of seedling development is known to be controlled by the prevailing light conditions during seed germination. Here we identify $^1O_2$-mediated signaling as an as yet unknown additional determinant of plastid differentiation that recruits abscisic acid (ABA) as a positive regulator of plastid formation in etiolated and light-grown seedlings.

3.2 Introduction

Higher plants are characterized by the formation of seeds that originate from fertilized ovules and include embryos and maternally derived tissues (Vicente-Carbajosa and Carbonero 2005). Embryogenesis can be divided into a morphogenetic phase characterized by rapid cell division followed by the maturation phase during which cells discontinue dividing and enlarge their size and accumulate storage material. This second phase ends with the onset of desiccation and the dispersal of dried seeds. Seeds remain dormant until stimuli are right for germination (Borisjuk et al. 2004; Vicente-Carbajosa and Carbonero 2005; Braybrook et al. 2006). Seedlings derived from seeds buried in the soil grow heterotrophically on seed reserves in the absence of chlorophyll accumulation and functional chloroplast development. Upon reaching the soil surface and being exposed to light they undergo a rapid transition from heterotrophic to autotrophic growth that requires the light-induced transformation of etioplasts to functional chloroplasts and chlorophyll accumulation (Albrecht et al. 2006).

Evidence implicating $^1O_2$-mediated signaling with the control of plastid differentiation during seedling development was derived from the analysis of *executer (ex)* mutants. As shown in our previous work, the conditional *flu* mutant accumulates in the dark the tetrapyrrole intermediate protochlorophyllide (Pchlide) that upon re-illumination acts as a potent photosensitizer and generates $^1O_2$ by energy transfer (Meskauskiene et al. 2001; op den Camp et al. 2003). Seedlings of *flu* exposed to a dark/light shift bleach and die, whereas mature *flu* plants stop growing (Wagner et al. 2004). The genetic basis of these singlet oxygen-mediated stress reactions was revealed by the discovery of two nuclear genes encoding the closely related plastid proteins EXECUTER1 and EXECUTER2 that are required for transmitting $^1O_2$-dependent signals from the plastid to the nucleus (Lee et al. 2007).

As shown in the present work EX-dependent $^1O_2$-signaling operates not only in *flu* but also in wild type Arabidopsis and prior to seed dormancy pre-determines differentiation of plastids during seedling development.

3.3 Results

In seedlings of the *ex1/ex2* double mutant chloroplast formation was severely disturbed. The chlorophyll (Chl) content and Chl fluorescence of cotyledons were reduced (Fig. 3.1A) and chloroplasts of *ex1/ex2* seedlings were much smaller than in wild type (Fig. 3.2A, C) and resembled undifferentiated proplastids (Supplementary Fig. 3.1).

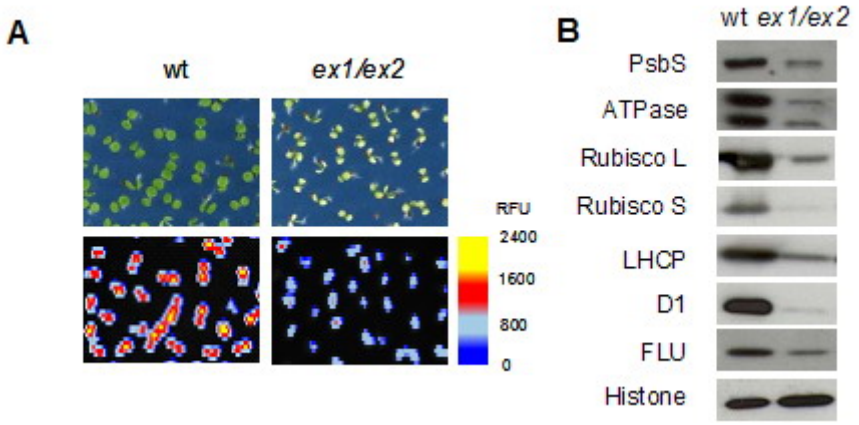

Fig. 3.1. Chloroplast development in seedlings of Arabidopsis depends on the activity of the nuclear encoded plastid proteins EXECUTER 1 and EXECUTER 2. A) Chlorophyll (Chl) accumulation and Chl fluorescence images of 4-day-old wild-type (wt) and *ex1/ex2* seedlings. B) The impact of *ex1/ex2* on the accumulation of chloroplast proteins (PsbS: photosystem II subunit S; ATPase: β-subunit of chloroplast ATPase; Rubisco L, S: large (L) and small (S) subunit of the ribulose-1.5-bisphosphate carboxylase; LHCP: light-harvesting Chl a/b protein; D1: D1 reaction center protein of PSII; FLU: 'fluorescent' protein, mediating feed-back control of Chl biosynthesis). As a loading control the relative concentration of histone was determined. Total proteins were extracted from 4-day-old light-grown seedlings of wild type and *ex1/ex2*, separated electrophoretically and detected by immunoblotting as described under 'Materials and Methods'.

The arrest of plastid differentiation in *ex1/ex2* was not evenly distributed across the cotyledon but occurred primarily within its central part as indicated by the Chl fluorescence that is confined to the marginal zone of the cotyledon (Fig. 3.2A). The disturbance of chloroplast development was also reflected in reduced levels of chloroplast proteins (Fig. 3.1B). All these deficiencies were observed in cotyledons, but not in true leaves of the mutant (Supplementary Fig. 3.2A, B, C). The arrest of plastid differentiation in cotyledons of *ex1/ex2* mutant seedlings indicates that $^1O_2$-mediated signaling may be involved in controlling plastid development. Generation of $^1O_2$ in plastids by energy transfer occurs under aerobic conditions only in the light (Apel and Hirt 2004; Krieger-Liszkay 2005). Since the impairment of plastid differentiation in *ex1/ex2* mutant seedlings affected also etioplast differentiation in dark-grown seedlings (Fig. 3.2B, C), *ex1/ex2*-dependent signaling is likely to occur not during seedling development but rather at an earlier developmental stage, when growing embryos are exposed to light.

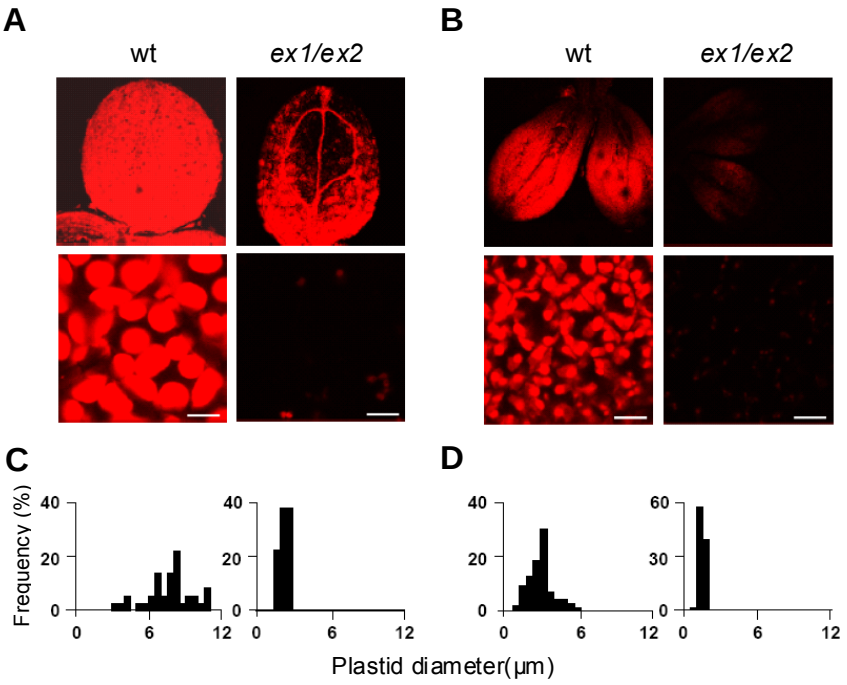

Fig. 3.2. The arrest of plastid differentiation in cotyledons of 4-day-old wild-type (wt) and *ex1/ex2* seedlings.
A) Chl fluorescence images of cotyledons (upper panel) and chloroplasts (lower panel) of light-grown seedlings of wild type (wt) and *ex1/ex2*. B) Pchlide fluorescence images of cotyledons and etioplasts of etiolated seedlings of wild type and *ex1/ex2*. C) Size distribution of chloroplasts from both lines. D) Size distribution of etioplasts from both lines. Bars: 5µm

Etioplasts and chloroplasts of seedlings are derived from undifferentiated progenitors in embryos named proplastids that descend from maternal plastids (Lopez-Juez and Pyke 2005). During the transition from the morphogenetic to the maturation phase of embryogenesis some of the proplastids start to increase in size and to differentiate into functional photoheterotrophic chloroplasts and acquire photosynthetic activity (Gutierrez-Nava Mde et al. 2004). With the onset of desiccation embryos lose again their chlorophyll and chloroplasts disintegrate, while proplastids are retained in quiescent embryos and upon germination differentiate into etioplasts in the dark or chloroplasts in the light (Parcy et al. 1997; Borisjuk et al. 2005; Albrecht et al. 2006). To test directly, whether the combined *ex1* and *ex2* mutations perturb chloroplast differentiation from the very beginning of the maturation phase, green immature seeds of wild type and *ex1/ex2* plants grown under continuous light were removed 10 days after anthesis from siliques and their chlorophyll contents and the size distributions of chloroplasts were compared. Embryos of both plant lines were green and their chloroplasts were similar in size and emitted the same Chl fluorescence (Fig. 3.3).

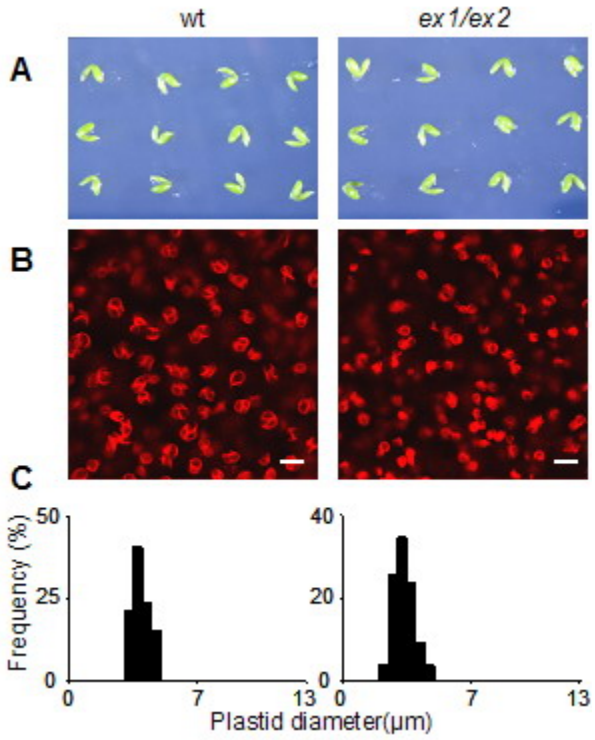

Fig. 3.3. The impact of *ex1/ex2* mutations on plastid development during embryogenesis. Immature embryos were taken 10 days after anthesis (DAA) from siliques of wild-type and *ex1/ex2* plants grown under continuous light. After plating them on agar plates they were allowed to grow for one day under dim light. The Chl content (A), Chl fluorescence (B) and size distribution of plastids (C) were indistinguishable between wild type and *ex1/ex2*. Bars: 5µm

Taken together these data indicate that the impact of the *ex1/ex2* mutations on plastid differentiation seems to be confined to a short period during late embryogenesis. At this stage the concentration of ABA in immature seeds has increased and marks a major developmental switch that initiates the onset of seed dormancy and the disintegration of chloroplasts in embryos (Rohde et al. 2000; Gazzarrini et al. 2004). This latter change is expected to enhance the release of free chlorophyll and the formation of chlorophyll catabolites that have been shown previously to be potent photosensitizers and to generate singlet oxygen in the light (Pruzinska et al. 2007). To measure $^1O_2$ production during embryogenesis, infiltration methods used previously (Flors et al. 2006) for the determination of $^1O_2$ in leaves of the *flu* mutant could not be applied because of the small size and delicate structure of immature seeds. Instead, a $^1O_2$-specific reporter gene cassette was constructed to probe non-invasively the release of $^1O_2$ *in vivo* during late embryogenesis. The *AAA-ATPase* gene was selected from a group of $^1O_2$-specific genes that had been identified earlier. This gene is hardly expressed in *flu* mutants grown in the dark or kept under continuous light, but is strongly up-regulated after a dark/light shift (op den Camp et al. 2003). The promoter of this gene was fused to the *LUCIFERASE (LUC)* gene (Fig. 3.4A). The sensitivity and selectivity of the *AAA-LUC* reporter gene was first

tested by expressing it in *flu* plants (Fig. 3.4B). In light-grown *flu*/*AAA:LUC* plants treated with Rose Bengal, a $^1O_2$-specific photosensitizer, or in *flu*/*AAA:LUC* plants subjected to a dark/light shift, the expression of the endogenous *AAA-ATPase* and the *AAA:LUC* reporter gene were strongly up-regulated (Supplementary Fig. 3.3), but not the expression of *Ferritin I*, a H_2O_2-responsive marker gene (Supplementary Fig. 3.3). Conversely, when *flu*/*AAA:LUC* plants grown under continuous light were treated with paraquat, a terminal oxidant of photosystem I that in the light leads to the enhanced generation of superoxide and hydrogen peroxide, the expression of the *AAA:LUC* reporter gene was not affected., but *Ferritin 1* expression was rapidly up-regulated (Supplementary Fig. 3.3). Inactivation of EX1 and EX2 attenuated the $^1O_2$-mediated up-regulation of *AAA:LUC* in *flu/AAA:LUC* following a dark/light shift. Collectively, these data indicate that the *AAA:LUC* reporter gene is suitable for the detection of $^1O_2$-production in intact plants.

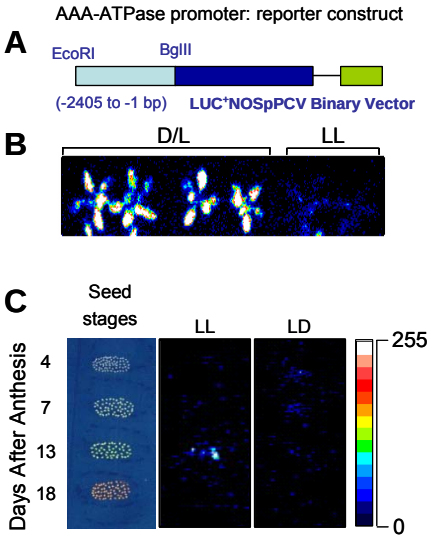

Fig. 3.4. The noninvasive detection of $^1O_2$-production during embryogenesis by using the $^1O_2$-specific *AAA-ATPase:LUCIFERASE* reporter gene. A) The promoter of the *AAA-ATPase* gene (*AAA*) drives the $^1O_2$ -induced rapid increase in the expression of the *LUCIFERASE* reporter gene (*LUC*$^+$*)*. B) $^1O_2$-induced transcription of *LUC*$^+$ *in planta*. Transgenic *flu* plants grown under continuous light were either shifted to the dark for 8 h and re-exposed to light (D/L) or kept under continuous light (LL). C) LUCIFERASE activity at different stages of embryogenesis (4, 7, 13, and 18 DAA) is only detectable in immature seeds 11 DAA prior to the onset of seed dormancy, when they are exposed to dim light. When transferred to the dark for 4 h they no longer show Luciferase activity.

Therefore, we analyzed in transgenic wild type/*AAA:LUC* reporter lines $^1O_2$ production in immature seeds at four different developmental stages, “pale” immature seeds taken from young siliques 4 days after anthesis at the beginning of the maturation phase, seeds with “pale-green” embryos 7 days after the anthesis that green and develop functional chloroplasts, “green” seeds collected 13 days after anthesis with embryos approaching the end of the maturation phase and “brown” immature seeds taken 18 days after anthesis that initiate already desiccation. Fifty to 60

seeds of each stage were collected and probed for luciferase activity. In wild type only “green” seeds showed luciferase activity (Fig. 3.4C). When plants were shifted from continuous light to the dark for 4 hours prior to the luciferase assay the activity in “green” immature seeds had vanished (Fig. 3.4C). These results support the notion that generation of $^1O_2$ depends on light absorption.

To assess the impact of EXECUTER1 and EXECUTER2-dependent signaling on nuclear gene transcription changes at different stages of embryogenesis, total RNA was extracted from immature seeds of wild type and *ex1/ex2* isolated 6 to 7 days (“pale-green”) and 15 to 16 days (“green-brown”) after anthesis, respectively, and analyzed on Affymetrix ATH1 gene chips that represent close to 95 % of all Arabidopsis genes. Major differences between global gene expression profiles of “pale-green” and “green-brown” immature seeds became apparent that correlate with reported differences in cell differentiation and metabolism of these two developmental stages of embryogenesis (Fig. 3.5). Transcripts of more than 13,000 genes were up-regulated at least 2-fold in “green-brown” immature wild-type seeds relative to “pale-green” seeds (Fig. 3.5A), whereas transcripts of approximately 3600 genes were inversely affected. Similar dramatic changes in transcript levels occurred also during the transition from “pale-green” seeds to the “brown-green” seeds of *ex1/ex2* mutant plants. Transcript levels of “pale-green” wild-type and *ex1/ex2* seeds were quite similar (Fig. 3.5C), whereas transcript levels of “brown-green” seeds were more strongly affected by the inactivation of EX1 and EX2, indicating that the impact of EX1- and EX2-dependent signaling during seed formation occurs primarily during late embryogenesis, when $^1O_2$ generation takes place. Among the genes that were differentially affected in “brown-green” seeds of wild type and *ex1/ex2* plants, 203 were at least 2-fold up-regulated in wild type relative to *ex1/ex2* double mutants that seem to be associated with $^1O_2$–mediated stage-specific alterations during late embryogenesis and require the presence of functional EXECUTER1 and EXECUTER2 proteins. Only one of these genes has previously been shown to respond to the release of $^1O_2$ in leaves of the *flu* mutant (Fig. 3.5D, (Lee et al. 2007)). A major fraction of these genes encodes embryogenesis-specific proteins (Supplementary Table 3.1). Part of these proteins may be essential for sustaining plastid differentiation during post-embryonic development.

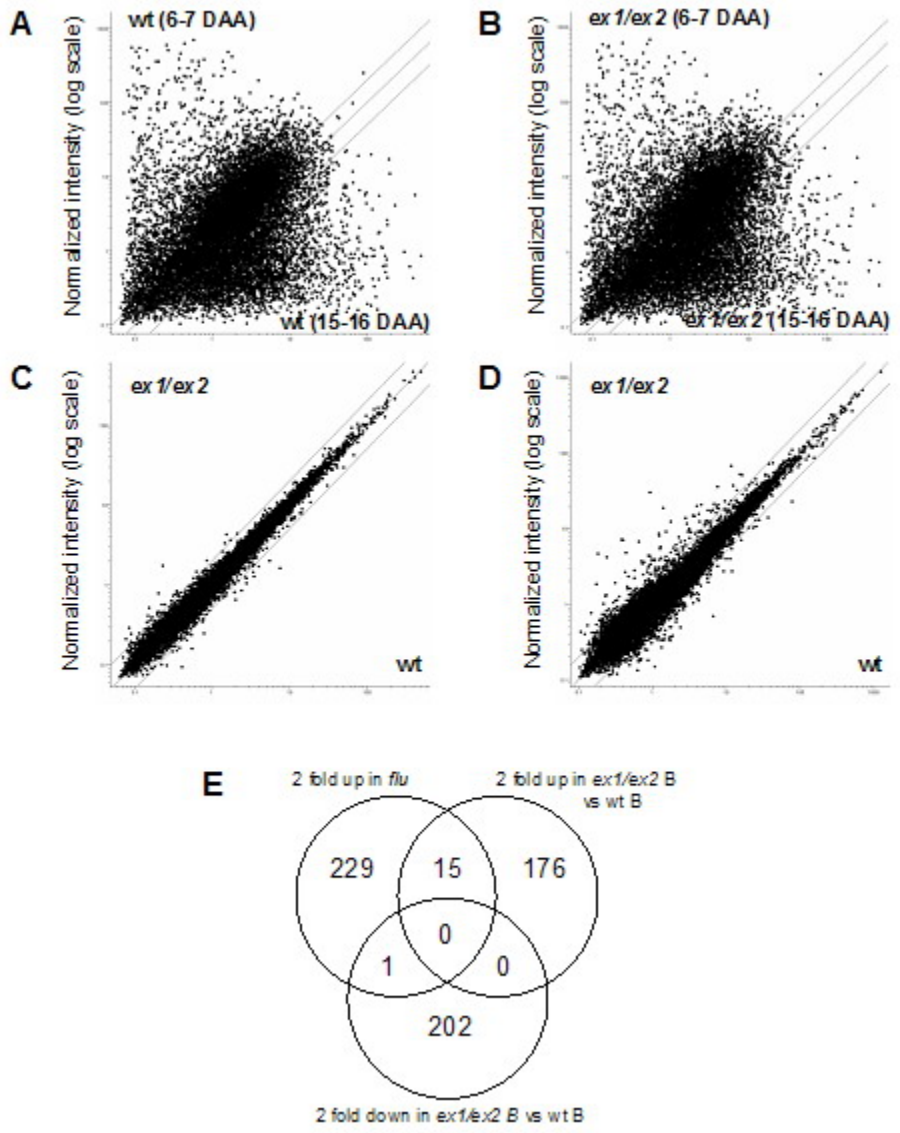

Fig. 3.5. The impact of *ex1/ex2* mutations on transcript changes during embryogenesis. Embryos were collected 6-7 DAA and 15-16 DAA from siliques of wild-type (wt) and *ex1/ex2* plants grown under continuous light. Global changes in transcript levels were determined using Affymetrix ATH1 gene chips. Major transcript changes occurred during the transition from the morphogenetic to the maturation phase of embryogenesis with more than half of all genes being affected as revealed by scatter blots of wild type (wt) (6-7 DAA) versus wild type (15-16 DAA) (A) and *ex1/ex2* (6-7 DAA) versus *ex1/ex2* (15-16 DAA) (B). Inactivation of EX1/EX2 had almost no effect on transcript levels in young embryos, as shown by the scatter blot *ex1/ex2* versus wild type (6-7 DAA) (C), whereas during late embryogenesis the number of differentially affected genes was strongly enhanced (D). 191 genes were at least twofold up-regulated in *ex1/ex2* relative to wild type, whereas 203 genes were at least twofold down-regulated in *ex1/ex2* versus wild type. Only a very few of these genes had previously been found among the $^1O_2$-responsive genes in leaves of the *flu* mutant (E).

Since $^1O_2$-mediated gene expression changes occur only in the light, plastid differentiation should not only be impaired in *ex1/ex2* but also in wild-type plants, when seed development of these latter plants occurs in the absence of light. This prediction was tested by covering half of the siliques of the primary inflorescence of light-grown wild-type plants with aluminum foil, while

the second half remained under continuous illumination, until maturation of seeds had been completed. Chloroplast formation and photosynthesis during embryogenesis had been proposed to support synthesis and deposition of storage material by increasing oxygen production and improving the energy supply in developing embryos (Rolletschek et al. 2003; Borisjuk et al. 2007). However, in contrast to this prevailing view seeds derived from siliques that had been kept in the dark for various durations showed the same germination rate and only slightly reduced weight as compared to seeds from control siliques that had been kept under continuous light (Supplementary Fig.3.4). Unexpectedly, in wild-type seedlings derived from seeds kept in the dark during embryogenesis proplastid differentiation was not perturbed (Fig. 3.6).

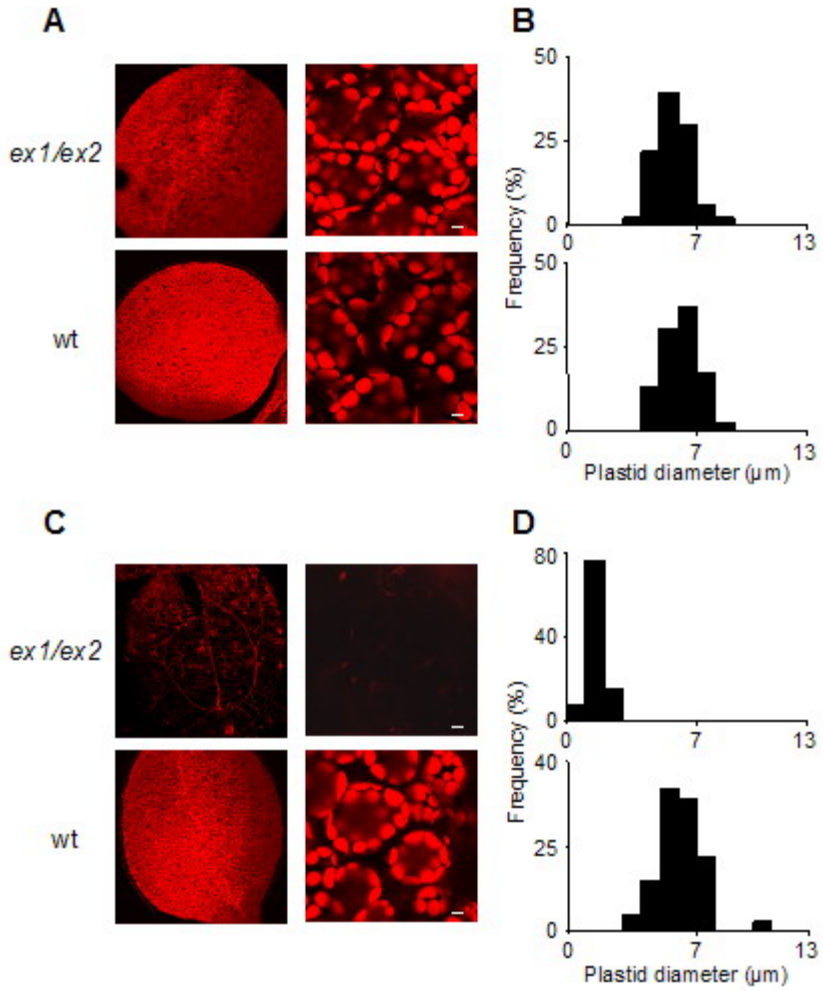

Fig. 3.6. Restoration of plastid differentiation during *ex1/ex2* seedling development by placing siliques into the dark. A) Siliques of *ex1/ex2* and wild-type plants grown under continuous light were covered with aluminum foil starting 10 DAA until the end of seed maturation. In contrast to *ex1/ex2* control plants kept under continuous light (C, D) seedlings derived from seeds taken from darkened siliques contained normal chloroplasts with Chl contents (A) and size distributions (B) similar to those of wild-type chloroplasts. Bars: 5µm

However, when a similar experiment was performed with *ex1/ex2* plants, plastid differentiation in seedlings derived from seeds kept in the dark was no longer impaired, very much in contrast to the arrest of proplastid differentiation in seedlings derived from seeds of the same plant that had developed under continuous illumination (Fig. 3.6). Taken together these data indicate that in immature seeds kept in the dark $^1O_2$-mediated signaling does not take place and plastid differentiation during post-embryonic development of wild type and *ex1/ex2* is not impaired. However, in light-grown plants that lack functional EX1 and EX2 proteins, $^1O_2$-mediated signaling prior to seed dormancy results in the severe disturbance of plastid formation during seedling development (Fig. 3.6).

Among the genes preferentially expressed during late embryogenesis and differentially affected, transcripts of 191 genes reached at least two-fold higher levels in *ex1/ex2* than in wild type (Fig. 3.5D). Fifteen of these genes have been identified previously as $^1O_2$-responsive genes in the *flu* mutant (Fig. 3.5D, (Lee et al. 2007)). In leaves up-regulation of the vast majority of these $^1O_2$-responsive genes was abrogated in *ex1/ex2/flu* triple mutants. During late embryogenesis, however, inactivation of *EX1* and *EX2* failed to suppress up-regulation of these genes. It is not known yet whether these genes are direct targets of $^1O_2$-mediated signaling or are more indirectly affected e.g. by $^1O_2$-mediated changes in phytohormone levels. Up-regulation of genes during late embryogenesis that are associated with the light-dependent release of $^1O_2$ seems to be triggered by two different signaling routes. One proceeds independently of EX1 and EX2 and leads to the perturbance of plastid differentiation during post-embryonic development, whereas the second signaling pathway depends on EX1 and EX2 and suppresses during late embryogenesis the negative impact of the former signaling on plastid differentiation (Fig. 3.7).

This seemingly complex interaction of two opposing signaling events may help the plant to coordinate and separate two conflicting developmental steps that take place during late embryogenesis in the same cell, chloroplast disintegration and chlorophyll catabolism on the one hand and the conservation and protection of proplastids on the other.

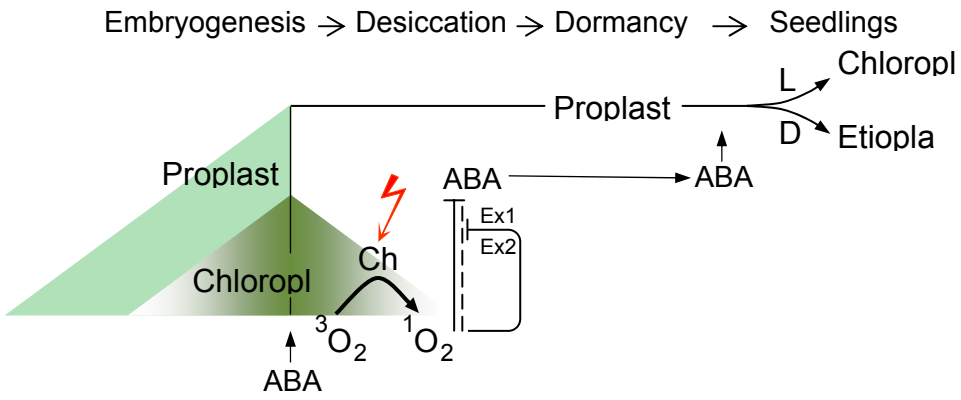

Fig. 3.7. Schematic diagram illustrating the interaction of two regulatory circuits during late embryogenesis that predetermines the fate of plastid differentiation during seedling development. Two types of plastids are present in younger embryos, proplastids and heterotrophic chloroplasts, the latter derived from proplastids. During late embryogenesis enhanced levels of ABA are known to initiate the onset of seed dormancy and chloroplasts start to disintegrate, releasing free Chl and Chl catabolites, potent photosensitizers that in the light generate $^1O_2$ by energy transfer. $^1O_2$ activates two antagonistic signaling pathways. In the absence of active EXECUTER1 and EXECUTER2 a subset of gene transcripts is up-regulated that results in the perturbance of plastid differentiation during seedling development. One of these transcripts encodes a ABA hydroxylase. Inactivation of this gene in the *ex1/ex2* background or the addition of exogenous ABA to *ex1/ex2* seedlings restores at least partially normal plastid development in *ex1/ex2* seedlings. In immature wild-type seeds, a second $^1O_2$-mediated signaling pathway suppresses the inhibitory effect of the former signaling event. In contrast to this former pathway, the second signaling pathway depends on the activity of the two EXECUTER proteins. A major prediction of this model is a positive effect of ABA on plastid differentiation in cotyledons.

Plastid differentiation in seedlings may be due to the activation of transcripts during seed germination that had been synthesized already prior to dormancy during late embryogenesis and stored in quiescent embryos. In such a case, differences in transcript levels between wild type and *ex1/ex2* would be expected to persist after the beginning of seed germination. We therefore extracted total RNA from seedlings 48 h after seed imbibition that had started to grow in the dark. RNA was hybridized to ATH1 Affymetrix gene chips. When global expression profiles of the 48 h old dark-grown seedlings of *ex1/ex2* and wild type were compared they turned out to be remarkably similar (Supplementary Fig. 3.5). Transcripts of genes that in late embryos of light-grown *ex1/ex2* and wild type plants had differentially been affected, reached the same levels in emerging seedlings of both lines. Only five of the Arabidopsis genes were found to be two-fold up-regulated in *ex1/ex2* seedlings relative to wild type (Supplementary Table 3.2). Since the extent of up-regulation of these genes was very minor, the biological significance of these transcript changes is not clear. On the other hand, transcript levels of 111 genes were at least twofold down-regulated in *ex1/ex2* relative to wild type (Supplementary Fig. 3.4B, Supplementary Table 3.2). More than 95 % of these genes are known to encode plastid proteins, roughly one third of these proteins are encoded by plastid genes, whereas the remaining two thirds are encoded by nuclear genes (Supplementary Fig. 3.4C). This remarkable

selectivity and specificity of transcript changes due to the inactivation of EX1/EX2-dependent signaling during late embryogenesis implicates a factor that remains active right after the breaking of dormancy and might have been stored throughout dormancy in quiescent embryos. Since the arrest of proplastid differentiation occurs only in *ex1/ex2* seedlings derived from light-exposed seeds, formation of this regulator may be linked to gene transcripts that are selectively up-regulated during late embryogenesis of light-grown *ex1/ex2* plants but not in wild-type plants. The genes that were up-regulated during late embryogenesis and whose expression was enhanced in light-grown *ex1/ex2* relative to wild type, were reexamined. Most of these genes encode transcription factors and signaling components known to be involved in triggering stress-related responses. One of the remaining genes, however, *At5g45340*, was of particular interest. It encodes a cytochrome P450 protein with ABA 8-hydroxylase activity involved in ABA catabolism (Millar et al. 2006; Umezawa et al. 2006). Transcripts of this gene, together with transcripts of two other genes encoding closely related P450 proteins reached 5- to 30-fold higher levels in "brown-green" embryos (15 to 16 days after anthesis) than in "pale-green" embryos (6 to 7 days after anthesis). Transcript levels of a fourth closely related gene remains constant throughout embryogenesis (Fig. 3.8).

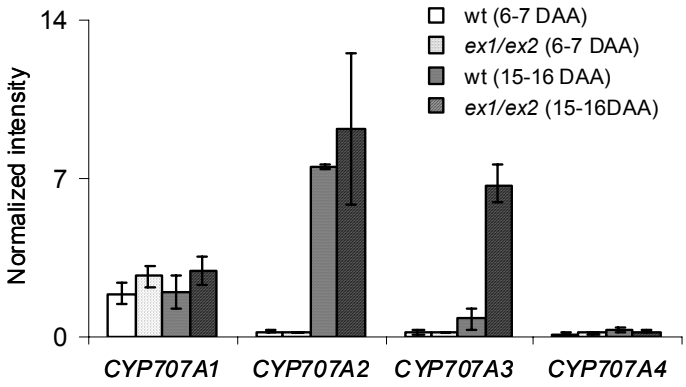

Fig. 3.8. Transcript changes of four *CYP707As* genes encoding different putative ABA hydroxylases during seed development of wild-type and *ex1/ex2* plants grown under continuous light. One of the transcripts (*CYP 707A1*) maintains the same relative concentration in young (6-7 DAA) and more mature (15-16 DAA) seeds of *ex1/ex2* and wild type (wt). Transcript levels of the three other genes (*CYP70A2, CYP707A3* and *CYP704*) increase during late embryogenesis. Transcript levels of *CYP707A3* are similar in young seeds of *ex1/ex2* and wild type (wt) and increase strongly during seed development like those of *CYP707A2* and *CYP703A4*, but in the absence of active EX1 and EX2 increase further to a 10-fold higher level in *ex1/ex2* relative to wild type. Transcript levels has been derived from two independent microarray expression experiments.

.

Among the three up-regulated cytochrome P450 genes, only the expression of *CYP707A3* was differentially affected in *ex1/ex2* versus wild type during late embryogenesis (Fig. 3.8). Transcripts of this gene reached a more than 10-fold higher level in brown-green seeds of *ex1/ex2* than in wild type. To test directly whether the enhanced expression of *CYP707A3* during late embryogenesis impacts plastid differentiation in light-grown *ex1/ex2* seedlings, a T-DNA ko mutant of *CYP707A3* was crossed with *ex1/ex2* and triple mutants were identified among the segregating F2 progeny of this cross (Fig. 3.9A). In the T-DNA line the expression of *CYP707A3* was completely blocked. When seedlings derived from seeds of light-grown triple mutants were compared with seedlings of the parental *ex1/ex2* line, plastid differentiation in these two groups of seedlings clearly differed. Inactivation of *CYP707A3* in *ex1/ex2* restores partially the capacity of proplastids to differentiate into chloroplasts as indicated by the increase in chlorophyll content and the enlargement of plastids in cotyledons of the triple mutant (Fig. 3.9B, C). The expression of the three other genes in immature *ex1/ex2* seeds encoding closely related cytochrome P450 enzymes is likely to compensate in part for the lack of *CYP707A3* and may explain why disruption of *CYP707A3* did not fully restore chloroplast formation in the triple mutant. This result implicates ABA with the control of plastid differentiation during post-embryonic development.

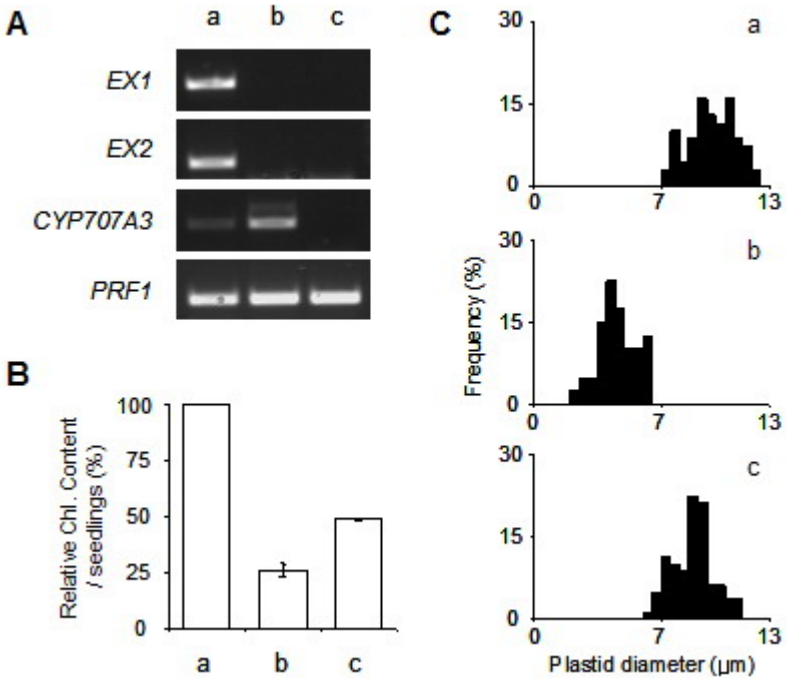

Fig. 3.9. Partial restoration of plastid differentiation in *ex1/ex2* seedlings by the inactivation of *CYP707A3*. A) Characterization of the T-DNA insertion mutant *cyp707a3*: Transcripts of *EX1*, *EX2* and *CYP707A3* in wild type (a), *ex1/ex2* double mutant (b) and the *ex1/ex2/cyp707a3* triple mutant (c). Chloroplast development in the triple mutant is partially restored as indicated by (B) an increase in Chl content and (C) the size distribution of plastids (a: wild type; b: *ex1/ex2*; c: *ex1/ex2/cyp707a3*).

To determine the physiological impact of ABA on plastid differentiation in *ex1/ex2* seedlings more directly, seeds were placed on agar plates in the absence or presence of different ABA concentrations and allowed to germinate in the dark.

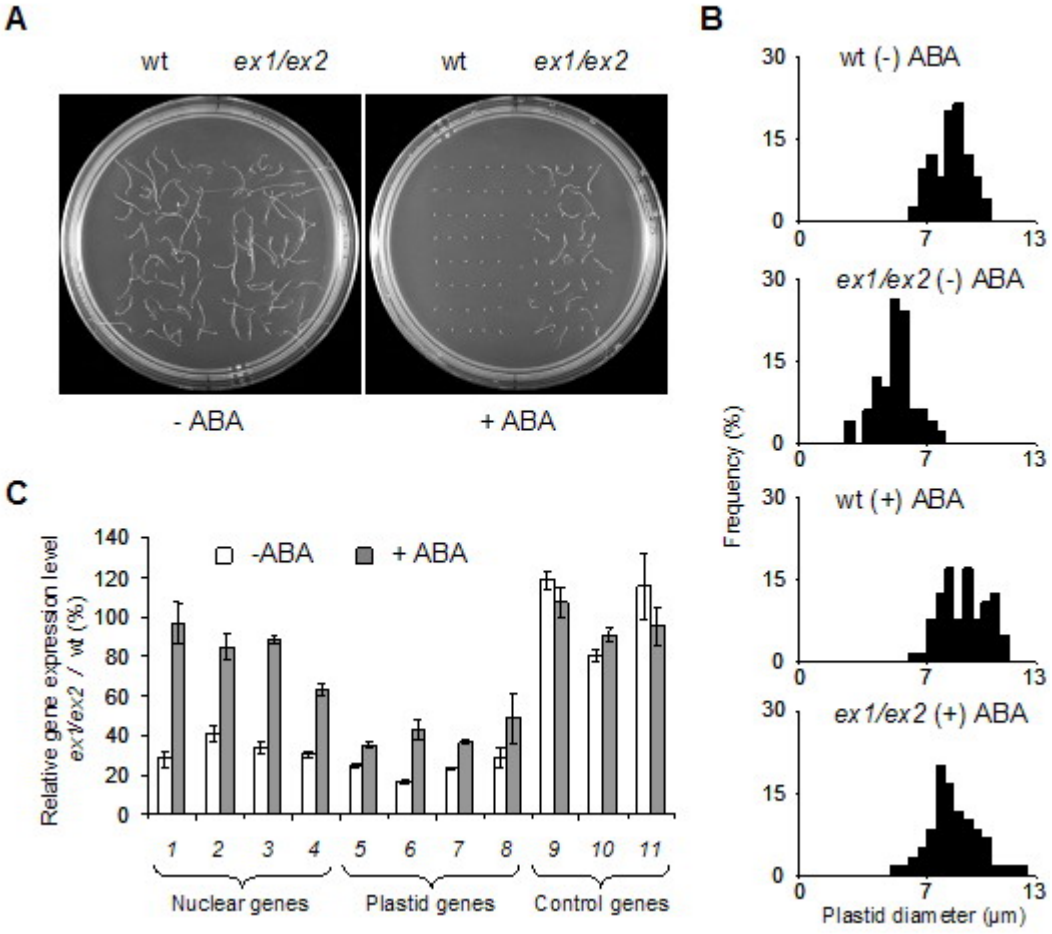

Fig. 3.10. Differential effects of exogenous ABA on seed germination, plastid differentiation and gene expression in young seedlings of wild type (wt) and *ex1/ex2*. Seeds were harvested from plants grown under continuous light. A) Wild-type (wt) and *ex1/ex2* seeds were germinated on Agar plates in the dark for 7 days in the absence (-) or presence (+) of ABA (0.2µM). B) Size distribution of plastids in cotyledons of wild-type (wt) and *ex1/ex2* seedlings grown in the light in the absence (-) or presence (+ABA) of ABA (0.5µM). Note that development of seedlings in the dark is more sensitive to exogenous ABA than in the light (data not shown). C) ABA-induced restoration of transcript levels of those genes encoding plastid proteins that are suppressed in *ex1/ex2* seedlings (See Suppl. Fig. 5). Seeds were harvested from *ex1/ex2* plants grown under continuous light and germinated in the dark for two days in the absence or presence of ABA (0.2µM). Transcript levels of four nuclear genes encoding plastid proteins (1: *At1g14150*; 2: *At3g16250*; 3: *At3g63140*; 4: *At4g28750*), four plastid genes (5: *PsbA*; 6: *PsbD*; 7: *RbcL*; 8: *PsaA*) and three control genes not affected by the *ex1/ex2* mutations (9: *At3g01790*; 10: *At5g60390*; 11: *At3g54280*) were measured by Real-Time PCR using gene-specific primers and were expressed relative to wild-type levels (-ABA). Values represent means and standard deviations of three independent measurements.

At 0.2 µM ABA seedling development of wild type was arrested, whereas the development of etiolated *ex1/ex2* seedlings was not disturbed. When exogenous ABA concentrations were lowered in the medium to 0.5µM to allow seedling development of both lines to proceed, the size distribution and Chl content of chloroplasts in ABA-treated light-grown *ex1/ex2* seedlings were

similar to wild-type seedlings in contrast to *ex1/ex2* control seedlings that were kept on agar plates without ABA (Fig. 3.10B). A similar ABA-dependent recovery of plastid formation was also observed in etiolated *ex1/ex2* seedlings (data not shown).

The ABA contents of seeds derived from siliques of light-grown *ex1/ex2* and wild-type plants that had been kept in the light or in the dark prior to seed dormancy were determined. ABA concentrations in all four seed samples were very similar with seeds from siliques kept in the dark having slightly lower ABA levels (Fig. 3.11). These results may suggest that the arrest of plastid differentiation is not due to a selective down-regulation of the ABA content of seeds derived from light-exposed siliques. However, global measurements of ABA contents of whole seeds may not reveal possible minor differences of local pools of ABA inside the plastids between the different seed samples.

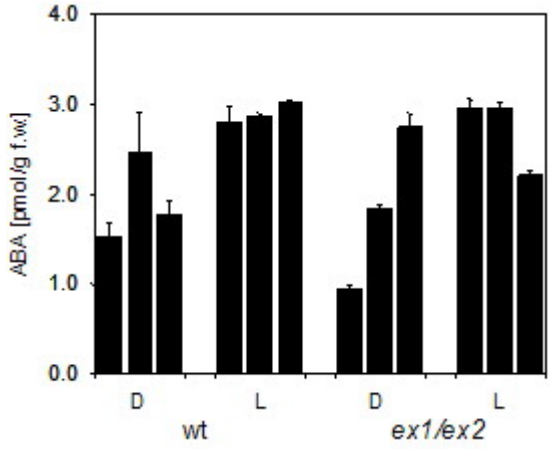

Fig. 3.11. ABA content of mature seeds of *ex1/ex2* and wild type (wt). Seeds were derived from siliques kept in the dark (D) or in the light (L). For each sample type three different seed samples were analyzed. Each value represents the means and standard deviation of four ABA measurements.

A likely reason for the recovery of plastid differentiation in ABA-treated *ex1/ex2* seedlings may be the readjustment of the expression of genes to wild-type level that encode plastid proteins and were shown to be down-regulated at the beginning of post-embryonic development of *ex1/ex2* mutant plants relative to wild type. Among the affected genes, four nuclear and four plastid genes were selected to determine the impact of exogenous ABA on their transcript levels in etiolated 2 day-old *ex1/ex2* seedlings. Addition of ABA to the growth medium restored the expression of the 4 nuclear genes close to the wild-type level, whereas the expression of the 4 plastid genes was up-regulated to a lesser extent. The expression of 3 control genes that had not been differentially affected by the inactivation of *EX1* and *EX2* was not altered grossly in their response to ABA (Fig. 3.10C).

3.4 Discussion

Thus far, plastid differentiation at the beginning of seedling development has been widely considered to be influenced by the prevailing external light conditions (Robertson and Laetsch 1974; Duysen et al. 1980). The present study identifies $^1O_2$-mediated signaling as an as yet unknown additional determinant of plastid differentiation that acts already prior to seed dormancy. Our work provides new insights but raises also new questions concerning the control of seedling development and plastid differentiation. During seed development proplastids in embryonic cells may differentiate into chloroplasts that have generally been thought to be necessary for the synthesis and deposition of storage material (Goldberg et al. 1989; Gazzarrini et al. 2004; Lopez-Juez and Pyke 2005). Developing seeds are entrapped in green siliques and thus receive only very little photosynthetically active light that does not seem to be essential for the survival of seeds. When siliques are placed in the dark, the growth and viability of seeds are not visibly impaired, suggesting that in the absence of photosynthesis developing seeds may attract sufficient nutrients from other parts of the plant. This raises the question as to why plants invest in a costly transformation of proplastids into chloroplasts and the accumulation of Chl that soon afterwards prior to seed dormancy will be catabolized. One of the consequences of this transient accumulation and catabolism of chlorophyll is the release of $^1O_2$ (Pruzinska et al. 2007) that forms an integral part of seed development. $^1O_2$ affects downstream gene expression via two antagonistic signaling events, thereby adjusting ABA levels that seem critical for retaining the competence of proplastids to differentiate into chloroplasts or etioplasts shortly after seed germination. ABA has been shown previously to regulate several key steps of seed formation such as the deposition of storage reserves, prevention of precocious germination, acquisition of desiccation tolerance, induction of primary dormancy and the transition from dormancy to germination and from germination to growth (Goldberg et al. 1989; Goldberg et al. 1994; Leung and Giraudat 1998; Gazzarrini et al. 2004). Its role as a key regulator of plastid differentiation during post-embryonic development, however, has remained unnoticed. Despite the reported pleiotropic effects of ABA during seed formation (Finkelstein et al. 1998; Finkelstein and Lynch 2000), differences in ABA levels of *ex1/ex2* and wild type seeds result in a remarkably selective down-regulation of gene expression in germinating *ex1/ex2* seedlings that is restricted to genes encoding plastid proteins.

This selective effect of ABA implies the existence of a plastid-specific ABA-responsive switch that coordinates and integrates activities of nuclear and plastid genes involved in the control of plastid development. Recently several distinct ABA receptors have been identified that support

the hypothesis of multiple sites of ABA perception with each of them controlling different sets of downstream genes. One of these receptors, the Mg^{2+} chelatase H subunit (Shen et al. 2006), is confined to the plastid compartment and may be involved in conferring the specificity of ABA-dependent signaling during post-embryonic plastid differentiation described in our present work.

3.5 Materials and Methods

3.5.1 Plant material

All experiments were performed with *Arabidopsis thaliana* ecotype *Columbia* (Col-0). Seeds were surface-sterilized and plated on Murashige and Skoog media with vitamins and 0.8% agar. Seeds were first kept at + 4°C for 4 days in the dark and then grown under continuous light (80 - 100 µmol m^{-2} s^{-1}) at 20 - 21°C. Light was provided by white light tubes (Philips Master TDL 36W, Philips Electronics N.V., Eindhoven, Netherlands and Sylvania Gro Lux F36W, SLI Lichtsysteme GmbH, Erlangen, Germany). The *ex1* and *ex2* mutants used in this study have been described previously (Lee et al. 2007). Seeds of the *CYP707A3* (At5g45340) T-DNA insertion line (SALK_078170) were obtained from the European Arabidopsis stock centre (NASC). *ex1/ex2* double mutant lines were generated by crossing *ex1* and *ex2* mutants. The *ex1/ex2cyp707A3* triple mutant was obtained by crossing *ex1/ex2* and *cyp707a3* mutant lines. Within the segregating F2 population triple mutants were identified by PCR-based genotyping.

3.5.2 Determination of chlorophyll autofluorescence and plastid size

The chlorophyll auto-fluorescence of cotyledons and leaves was recorded with a FluorCam system (Photon Systems Instruments, Brno, Czech Republic) and a Confocal Laser Scanning Microscope (TCS-NT; Leica Microsystems, Heidelberg, Germany). For measurements of plastid size, the sections of cotyledons and leaves were digitally scanned by using a Confocal Laser Scanning Microscope (Leica Microsystems). The Image program software (TCS NT, version 1.6.587, Leica Microsystems) was used to trace plastid outlines and to determine the diameter of each plastid.

3.5.3 RNA extraction and RT-PCR

Total RNA was extracted from seedlings by using an RNeasy plant mini kit (Qiagen, Hilden, Germany). Plant material was frozen under liquid nitrogen and homogenized with a mortal and a pestle. Total RNA from immature seeds of wt and *ex1/ex2* was extracted as described by Vicient and Delseny (Vicient and Delseny 1999). Immature seeds were isolated from siliques 6 to 7 days (“pale-green”), 10 to 11 days (“green”) and 15 to 16 days (“green-brown”) after anthesis.
cDNA was synthesized from 1*µg* of DNase-treated (Promega) RNA by using random primers (Promega) and Improm II reverse transcriptase (Promega) according to the manufacturer’s instructions. RT-PCR was performed with equal amounts of cDNAs by using the GeneAmp®

PCR system 9700 (Applied Biosystems, Foster City, CA, USA). Real-Time PCR using SYBR Green I was performed as described previously (Lee et al. 2007). The sequences of the primers for the selected genes are shown in Table 3.1.

Table 3.1 List of selected genes and sequences of the primers

Gene Name	Forward Primer	Reverse Primer
PsaA	5'-GCCAAGAAATCCTGAATGGA-3	5'-CATCTTGGAACCAAGCCAAT-3'
PsbB	5'-TATCGCATTCATTGCTGCTC-3'	5'-CATAAGGACCGCCGTTGTAT-3'
PsbD	5'-TTCCGTGCTTTTAACCCAAC-3'	5'-TGGGAAACGAAGTCATAGGC-3'
RbcL	5'-GACAACTGTGTGGACCGATG-3'	5'-CAGGGCTTTGAACCCAAATA-3'
At1g14150	5'-TATCATCGCCGTGTAAACCA-3'	5'-CCGCATCCTCAGGTGATAGT-3'
At3g16250	5'-ACCTCCTGCTGTCGATTTTG-3'	5'-TTCCTACTCCTGCGCAGTTT-3'
At3g63140	5'-CTGTTAGGCCAGTGGTGGAT-3'	5'-TCATGTACTGCGGTCGAAAG-3'
At4g28750	5'-GGAGCTCCGTGTCTTTCTTG-3'	5'-CTTAGGACCAATCGGTGGTG-3'
At3g01790	5'-CCCAGATATCAACCGTGCTT-3'	5'-ACCCAGTATGCCAACGGTAG-3'
At5g60390	5'-ACCAAGATTGACAGGCGTTC-3'	5'-TCCTTCTTGTCCACGCTCTT-3'
At3g54280	5'-CCTAGCGAAACACCTCAAGC-3'	5'-TGTCAAACAAGGAACCACCA-3'
At2g19760 (*PRF1*)	5'-AGAGCGCCAAATTTCCTCAG-3',	5'-CCTCCAGGTCCCTTCTTCC-3'

3.5.4 Protein analysis

Seedlings were grown for 4 days and 14 days, respectively, under continuous light. 4-day-old seedlings or primary leaves of 14-day-old seedlings were harvested, frozen under liquid nitrogen and homogenized. Total protein was extracted for each sample from approximately 0.1g of the powder in 0.5ml of homogenization buffer (0.0625M Tris-HCl pH 6.8; 1% (w/v) Sodium dodecyl sulfate (SDS); 10% (v/v) Glycerin, 0.01% (v/v) 2-Mercaptoethanol). For each sample 20µg of protein were separated electrophoretically and blotted onto xxx membranes. PSBS, ATPase, RBCL, RBCS, LHCP, D1 proteins were immunologically detected using monoclonal antibodies obtained from AgriSera (Sweden). For the detection of the FLU protein a monospecific antiserum was used that previously had been raised by Dr. Rasa Meskauskiene (ETH, Zurich). For the loading control a histone antibody obtained from Prof. Wilhelm Gruissem (ETH, Zurich) was used.

3.5.5 Precocious germination of immature seeds

The possible impact of *ex1/ex2* mutations on plastid differentiation during seed development was analyzed by removing green immature seeds of wild type and *ex1/ex2* grown under continuous light from siliques 10 days after anthesis. The isolated immature seeds were placed onto 0.8% agar plates containing 1X MS salts and allowed to grow under continuous light.

3.5.6 *In vivo* detection of singlet oxygen production in immature seeds using the pAAA-ATPase luciferase reporter line

For the detection of singlet oxygen production during seed development, transgenic lines overexpressing a singlet-oxygen-specific *AAA-ATPase:LUCIFERASE* (*AAA:LUC*) reporter gene were used. The promoter construct and the transgenic lines have been described previously (Baruah, unpublished). For the detection of luciferase activity during seed development, each day newly formed siliques following the opening of flowers were marked by threads of different colors to keep track of silique age. 50-60 seeds from siliques of different developmental stages (4, 7, 13, and 18 days after anthesis (DAA)) were isolated under dim light and placed on MS medium. The luciferase activities of seed samples were measured by spraying the luciferin solution with a home-made fine misting sprayer. A 100mM luciferin stock solution was prepared by dissolving D-Luciferin sodium salt monohydrate (ACROS ORGANICS) in sterile water and storing it at -20°C. A 1mM luciferin working solution was made by diluting the stock solution with 0.1% Tween20 just before spraying. An intensified CCD camera system from Hamamatsu Photonic Systems (MODEL XC-77, C2400) was used for the *in vivo* imaging of immature seeds. Images were viewed as photon counting using the ARGUS-50 image processing software. The images were acquired with sensitivity level 5 using slice/gravity mode.

3.5.7 Germination tests on abscisic acid (ABA)-containing medium

For germination and post-germination growth analysis in the absence or presence of different concentrations of (±)-ABA (Sigma-Aldrich Chemie GmbH, Switzerland), freshly harvested seeds were germinated. After 4 days of stratification at 4°C, the plates were placed at 22°C under continuous light or continuous darkness for 7days. Germination rates were scored based on radicle emergence and post-germination was scored based on the greening of cotyledons of plants growing under light or on the appearance of roots for plants growing in the dark, respectively. In all experiments approximately 40 seeds were used and each experiment was repeated three times.

3.5.8 Determination of ABA levels in seeds.

ABA measurement of wild-type and *ex1/ex2* seeds was performed by Dr. Cornelia Göbel and Prof. Ivo Feussner from the University Göttingen, Germany. Arabidopsis seeds of about 25 mg were extracted with 5 ml of acetone/water/acetic acid (20:79:1, v/v/v) containing 2 ng of D_6-(2*Z*,4*E*)-ABA (D_6-ABA) standard (Icon Services, Summit, NJ, USA) for 2 h at 4 ºC in darkness. The extract was centrifuged at 3200 x *g* at 4 °C for 10 min. The clear upper phase was

delipidated with 5 ml *n*-hexane and centrifuged at 3200 x *g* at 4 °C for 2 min. The lower phase was acidified by adding acetic acid to 0.1 % (v/v) and extracted twice with 5 ml diethyl ether. The solvent was dried under streaming nitrogen, and the residues were dissolved in 1 ml methanol, filtered through a 0.2 µm Teflon filter and dried under streaming nitrogen. The dried extract was resuspended in 50 µl of methanol/water/acetic acid (55:45:0.1, v/v/v).

The analysis of constituents was performed using an Agilent 1100 HPLC system (Agilent, Waldbronn, Germany) coupled to an Applied Biosystems 3200 hybrid triple quadrupole/linear ion trap mass spectrometer (MDS Sciex, Ontario, Canada). Nanoelectrospray (nanoESI) analysis was achieved using a chip ion source (TriVersa NanoMate; Advion BioSciences, Ithaca, NY, USA). Reversed-phase HPLC separation was performed on an EC 250/2 Nucleodure 100-5 $C18_{ec}$ column (250 x 2.1 mm, 5 µm particle size; Macherey and Nagel, Düren, Germany). The binary gradient system consisted of solvent A, methanol/water/acetic acid (55:45:0.1, v/v/v) and solvent B, methanol/acetic acid (100:0.1, v/v) with the following gradient program: 100 % solvent A for 2 min, followed by a linear increase of solvent B up to 100 % within 8 min and an isocratic run at 100 % solvent B for 8 min. The flow rate was 0.2 ml min^{-1}. For stable nanoESI, 30 µl min^{-1} of 2-propanol/acetonitrile/water/formic acid (70:20:10:0.1, v/v/v/v) delivered by a 515 HPLC pump (Waters, Milford, MA, USA) were added just after the column via a mixing tee valve. By using another post column splitter, 490 nl min^{-1} of the eluent were directed to the nanoESI chip. Ionization voltage was set to -1.7 kV. ABA was ionized in a negative mode and determined in multiple reaction monitoring mode. The transitions monitored for ABA and D_6-ABA were *m/z* 263 to 153 and 269 to 159, respectively. The collision energy, with nitrogen in the collision cell, was -16 V. Declustering potential was -55 V. Entrance potentials were -9 V for ABA and -10 V for D_6-ABA, respectively. The mass analyzers were adjusted to a resolution of 0.7 amu full width at half-height. The ion source temperature was 40 °C, and the curtain gas was set at 10 (given in arbitrary units). Quantification was carried out using a calibration curve of intensity (*m/z*) ratios of [ABA]/[D_6-ABA] *versus* molar amounts of ABA input (0.3-150 pmol).

3.5.9 Microarray analysis

For one set of experiments total RNA was extracted from young emerging seedlings of wild type and *ex1/ex2* that had started to grow in the dark for 48h after seed imbibition. Three individual biological replicates of wild-type and *ex1/ex2* seedlings were used for the microarray analysis.

In a second set of experiments gene expression changes were assessed during seed development. Total RNA was extracted from immature seeds of wild type and *ex1/ex2* isolated 6-7 days (“pale-green”) and 15-16 days (“green-brown”) after anthesis. Preparation of total RNA

and microarray analysis using Affymetrix ATH1 gene chips were performed as described previously (Lee et al. 2007).

3.5.10 Transmission Electron Microscopy

Cotyledons of 3-days-old light- or dark-grown seedlings and true leaves of 14-days-old light-grown plants of wild type and *ex1/ex2* were used. The cotyledons and leaves were prefixed in 4% paraformaldehyde and 5% glutaraldehyde for 1 hour, and then fixed in 1% OsO_4 for 1 hour. After dehydration through an acetone series (10 steps from 25% to 100%), samples were embedded in Agar resin 100 and sectioned using a glass knife. The sections were examined under a transmission electron microscope.

3.5.11 Extraction and measurement of Pchlide

Total Pchlide was extracted with 90% acetone/10% 0.1 M NH_4OH in water. Relative amounts of Pchlide were determined as previously described (Kim and Apel 2004). The relative units were normalized either per fresh weight of seedlings with five independent biological replicas or per chlorophyll content with three replicas.

3.5.12 Chlorophyll measurement

Chlorophyll was extracted from seedlings boiling in 95% ethanol at 80°C for 20 minutes. The relative chlorophyll content per seedling was calculated as described by Lichtenthaler (Lichtenthaler 1987).

3.6 Acknowledgements

We thank the editorial work of Ursula Baldenweg, Dr. Dieter Rubli for art work, André Imboden for taking care of plants, and Dr. Frank Landgraf for technical support. We thank members of our group, in particular Dr. Rasa Meskauskiene, Dr. Christophe Laloi, Dr. Veronica Albrecht for helpful discussions during the completion of the manuscript. This study was supported by grants from ETH-Zurich, the Swiss National Science Foundation (NSF), and the Functional Genomics Center Zurich (FGCZ) .

3.7 References

Albrecht, V., Ingenfeld, A., and Apel, K. 2006. Characterization of the snowy cotyledon 1 mutant of Arabidopsis thaliana: the impact of chloroplast elongation factor G on chloroplast development and plant vitality. *Plant Mol Biol* 60(4): 507-518.

Apel, K. and Hirt, H. 2004. Reactive oxygen species: metabolism, oxidative stress, and signal transduction. *Annu Rev Plant Biol* 55: 373-399.

Borisjuk, L., Macherel, D., Benamar, A., Wobus, U., and Rolletschek, H. 2007. Low oxygen sensing and balancing in plant seeds: a role for nitric oxide. *New Phytol* 176(4): 813-823.

Borisjuk, L., Nguyen, T.H., Neuberger, T., Rutten, T., Tschiersch, H., Claus, B., Feussner, I., Webb, A.G., Jakob, P., Weber, H., Wobus, U., and Rolletschek, H. 2005. Gradients of lipid storage, photosynthesis and plastid differentiation in developing soybean seeds. *New Phytol* 167(3): 761-776.

Borisjuk, L., Rolletschek, H., Radchuk, R., Weschke, W., Wobus, U., and Weber, H. 2004. Seed development and differentiation: a role for metabolic regulation. *Plant Biol (Stuttg)* 6(4): 375-386.

Braybrook, S.A., Stone, S.L., Park, S., Bui, A.Q., Le, B.H., Fischer, R.L., Goldberg, R.B., and Harada, J.J. 2006. Genes directly regulated by LEAFY COTYLEDON2 provide insight into the control of embryo maturation and somatic embryogenesis. *Proc Natl Acad Sci U S A* 103(9): 3468-3473.

Duysen, M.E., Freeman, T.P., and Zabrocki, R.D. 1980. Light and the correlation of chloroplast development and coupling of phosphorylation to electron transport. *Plant Physiol* 65(5): 880-883.

Finkelstein, R.R. and Lynch, T.J. 2000. The Arabidopsis abscisic acid response gene ABI5 encodes a basic leucine zipper transcription factor. *Plant Cell* 12(4): 599-609.

Finkelstein, R.R., Wang, M.L., Lynch, T.J., Rao, S., and Goodman, H.M. 1998. The Arabidopsis abscisic acid response locus ABI4 encodes an APETALA 2 domain protein. *Plant Cell* 10(6): 1043-1054.

Flors, C., Fryer, M.J., Waring, J., Reeder, B., Bechtold, U., Mullineaux, P.M., Nonell, S., Wilson, M.T., and Baker, N.R. 2006. Imaging the production of singlet oxygen in vivo using a new fluorescent sensor, Singlet Oxygen Sensor Green. *J Exp Bot* 57(8): 1725-1734.

Gazzarrini, S., Tsuchiya, Y., Lumba, S., Okamoto, M., and McCourt, P. 2004. The transcription factor FUSCA3 controls developmental timing in Arabidopsis through the hormones gibberellin and abscisic acid. *Dev Cell* 7(3): 373-385.

Goldberg, R.B., Barker, S.J., and Perez-Grau, L. 1989. Regulation of gene expression during plant embryogenesis. *Cell* 56(2): 149-160.

Goldberg, R.B., de Paiva, G., and Yadegari, R. 1994. Plant Embryogenesis: Zygote to Seed. *Science* 266(5185): 605-614.

Gutierrez-Nava Mde, L., Gillmor, C.S., Jimenez, L.F., Guevara-Garcia, A., and Leon, P. 2004. CHLOROPLAST BIOGENESIS genes act cell and noncell autonomously in early chloroplast development. *Plant Physiol* 135(1): 471-482.

Kim, C. and Apel, K. 2004. Substrate-dependent and organ-specific chloroplast protein import in planta. *Plant Cell* 16(1): 88-98.

Krieger-Liszkay, A. 2005. Singlet oxygen production in photosynthesis. *J Exp Bot* 56(411): 337-346.

Lee, K.P., Kim, C., Landgraf, F., and Apel, K. 2007. EXECUTER1- and EXECUTER2-dependent transfer of stress-related signals from the plastid to the nucleus of Arabidopsis thaliana. *Proc Natl Acad Sci U S A* 104(24): 10270-10275.

Leung, J. and Giraudat, J. 1998. Abscisic Acid Signal Transduction. *Annu Rev Plant Physiol Plant Mol Biol* 49: 199-222.

Lichtenthaler, H.K. 1987. Chlorophylls and carotenoids: Pigments of photosynthetic biomembranes. *Methods Enzymol* 148: 350-382.

Lopez-Juez, E. and Pyke, K.A. 2005. Plastids unleashed: their development and their integration in plant development. *Int J Dev Biol* 49(5-6): 557-577.

Meskauskiene, R., Nater, M., Goslings, D., Kessler, F., op den Camp, R., and Apel, K. 2001. FLU: a negative regulator of chlorophyll biosynthesis in Arabidopsis thaliana. *Proc Natl Acad Sci U S A* 98(22): 12826-12831.

Millar, A.A., Jacobsen, J.V., Ross, J.J., Helliwell, C.A., Poole, A.T., Scofield, G., Reid, J.B., and Gubler, F. 2006. Seed dormancy and ABA metabolism in Arabidopsis and barley: the role of ABA 8'-hydroxylase. *Plant J* 45(6): 942-954.

op den Camp, R.G., Przybyla, D., Ochsenbein, C., Laloi, C., Kim, C., Danon, A., Wagner, D., Hideg, E., Gobel, C., Feussner, I., Nater, M., and Apel, K. 2003. Rapid induction of distinct stress responses after the release of singlet oxygen in Arabidopsis. *Plant Cell* 15(10): 2320-2332.

Parcy, F., Valon, C., Kohara, A., Misera, S., and Giraudat, J. 1997. The ABSCISIC ACID-INSENSITIVE3, FUSCA3, and LEAFY COTYLEDON1 loci act in concert to control multiple aspects of Arabidopsis seed development. *Plant Cell* 9(8): 1265-1277.

Pruzinska, A., Anders, I., Aubry, S., Schenk, N., Tapernoux-Luthi, E., Muller, T., Krautler, B., and Hortensteiner, S. 2007. In vivo participation of red chlorophyll catabolite reductase in chlorophyll breakdown. *Plant Cell* 19(1): 369-387.

Robertson, D. and Laetsch, W.M. 1974. Structure and function of developing barley plastids. *Plant Physiol* 54(2): 148-159.

Rohde, A., De Rycke, R., Beeckman, T., Engler, G., Van Montagu, M., and Boerjan, W. 2000. ABI3 affects plastid differentiation in dark-grown Arabidopsis seedlings. *Plant Cell* 12(1): 35-52.

Rolletschek, H., Weber, H., and Borisjuk, L. 2003. Energy status and its control on embryogenesis of legumes. Embryo photosynthesis contributes to oxygen supply and is coupled to biosynthetic fluxes. *Plant Physiol* 132(3): 1196-1206.

Shen, Y.Y., Wang, X.F., Wu, F.Q., Du, S.Y., Cao, Z., Shang, Y., Wang, X.L., Peng, C.C., Yu, X.C., Zhu, S.Y., Fan, R.C., Xu, Y.H., and Zhang, D.P. 2006. The Mg-chelatase H subunit is an abscisic acid receptor. *Nature* 443(7113): 823-826.

Umezawa, T., Okamoto, M., Kushiro, T., Nambara, E., Oono, Y., Seki, M., Kobayashi, M., Koshiba, T., Kamiya, Y., and Shinozaki, K. 2006. CYP707A3, a major ABA 8'-hydroxylase involved in dehydration and rehydration response in Arabidopsis thaliana. *Plant J* 46(2): 171-182.

Vicente-Carbajosa, J. and Carbonero, P. 2005. Seed maturation: developing an intrusive phase to accomplish a quiescent state. *Int J Dev Biol* 49(5-6): 645-651.

Vicient, C.M. and Delseny, M. 1999. Isolation of total RNA from Arabidopsis thaliana seeds. *Anal Biochem* 268(2): 412-413.

Wagner, D., Przybyla, D., Op den Camp, R., Kim, C., Landgraf, F., Lee, K.P., Wursch, M., Laloi, C., Nater, M., Hideg, E., and Apel, K. 2004. The genetic basis of singlet oxygen-induced stress responses of Arabidopsis thaliana. *Science* 306(5699): 1183-1185.

Supplementary Materials

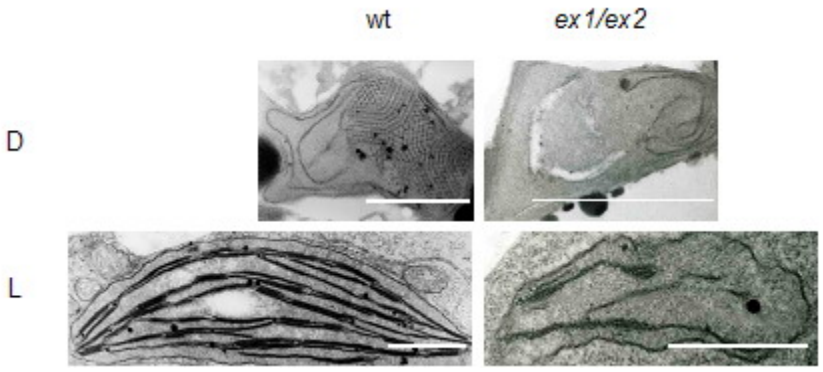

Supplementary Fig. 3.1. Transmission electron micrographs of plastids from 3-day-old etiolated (D) and light-grown (L) seedlings of wild type (wt) and *ex1/ex2* mutants. Bars: 1 µm.

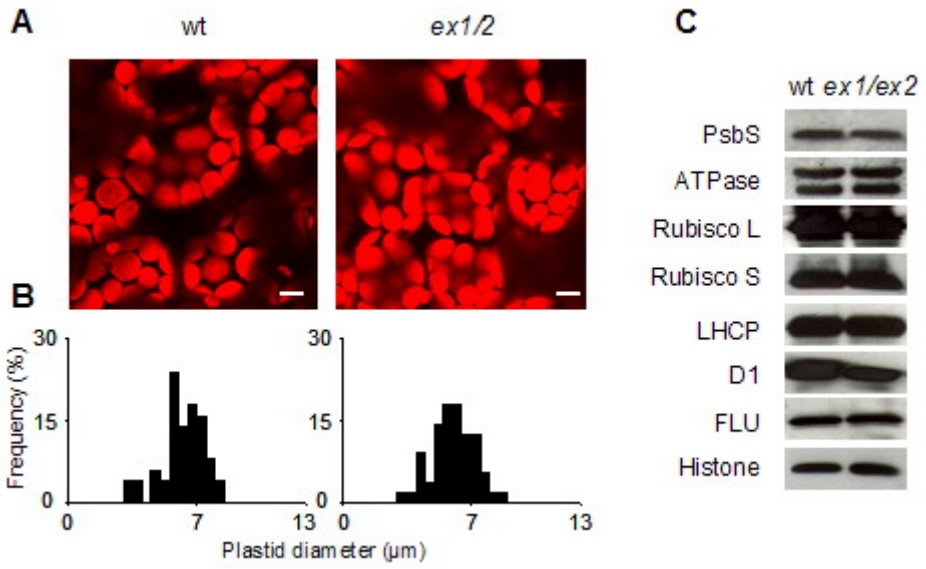

Supplementary Fig. 3.2 Chloroplast development in true leaves of wild-type (wt) and *ex1/ex2* seedlings grown for 10 days under continuous light. A) Chl fluorescence images of chloroplasts, (B) the size distribution of chloroplasts and (C) the relative concentrations of chloroplast proteins are similar in wild type and *ex1/ex2*, indicating that the suppressive effect of *ex1/ex2* mutations is restricted to plastid differentiation in cotyledons. Abbreviations of proteins (C) are the same as in Fig. 1B. Bars: 5µm.

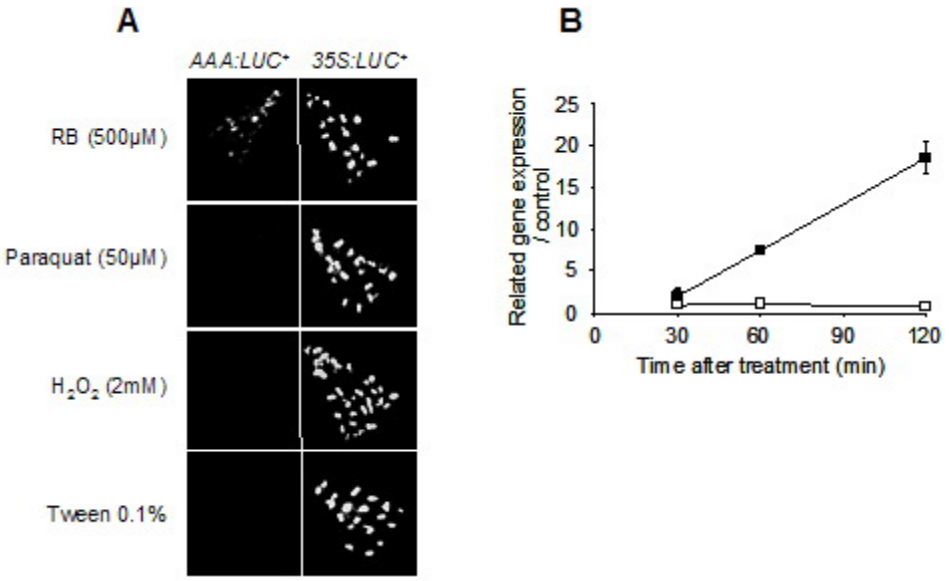

Supplementary Fig. 3.3. The selectivity of 1O2-mediated activation of the *AAA:LUC*$^+$ reporter gene. A) Seedlings of transgenic wild-type lines expressing *AAA:LUC*$^+$ or *LUC*$^+$ under control of the constitutively active *35S CamV*-promoter (*35S:LUC*$^+$) were grown for 4 days under continuous light. Activation of *AAA:LUC*$^+$ was seen only in light-grown seedlings sprayed with Rose Bengal (RB), a photosensitizer generating $^1O_2$ by energy transfer, but not in seedlings treated with paraquat, a herbicide that gives rise to H_2O_2 and superoxide or with H_2O_2. As controls, plants were also sprayed with 0.1% Tween20. B) Specific up-regulation of the $^1O_2$-specific *AAA-ATPase* gene (■), but not the H_2O_2-responsive gene *FERRITIN1* (□) in 4-day-old wild-type seedlings sprayed with Rose Bengal.

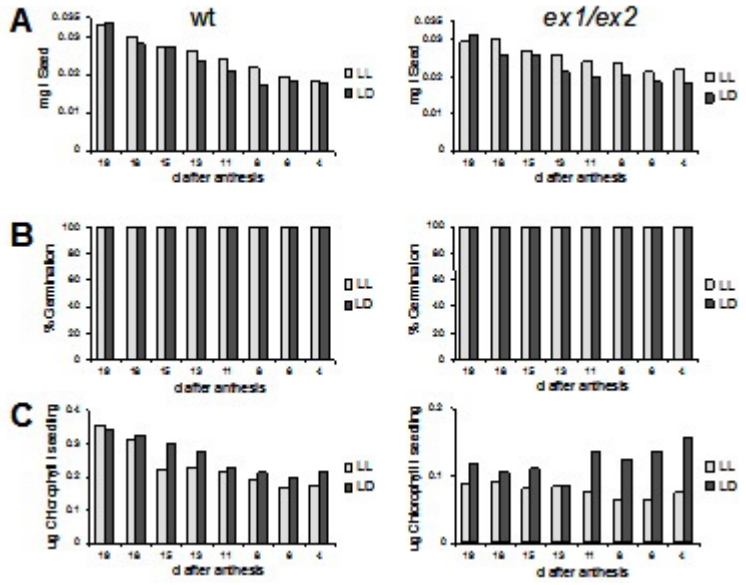

Supplementary Fig. 3.4. The effect of darkening siliques of wild-type (wt) and *ex1/ex2* plants grown under continuous light with aluminum foil on (A) seed weight, (B) germination rate and (C) chlorophyll content of light-grown seedlings derived from dark- and light-treated siliques. Gray and black bars represent measurements with light-exposed and darkened siliques, respectively. Siliques were first covered at different days after anthesis and kept in the dark until mature dry seeds could be harvested. Each value represents the means of at least 50 seeds. The experiment was repeated two times and gave very similar results. Note that only Chl accumulation of *ex1/ex2* seedlings was differentially affected by the absence or presence of light during seed development. The effect of darkening *ex1/ex2* seedlings was effective only if started before 13 DAA.

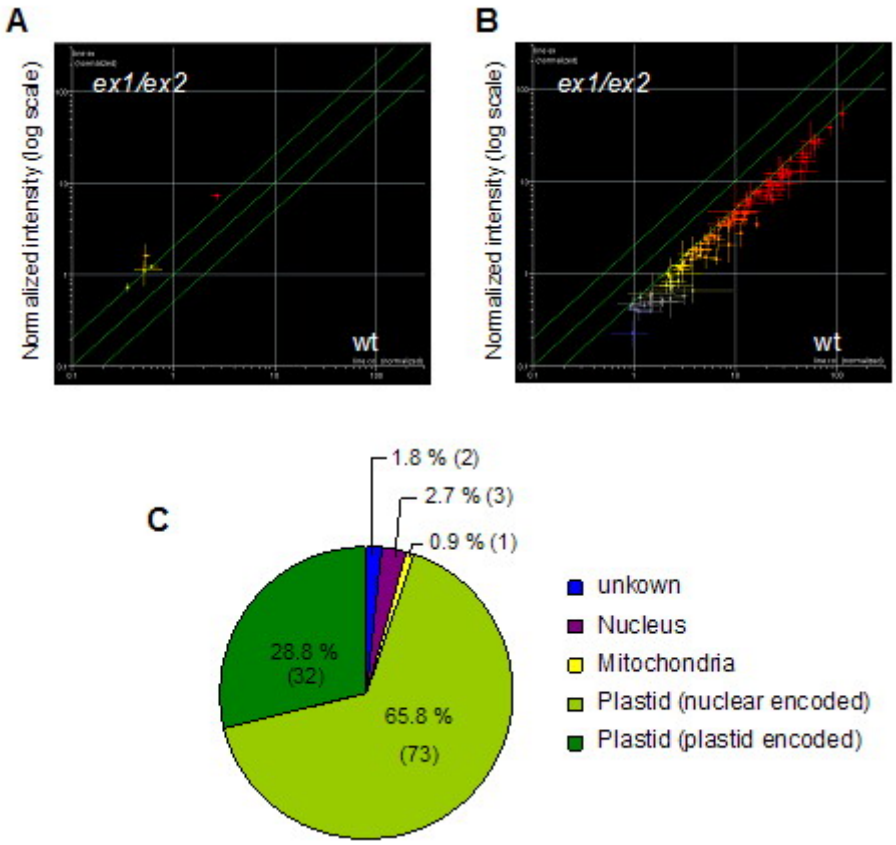

Supplementary Fig. 3.5. Selective down-regulation of transcripts encoding plastid proteins in 2-day-old *ex1/ex2* seedlings relative to wild type. Seeds of *ex1/ex2* and wild-type plants grown under continuous light were plated in the dark on Agar plates and 48 h later after radical emergence total RNA was extracted from *ex1/ex2* and wild-type embryos and analyzed on Affymetrix ATH1 gene chips. A) Scatter blot showing transcripts that reached an at least a two-fold higher level in *ex1/ex2* versus wild type. Only 5 genes were affected. B) Scatter blot showing genes that were at least twofold down-regulated in *ex1/ex2* versus wild type. A total of 111 genes were affected. C) Unexpectedly, almost 95% of these genes encode plastid proteins. Roughly two thirds of these genes are localized in the nucleus, whereas the remainders are of plastid origin.

Supplementary Table 3.1. List of genes (at least three-fold up- or down-regulated in ex1/ex2 "green-brown" vs. wt "green-brown" embryos)

Up (74)

Gene ID	Common	Description	Localization	Fold (+)
At2g26150	ATHSFA2	heat shock transcription factor family protein	nucleus	3.01
At4g01250	WRKY22	member of WRKY Transcription Factor; Group II-e	nucleus	4.24
At1g68670		myb family transcription factor	nucleus	5.64
At4g34410		a member of the ERF subfamily B-3 of ERF/AP2 transcription factor	nucleus	11.02
At2g47520		a member of the ERF subfamily B-2 of ERF/AP2 transcription factor	nucleus	4.72
At4g17490	ATERF6	a member of the ERF subfamily B-3 of ERF/AP2 transcription factor	nucleus	4.99
At3g54810		zinc finger (GATA type) family protein,	nucleus	4.98
At1g32640	ATMYC2	basic helix-loop-helix (bHLH) protein (RAP-1)	nucleus	3.62
At1g19210		a member of the DREB subfamily A-5 of ERF/AP2 transcription factor	nucleus	17.89
At5g59820	RHL41	Encodes a zinc finger protein	nucleus	4.55
At2g18160	GBF5	bZIP transcription factor family protein	nucleus	5.25
At2g38470	WRKY33	putative WRKY-type DNA binding protein	nucleus	17.47
At3g55980		zinc finger (CCCH-type) family protein,	Unknown	4.70
At3g10040		expressed protein	Chloroplast	21.97
At4g10270		wound-responsive family protein	Chloroplast	8.68
At3g19680		expressed protein	Chloroplast	3.63
At3g13310		DNAJ heat shock N-terminal domain-containing protein	Chloroplast	9.48
At3g52760		integral membrane Yip1 family protein, Yip1 domain	Chloroplast	3.11
At4g27280		calcium-binding EF hand family protein	Chloroplast	3.81
At5g26030		ferrochelatase-I	Chloroplast	3.37
At1g20310		expressed protein	Chloroplast	10.80
At1g72520	LOX	lipoxygenase	Chloroplast	6.15
At2g22880		VQ motif-containing protein,	Chloroplast	4.74
At2g26530		similar to calmodulin-binding protein (At2g15760.1)	Chloroplast	3.12
At5g59730		leucine zipper-containing protein	Chloroplast	4.32
At3g02540		ubiquitin family protein	nucleus	3.60
At1g76600		expressed protein	nucleus	3.12
At4g11280	ACS6	1-aminocyclopropane-1-carboxylate synthase 6 / ACC synthase 6	Unknown	3.39
At5g37770	TCH2	CALMODULIN-RELATED PROTEIN 2, TOUCH-INDUCED (TCH2)	Unknown	6.63
At5g57560	TCH4	xyloglucan:xyloglucosyl transferase	Unknown	7.09
At2g17850		unknown protein	Unknown	25.85
At1g75030	ATLP-3	pathogenesis-related thaumatin family protein (PR5 like protein)	endomembrane	3.34
At5g06320	NHL3	Similar to non-race specific disease resistance gene (NDR1).	membrane	4.68
At5g62520		similarity to RCD1(Radical induced cell death 1)	mitochondrion	3.62
At4g25810	XTR6	xyloglucan endo-1,4-beta-D-glucanase (XTR-6),	endomembrane	4.96
At2g22500		mitochondrial substrate carrier family protein	mitochondrial	13.57
At2g31880		leucine-rich repeat transmembrane protein kinase	endomembrane	3.57
At5g27920		a similarity to leucine-rich repeats containing F-box protein	Unknown	3.50
At1g35140	PHI-1	PHOSPHATE-INDUCED 1	Cell wall	19.05
At4g23180	CRK10	CYSTEINE-RICH receptor-like protein kinase 4 (RLK10)	Unknown	3.81
At1g66400		calmodulin-related protein	Unknown	3.52
At5g19120		conglutin gamma - like protein conglutin gamma precursor	endomembrane	3.22
At1g31290		PAZ domain-containing protein / piwi domain-containing protein,	Unknown	3.61
At5g45340	CYP707A3	cytochrome P450	endomembrane	10.33
At2g44460	AtBG1	beta-glucosidase 1	endomembrane	6.32
At2g27080		harpin-induced protein-related	Unknown	4.78

At1g55450		similar to embryo-abundant protein	Unknown	5.73
At5g41060		zinc finger (DHHC type) family protein	Unknown	3.45
At1g57990	ATPUP18	purine permease-related,	membrane	4.11
At4g24570		mitochondrial substrate carrier family protein	mitochondrial	32.88
At4g04830		similar to transcriptional regulator	Unknown	11.13
At5g64660		U-box domain-containing protein,	ubiquitin ligase	3.70
At5g09800		U-box domain-containing protein	ubiquitin ligase	3.98
At4g30440	GAE1	UDP-D-glucuronate 4-epimerase,	Unknown	3.38
At1g32920		expressed protein	endomembrane	5.82
At1g33055		Expressed protein	endomembrane	11.61
At5g15120		expressed protein	Unknown	9.62
At3g27220		Myb DNA-binding domain repeat signature 2	mitochondrion	5.88
At3g23170		expressed protein	mitochondrion	5.51
At1g04770		male sterility MS5 family protein	mitochondrion	3.09
At5g46295		expressed protein	mitochondrion	3.12
At3g57450		expressed protein	mitochondrion	6.29
At3g02550		lateral organ boundaries domain protein 41 (LBD41),	Unknown	7.10
At1g19380		expressed protein	Unknown	3.97
At1g03610		expressed protein	Unknown	3.10
At1g18740		expressed protein , similar to AT1G43630	Unknown	7.03
At1g74450		expressed protein	Unknown	3.22
At3g33066		pseudogene	Unknown	3.65
At1g19020		expressed protein	Unknown	4.04
At5g39890		expressed protein	Unknown	7.47
At5g17350		expressed protein	Unknown	5.21
At4g24110		expressed protein	Unknown	3.56
At5g66985		expressed protein	Unknown	4.91
At4g29780		expressed protein	Unknown	4.78

Down (29)

Gene ID	Common	Descriptions	Localization	Fold (-)
At1g62500		seed storage/lipid transfer protein (LTP) family protein	endomembrane	5.12
At1g01520		myb family transcription factor	nucleus	3.17
At1g17310		MADS-box protein (AGL100), similar to transcription factor	nucleus	3.47
At3g18850		phospholipid/glycerol acyltransferase family protein	Unknown	3.11
At3g55630	ATDFD	dihydrofolate synthetase/folylpolyglutamate synthetase	cytosol	3.01
At1g09660		putative elongation factor or KH domain-containing quaking protein	Unknown	3.15
At3g52820		purple acid phosphatase (PAP22)	endomembrane	7.12
At4g10250	HSP22.0	22.0 kDa ER small heat shock protein (HSP22.0-ER)	endomembrane	4.39
At2g41390		expressed protein	endomembrane	3.98
At1g12845		expressed protein	endomembrane	5.18
At2g03540		expressed protein	chloroplast	3.42
At3g04190		Similar to germin type2	endomembrane	6.12
At2g45870		expressed protein	chloroplast	3.42
At3g47420		glycerol-3-phosphate transporter	membrane	4.96
At4g27670	HSP21	heat shock protein 21, 25.3 kDa small heat shock protein,	Chloroplast	9.58
At5g24160		squalene monooxygenase 1,2	endomembrane	3.37
At4g25200	HSP23.6	23.6 kDa mitochondrial small heat shock protein	mitochondrion	3.38
At5g07710		exonuclease family protein, contains exonuclease domain	intracellular	3.07

At4g14780		similar to protein kinase ATMRK1	Unknown	4.64
At5g34895		hypothetical protein,	Unknown	4.87
At3g07850		Galacturan 1,4-alpha-galacturonidase	endomembrane	3.74
At1g55690		Phosphatidylinositol Transfer Protein	Unknown	3.51
At3g50620		nodulation protein-related	Unknown	4.07
At1g62210		expressed protein	endomembrane	3.40
At2g38940	ATPT2	phosphate transporter (AtPT2)	membrane	4.79
At2g14620		xyloglucan:xyloglucosyl transferase	endomembrane	3.45
At5g50000		similar to protein kinase ATMRK1	Unknown	3.57
At5g13930	CHS	chalcone synthase	ER, nucleus	6.54
At3g12203		serine carboxypeptidase S10 family protein,	endomembrane	4.76

Supplementary Table 3.2. List of genes (at least two-fold up- or down-regulated in 2days old etiolated *ex1ex2* seedlings vs 2days old etiolated wt seedlings)

Up (5)

Gene ID	Common	Description	Localization	Fold (+)
At3g60140		beta-glucosidase-like protein several beta-glucosidases , DIN2	endomembrane	2.21
At5g51440	HSP23.5M	mitochondrial heat shock 22 kd protein-like	mitochondrion	3.01
At2g21640		unknown protein	mitochondrion	2.74
At2g30250		putative WRKY-type DNA binding protein, transcription factor	nucleus	2.10
At1g71330		putative ABC transporter , ATNAP5	unknown	2.05

Down (111)

Gene ID	Common	Description	Localization	Fold (-)
At1g03130		putative photosystem I reaction center subunit II precursor	chloroplast	2.06
At1g03630		putative protochlorophyllide reductase	chloroplast	2.10
At1g08380		unknown protein	chloroplast	2.54
At1g14150		oxygen evolving enhancer 3 (PsbQ) family protein	chloroplast	3.76
At1g15820	LHCB6	Lhcb6 protein (Lhcb6),chlorophyll binding protein	chloroplast	2.08
At1g15980		unknown protein	chloroplast	2.73
At1g18730		unknown protein	chloroplast	2.73
At1g19150		PSI type II chlorophyll a/b-binding protein	chloroplast	2.52
At1g21500		1-phosphatidylinositol-4-phosphate kinase, class IA complex	chloroplast	2.75
At1g30380	PSAK	photosystem I subunit X precursor	chloroplast	2.90
At1g32060		phosphoribulokinase precursor	chloroplast	2.21
At1g32080		G-protein coupled receptor protein signaling pathway	chloroplast	2.47
At1g32470		glycine cleavage system H protein precursor	mitochondrion	2.00
At1g35420		dienelactone hydrolase family protein	chloroplast	2.05
At1g43800		stearoyl acyl carrier protein desaturase	mitochondrion	3.31
At1g44575	PSBS	photosystem II 22kDa protein	chloroplast	2.86
At1g51115		plastid-lipid associated protein PAP / fibrillin family protein	chloroplast	2.08
At1g52230	PSAH2	photosystem I subunit VI precursor	chloroplast	2.40
At1g55670	PSAG	photosystem I subunit V precursor	chloroplast	2.81
At1g61520	LHCA3.1	PSI type III chlorophyll a/b-binding protein	chloroplast	2.48
At1g62780		unknown protein	chloroplast	2.55
At1g64770		similar to putative antifreeze glycoprotein precursor [Oryza sativa]	chloroplast	2.17

At1g68010		hydroxypyruvate reductase (HPR)	chloroplast	2.23
At1g70760		putative inorganic carbon transport protein	chloroplast	2.81
At1g74730		unknown protein	chloroplast	2.21
At1g76080		thioredoxin family protein	chloroplast	2.42
At1g76100		plastocyanin	chloroplast	3.20
At2g03750		putative steroid sulfotransferase	chloroplast	2.41
At2g05070	LHCB2.2	putative chlorophyll a/b binding protein	chloroplast	2.67
At2g13360		alanine-glyoxylate aminotransferase	chloroplast	2.58
At2g20260	PSAE2	putative photosystem I reaction center subunit IV	chloroplast	2.13
At2g21330		putative fructose bisphosphate aldolase	chloroplast	2.27
At2g23670		hypothetical protein .	chloroplast	2.62
At2g39470		photosystem II reaction center PsbP family protein	chloroplast	2.13
At2g42220		rhodanese-like family protein	chloroplast	2.54
At2g42690		putative lipase	Unknown	2.20
At3g01440	PSBQ	oxygen evolving enhancer 3 (PsbQ) family protein	chloroplast	2.73
At3g01500	CA1	carbonic anhydrase	chloroplast	3.72
At3g02730		thioredoxin,similar to Thioredoxin F-type, (TRX-F) (Borisjuk et al.)	chloroplast	2.15
At3g04000		putative short-chain type dehydrogenase/reductase	chloroplast	2.07
At3g08940	LHCB4.2	putative chlorophyll a/b-binding protein	chloroplast	2.39
At3g15360		thioredoxin m4	chloroplast	2.06
At3g15840		unknown protein	chloroplast	2.51
At3g16140	PSAH1	photosystem I subunit VI precursor	chloroplast	2.47
At3g16250		putative 2Fe-2S iron-sulfur cluster protein	chloroplast	5.36
At3g46780		putative protein	chloroplast	3.73
At3g50685		Expressed protein	chloroplast	2.11
At3g50820	OEC33	psbO2. photosystem II oxygen-evolving complex protein 1	chloroplast	2.77
At3g54050		fructose-bisphosphatase precursor	chloroplast	2.46
At3g59400		GUN4	chloroplast	2.46
At3g61470	LHCA2	Lhca2 protein	chloroplast	2.84
At3g63140		mRNA binding protein precursor	chloroplast	3.24
At3g63160		putative protein	chloroplast	2.97
At4g02770		putative photosystem I reaction center subunit II precursor	chloroplast	2.22
At4g05180	OEC16	Oxygen-evolving enhancer protein 3 precursor	chloroplast	2.70
At4g10340	LHCB5	chlorophyll a/b-binding protein CP26 in PS II	chloroplast	2.29
At4g12800	PSI-L	probable photosystem I chain XI precursor	chloroplast	2.71
At4g28080		putative tetratricopeptide repeat(TPR)-containing protein	Unknown	2.79
At4g28660		photosystem II reaction centre W (PsbW) family protein,	chloroplast	2.47
At4g28750	PSAE1	Photosystem I reaction centre subunit IV / PsaE	chloroplast	3.25
At4g33630		Executer1	chloroplast	2.03
At4g34730		ribosome-binding factor A family protein	chloroplast	2.11
At4g39710	FKBP	immunophilin, putative / FKBP-type peptidyl-prolyl cis-trans isomerase	chloroplast	2.37
At5g04140	GLU1	glutamate synthase (GLU1)	chloroplast	2.33
At5g13630		GUN5	chloroplast	2.01
At5g13770		pentatricopeptide (PPR) repeat-containing protein	chloroplast	2.92
At5g14740	CA2/CA18	CARBONIC ANHYDRASE 2 (CA2-cytoplasm) or (CA1-chloroplast)	chloroplast	2.34
At5g16400		thioredoxin, putative Thioredoxin F-type, chloroplast precursor (TRX-F)	chloroplast	2.01
At5g17230	PSY	phytoene synthase	chloroplast	2.23
At5g19220	APL1	Glucose-1-phosphate adenylyltransferase (ApL1/adg2)	chloroplast	3.64
At5g20630	GER3	germin-like protein (GLP3)	chloroplast	2.37
At5g23060		unknown protein	mitochondrion	2.85

At5g36700		phosphoglycolate phosphatase	chloroplast	2.16
At5g38520		hydrolase, alpha/beta fold family protein	chloroplast	2.26
At5g44190		myb family transcription factor (GLK2)	nucleus	2.02
At5g55220		trigger factor type chaperone family protein	chloroplast	2.06
At5g58260		subunit NDH-N of NAD(P)H:plastoquinone dehydrogenase complex	chloroplast	2.48
At5g64040	PSI-N	PSI reaction centre subunit psaN precursor (PSI-N)	chloroplast	2.00
At5g66570	OEC33	33 kDa polypeptide of oxygen-evolving complex (OEC) in PSII	chloroplast	2.27
atpA		ATPase alpha subunit	chloroplast	2.03
atpE		ATPase epsilon subunit	chloroplast	2.10
atpF		ATPase I subunit	chloroplast	2.14
atpH		ATPase III subunit	chloroplast	2.80
ndhA		NADH dehydrogenase ND1	chloroplast	2.26
ndhC		NADH dehydrogenase D3	chloroplast	2.00
ndhD		NADH dehydrogenase ND4	chloroplast	2.26
ndhE		NADH dehydrogenase ND4L	chloroplast	4.12
ORF31		hypothetical protein	chloroplast	2.40
petB		cytochrome B6	chloroplast	2.26
psaA		PSI P700 apoprotein A1	chloroplast	4.20
psaB		PSI P700 apoprotein A2	chloroplast	3.49
psaC		PSI 9KDa protein	chloroplast	2.38
psaI		PSI I protein	chloroplast	2.25
psaJ		PSI J protein	chloroplast	2.57
psbA		PSII 32 KDa protein	chloroplast	5.79
psbC		PSII 43 KDa protein	chloroplast	4.73
psbD		PSII D2 protein	chloroplast	4.36
psbG		photosystem II G protein	chloroplast	2.01
psbH		PSII 10KDa phosphoprotein	chloroplast	3.16
psbI		PSII I protein	chloroplast	2.64
psbK		PSII K protein	chloroplast	3.46
rbcL		large subunit of riblose-1,5-bisphosphate carboxylase/oxygenase	chloroplast	4.05
rpl33		ribosomal protein L33	chloroplast	2.31
rpoC1		RNA polymerase beta' subunit-1	chloroplast	2.25
rps12.1		ribosomal protein S12 (trans-splice part 1 of 2)	chloroplast	2.49
rps12.2		ribosomal protein S12 (trans-splice part 2 of 2)	chloroplast	2.07
rps15		ribosomal protein S15	chloroplast	2.35
rps4		ribosomal protein S4	chloroplast	2.89
ycf3		hypothetical protein	chloroplast	4.19
ycf5		hypothetical protein	chloroplast	2.72
ycf9		encodes PsbZ, which is a subunit of photosystem II.	chloroplast	3.71

4. A new role of chloroplasts as the *alpha* and *omega* of a plant-specific programmed cell death pathway

Chanhong Kim[1,8,10], Keun Pyo Lee[1,10], Ashok M.L.[1], Karolina Blajecka[1], Magdalena Obazanek-Fojt[1,3], Hyesung Jeon[1,4], Rasa Meskauskiene[1], Hye Min Ham[1,5], Ji Young Kim[1,6], Diana Marcela Pazmiño Mantilla[1,7], Mena Nater[1], Karin Krupinska[2] and Klaus Apel[1,8,9]

[1] Swiss Federal Institute of Technology (ETH) Zürich, Institute of Plant Sciences, Switzerland

[2] Botanisches Institut der Christian-Albrechts-Universität zu Kiel, Germany

Present address:

[3] Department of Dermatology, CHUV, Lausanne, Switzerland

[4] School of Agricultural Biotechnology, Seoul National University, Seoul, Republic of Korea

[5] Kyungpook National University School of Medicine, Daegu, Republic of Korea

[6] Department of Molecular Biology, Pusan National University, Pusan, Republic of Korea

[7] Department of Biochemistry and Molecular and Cellular Biology of Plants, Estacion Experimental del Zaidin (EEZ), Spanish Council for Scientific Research (CSIC)

[8] Boyce Thompson Institute Plant Research, Ithaca, USA

[9] To whom correspondence should be addressed

[10] These authors contributed equally to this work

In preparation

4.1 Abstract

Programmed cell death (PCD) is a genetically controlled physiological process that is of central importance for the development and homeostasis of multicellular organisms. In several instances the execution of PCD involves the participation of mitochondria that act as sensors of cellular stress and initiate the onset of the cell death response. Here, we report the discovery of another form of PCD unique to photosynthetic eukaryotes that implicates chloroplasts rather than mitochondria with being the source and also the target of a cell death signaling pathway.

It leads to a genetically controlled rapid loss of chloroplast integrity and triggers the collapse of the affected cell. In contrast to PCD associated with mitochondria, the plastid-specific PCD is initiated by the release of singlet oxygen that acts in a dose-dependent manner and may induce a rapid suicide of the cell.

4.2 Introduction

Plants are sessile organisms that frequently encounter changes in their environment. One of the first reactions of plants to environmental stress is the enhanced production of chemically distinct reactive oxygen species (ROS) (Apel and Hirt 2004). Chloroplasts have been shown to be major sites of ROS production. The enhanced generation of ROS in these organelles has been attributed to the disturbance of the light-driven photosynthetic electron transport by a large variety of environmental stress factors (Foyer and Noctor 2000). One of the difficulties in elucidating the biological activity of ROS during these stress responses stems from the fact that several ROS with distinct biological activities are generated simultaneously. This problem has been alleviated by using the conditional *flu* mutant of Arabidopsis that allows inducing the production of only one ROS, singlet oxygen ($^1O_2$), within plastids in a non-invasive, controlled manner (op den Camp et al. 2003). The *flu* mutant accumulates excess protochlorophyllide (Pchlide) in the dark that upon illumination acts as a photosensitizer and generates $^1O_2$ (Meskauskiene et al. 2001; op den Camp et al. 2003). Immediately after the release of $^1O_2$ mature *flu* plants stop growing, whereas seedlings bleach and die. We have explored the genetic basis of $^1O_2$-mediated suicide of *flu* seedlings by isolating the *flu/ executer1* double mutant that under non-permissive dark/light conditions generates similar amounts of $^1O_2$ as the parental *flu* line, but in contrast to *flu* behaves like wild type in that seedlings remain viable and do not bleach (Wagner et al. 2004). Enhanced levels of $^1O_2$ within plastids of the *flu* mutant induce also rapid changes in nuclear gene expression (op den Camp et al. 2003; Lee et al. 2007). Inactivation of EXECUTER1 (EX1) attenuated the up-regulation of $^1O_2$-responsive nuclear genes, but did not fully eliminate these changes. A second related nuclear-encoded protein, dubbed EXECUTER2 (EX2), has been shown to be also involved in signaling of $^1O_2$-dependent nuclear gene expression changes (Lee et al. 2007). Like EX1, EX2 is confined to the plastid. The primary function of EX2 seems to be that of a modulator attenuating and controlling the activity of EX1 (Lee et al. 2007). When both EXECUTER proteins are inactive in the *flu/ex1/ex2* triple mutant, most of the $^1O_2$-responsive gene transcripts are close to the wild-type level (Lee et al. 2007). By extending the length of the dark period the photosensitizer Pchlide reaches levels that during illumination are sufficient to cause non-enzymatic peroxidation of polyunsaturated fatty acids and photodamage of chloroplasts, whereas conditions used in our present study support an enhanced enzymatic but not non-enzymatic lipid peroxidation (Przybyla et al. 2008).

4.3 Results

The impact of the *ex1/ex2* mutations on different lipid peroxidation reactions has been used to distinguish between cytotoxic effects of $^1O_2$ and its signaling role. Whereas non-enzymatic lipid peroxidation is not affected, $^1O_2$-mediated enzymatic lipid peroxidation is abolished in the *flu/ex1/ex2* triple mutant (Przybyla et al. 2008) (data not shown). After light-grown seedlings of wild type, *flu, flu/ex1, flu/ex2* and the triple mutant *flu/ex1/ex2* had been transferred to the dark for 4, 8, 12 and 16 h, the frequency of visible lesions in true leaves of *flu* and *flu/ex2* during re-illumination increased steadily with increasing lengths of the dark period (Fig. 4.1A). In the *flu/ex1/ex2* triple mutant and also in the *flu/ex1* double mutant visible cell death responses were completely or almost completely abolished, even though in the dark these mutant lines accumulated similar excess amounts of the photosensitizer Pchlide as *flu/ex2* and only slightly lower amounts than *flu* (Figure 4.1B). Similar results were obtained, when the spreading of cell death in different mutant lines and wild type was visualized by trypan blue staining (Fig. 4.1C).

During the execution of PCD the intactness of chloroplasts was monitored by first expressing the GFP-tagged small subunit of the ribulose-1,5-bisphosphate carboxylase and then determining its intracellular distribution under the confocal scanning microscope before and after the release of $^1O_2$. In all seedlings grown under continuous light or after transfer to the dark the SSU-GFP fusion protein accumulated exclusively within chloroplasts (Supplementary Fig. 4.1). However, in *flu* seedlings that had been subjected to a dark/light shift, chloroplasts started to release the fusion protein to the extraplastidic cytoplasm (Fig. 4.1). A similar re-localization of the SSU protein in the *flu* mutant could also be demonstrated with a tagged antibody against the SSU-subunit and by immunogold labeling (Supplementary Fig. 4.2). Even in *flu* seedlings that were exposed to the dark for only 30 min and did not display any visible cell death response of leaves during re-illumination, chloroplasts started to leak in a few cells (Supplementary Figure 4.2, Supplementary movie). The electrophoretic mobility of the SSU-GFP fusion protein during SDS PAGE and its relative amounts did not change following the release of stroma proteins from the chloroplast to the surrounding cytoplasm (Fig. 4.1E). Chloroplast leakage in *flu* seedlings correlated closely with the onset of cell death as indicated by the staining of cells with propidium iodine. This reagent is excluded from intact viable cells, but penetrates dying or dead cells and intercalates into double stranded nucleic acids (Liu et al. 2007)(Supplementary Fig. 4.3). In contrast to *flu*, the SSU-GFP fusion protein was not released from the plastids of the *flu/ex1/ex2* triple mutant to the surrounding cytoplasm even after 24 h of re-illumination (Supplementary Fig. 4.1).

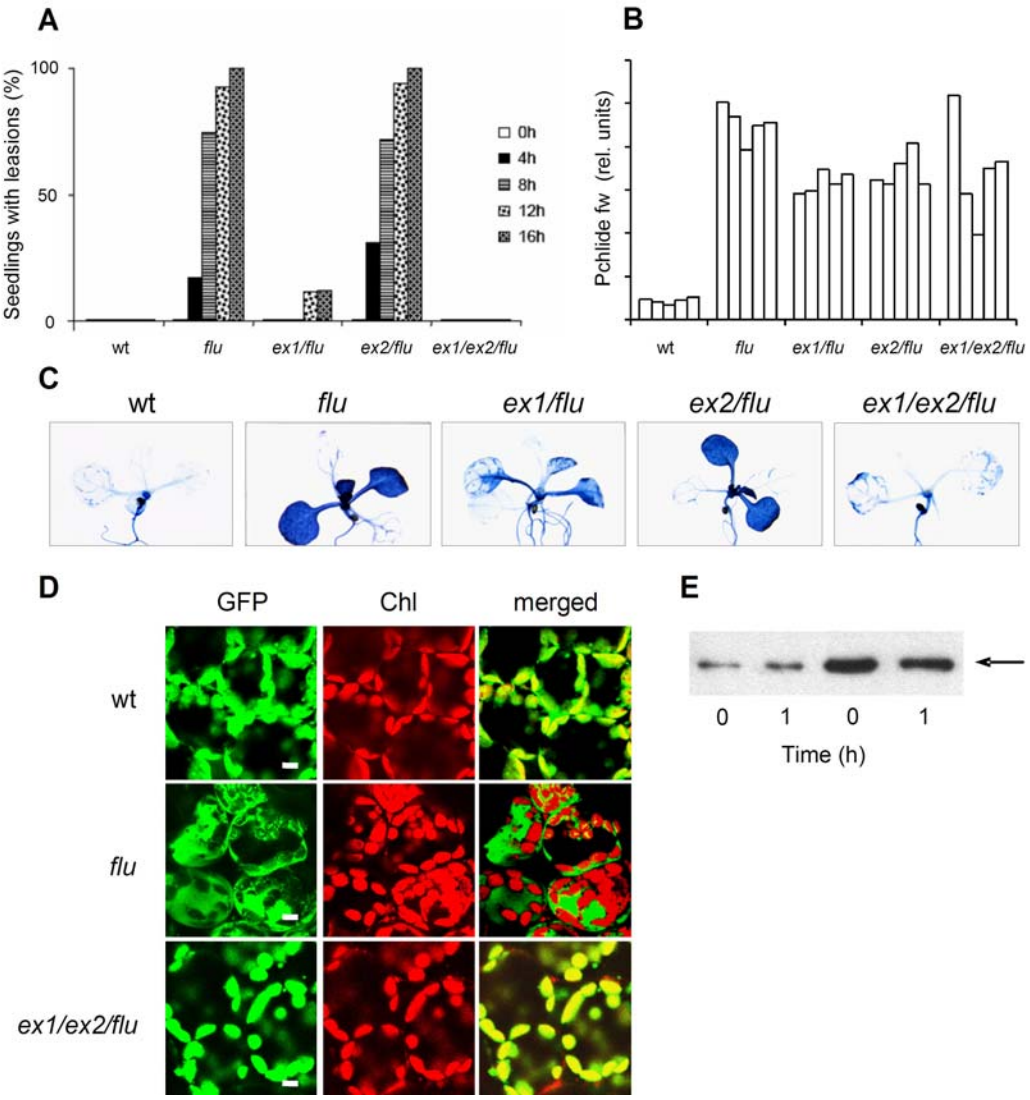

Fig. 4.1. The genetic control of $^1O_2$-mediated cell death. (A) Dose-dependent $^1O_2$-mediated lesion formation in 10 day-old seedlings of wild type, *flu, ex1/flu, ex2/flu* and *ex1/ex2/flu*. Seedlings were grown under continuous light, transferred to the dark for 0, 4, 8, 12 and 16 h and re-exposed to light for 24 h. The number of seedlings with visible lesions relative to the total number of seedlings was used to determine the frequency of lesion formation. A minimum of 100 seedlings were counted per sample. The experiment was repeated three times and gave very similar results. (B) Pchlide levels in seedlings of wild type, *flu*, *ex1/flu*, *ex2/flu* and *ex1/ex2/flu* at the end of a 16 h dark period. For each line 5 pigment extracts from 5 plants each were analyzed. Note that in *ex1/ex2/flu* triple mutants no lesion formation occurred, even though Pchlide reached similar excess levels as in the three other mutant lines (*flu*, *ex1/flu*, *ex2/flu*). (C) The genetic control of cell death as revealed by trypan blue staining of 10- day-old seedlings. Seedlings were treated as described in (A). Note that in cotyledons of 10 day-old *flu* seedlings trypan blue staining was no longer observed. At this developmental stage Pchlide accumulation in cotyledons kept in the dark has ceased. (D) 4-day-old seedlings expressing the SSU-GFP fusion protein were grown under continuous light, shifted to the dark for 8 h and re-exposed to light for 1 h. The green fluorescence of GFP and red fluorescence of Chl were monitored separately by CLSM and the two fluorescence images were merged. In *flu* $^1O_2$-mediated plastid leakage occurred, whereas in the *flu/ex1/ex2* triple mutant leakage was suppressed even though seedlings accumulated similar amounts of the photosensitizer Pchlide as *flu*. (E) During plastid leakage the size and relative concentration of GFP was not detectably altered. Two different concentrations of protein from total seedling extracts (10 and 30 µg per 50 µl) before (0) or 1 h (1) after re-illumination were separated electrophoretically by SDS PAGE, blotted and detected immunologically. As indicated by the arrow, only the full-sized GFP fusion protein was detected using the GFP antiserum. Bars (D): 10 µm.

Collectively, these results suggest that $^1O_2$-mediated leakage of plastids is not due to a direct modification of components of chloroplast envelopes by $^1O_2$. Instead, destabilization of these membranes seems to result more indirectly from $^1O_2$-mediated retrograde signaling from the plastid to the nucleus and changes in the expression of $^1O_2$-responsive genes that ultimately result in the loss of chloroplast integrity. The proposed requirement of nuclear gene expression changes for the $^1O_2$-mediated leakage of plastids was also supported by comparing the impact of $^1O_2$ on plastid integrity in *flu* protoplasts and on chloroplasts isolated from these protoplasts that both had accumulated similar amounts of the photosensitizer Pchlide in the dark (Fig. 4.2A, C). Protoplasts were isolated from light-grown *flu* and wild-type plants that express the SSU-GFP fusion protein. When placed in the dark *flu* protoplasts accumulated excess amounts of Pchlide that upon re-illumination had been shown previously to give rise to $^1O_2$ by energy transfer (op den Camp et al. 2003). At the end of the dark period, SSU-GFP fusion protein was found exclusively within chloroplasts of protoplasts (Fig. 4.2A). However, during re-illumination of *flu* protoplasts, the chloroplast integrity was rapidly lost as indicated by the extensive translocation of the SSU-GFP fusion protein from the chloroplast to the surrounding cytoplasm (Fig. 4.2B, D). In wild-type control protoplasts, chloroplast integrity was largely maintained throughout a re-illumination period of 4 hours (Fig. 4.2B, C). Part of the protoplast preparation was used for the isolation of chloroplasts at the end of the dark incubation. Isolated chloroplasts from *flu* protoplasts contained similar excess amounts of the photosensitizer Pchlide as chloroplasts within the protoplasts (Fig. 4.2F). The total number of intact chloroplasts isolated from *flu* and wild-type control protoplasts declined during incubation in the light, but the intactness of *flu* chloroplasts was not preferentially impaired during this incubation by the release of $^1O_2$ (Fig. 4.2E) . These results provide additional evidence that chloroplast leakage in the *flu* mutant is not caused by a direct reaction of $^1O_2$ with constituents of chloroplast envelope membranes, but results from the $^1O_2$-mediated activation of a PCD signaling pathway that depends on the intactness of the whole cell.

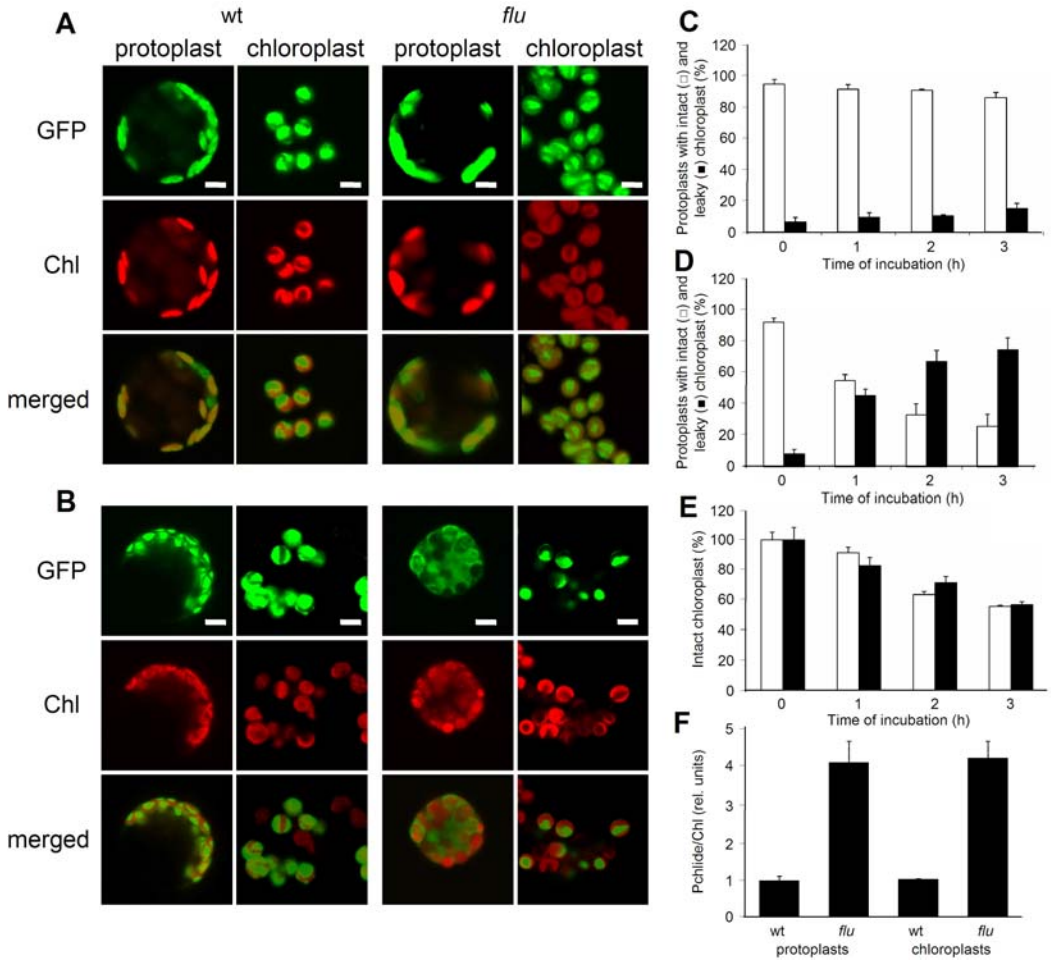

Fig. 4.2. The dependence of $^1O_2$-mediated plastid leakage on the intactness of cells. Protoplasts were isolated from 4-day-old seedlings of wild type and *flu* grown under continuous light by incubating them for 15 h in the dark in the presence of the cellulose/macerozyme digestion medium. The green fluorescence of GFP and the red fluorescence of Chl of protoplasts were monitored before (A) and after (B) light exposure. Protoplasts of wild type (C) and *flu* (D) with intact and leaky chloroplasts were identified and counted under the CLSM at various time points during re-illumination. The values represent the mean and standard deviations of three experiments. A minimum of 50 to 100 protoplasts per 100 µl of suspension were counted. Parts of the original protoplast suspensions kept in the dark were used for the isolation of chloroplasts (A, B, E). Even though protoplasts and chloroplasts of *flu* accumulated similar excess amounts of the photosensitizer Pchlide (F), an enhanced $^1O_2$-mediated plastid leakage occurred only in protoplasts but not in isolated chloroplasts (E). During illumination of isolated pre-darkened chloroplasts of wild type (white bars) and *flu* (black bars) the relative number of intact chloroplasts gradually declined, but no significant differences between the relative number of intact isolated chloroplasts of wild type and *flu* were detected. The values represent the mean and standard deviations of 6 samples. A minimum of 250 chloroplasts were counted per sample. Bars (A, B): 10µm.

A similar chloroplast leakage was shown to occur also in wild-type plants that were subjected to a combined high light/low temperature stress (Fig. 4.3A). Wild-type and *ex1/ex2* seedlings expressing SSU-GFP fusion protein were grown for 6 days at 21° C under continuous low light (12 µmol $m^{-2}s^{-1}$) and were then transferred to a higher light intensity (250 µmol $m^{-2}s^{-1}$) and kept at 12° C rather than at 21° C. Stress responses of seedlings were registered by measuring the maximum quantum efficiency of photosystem II (PSII). At the beginning of the combined high

light/low temperature stress, the Fv/Fm values of wild-type and *ex1/ex2* seedlings were similar (Fig. 4.3C). During the first 24 h of stress treatment, both groups of seedlings suffered similarly from photoinhibition as indicated by the reduction of the Fv/Fm values from 0.86 to 0.6. During the following stress treatment, however, wild-type and *ex1/ex2* seedlings diverged significantly in their stress susceptibility. In non-pretreated wild-type seedlings the maximum efficiency of PSII was further reduced and finally the stress treatment resulted in the bleaching and collapse of seedlings (Fig. 4.3B, D). *ex1/ex2* seedlings, however, remained viable under the same conditions and were not visibly damaged. Trypan blue staining revealed the spreading of cell death in wild-type seedlings five days after the beginning of the combined high light/low temperature treatment, whereas in *ex1/ex2* seedlings cells remained viable and intact (Fig. 4.3B, C). Chloroplast integrity was monitored in green seedlings after 4 days of stress treatment. In *ex1/ex2* seedlings chloroplast integrity had not been impaired, whereas in wild type seedlings most of the fusion protein had been translocated to the extraplastidic cytoplasm (Fig. 4.3A, data not shown).

Under the combined high light/low temperature stress chloroplasts would be expected to enhance not only the generation of $^1O_2$, but also the production of H_2O_2 and superoxide (Foyer and Noctor 2000). The two latter ROS have been shown previously to be involved in triggering a hypersensitive cell death response during plant-pathogen interactions (Liu et al. 2007). To determine which of these ROS triggers the observed plastid leakage in wild-type seedlings during high light/low temperature stress, changes in transcript levels of genes known to be controlled by either $^1O_2$ or H_2O_2 or superoxide were recorded in wild-type and *ex1/ex2* seedlings after different lengths of exposure to stress. Transcript levels of the superoxide-responsive gene *Fe SOD1* and the H_2O_2-responsive gene *Ferritin* (*FER1*) were up-regulated during the first 3 to 4 days of stress treatment and remained constant thereafter (*Fe SOD1*) or declined again (*FER1*) (Fig. 4.3E). These transcript changes were similar in wild type and *ex1/ex2*, supporting the previous finding that H_2O_2/superoxide-dependent retrograde signaling from the plastid to the nucleus does not involve EX1- and EX2-dependent signaling steps (op den Camp et al. 2003; Laloi et al. 2007). Relative to the H_2O_2- and superoxide-dependent up-regulation of genes, activation of the $^1O_2$-responsive marker genes *WRKY33* and *WRKY46* was delayed and started between the third and fourth day of stress treatment shortly before first visible damages of seedlings were detectable. These transcript changes were suppressed in *ex1/ex2* seedlings (Fig. 4.3E). The kinetics of transcript accumulation of different ROS-responsive genes revealed that H_2O_2 and superoxide production preceded the release of singlet oxygen. As the up-regulation of $^1O_2$-responsive genes, but not H_2O_2- or superoxide-responsive genes was

suppressed in *ex1/ex2* and correlated with a similar suppressive effect of *ex1/ex2* on plastid leakage and seedling lethality, these latter stress responses of wild type seem to be under the control of $^1O_2$.

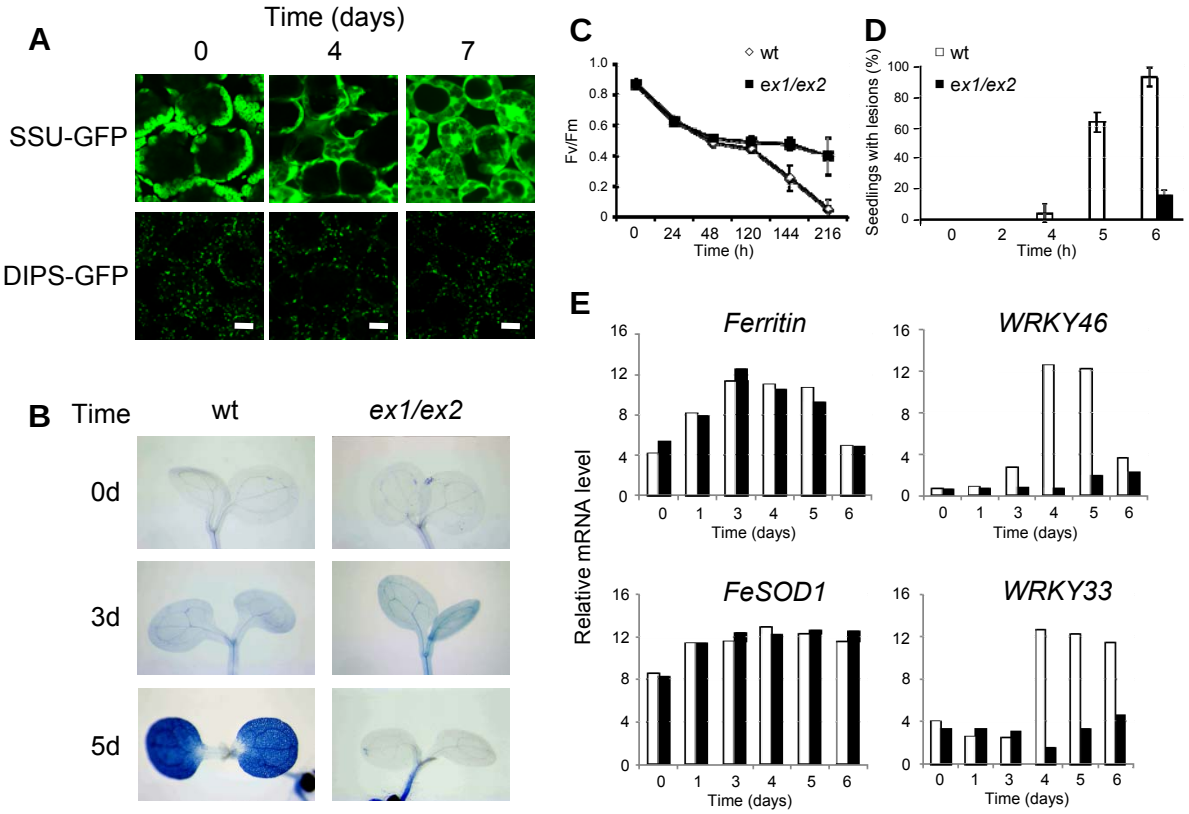

Fig. 4.3. Stress-induced plastid leakage (A), cell death (B), photoinhibition (C), lesion formation (D) and gene expression changes of H_2O_2- (*Ferritin*), superoxide- (*FeSOD1*) and $^1O_2$-responsive (*WRKY43, WRKY33*) genes of wild-type and *ex1/ex2* seedlings (E). Wild-type seedlings were initially grown for 6 days at 21°C and 12 µmol $m^{-2}s^{-1}$ and were then exposed to a combined low temperature (12°C)/high light (250 µmol $m^{-2}s^{-1}$) stress program. (A) Fluorescence images of leaf cells of transgenic seedlings expressing SSU-GFP or DIPS-GFP targeted to plastids and mitochondria, respectively, were taken under the CLSM before (0) or 4 or 7 days during the low temperature/high light stress . Extensive plastid leakage occurred already after 4 days of stress, whereas the fluorescence signal of DIPS-GFP-expressing seedlings was retained within mitochondria throughout the stress treatment. (B) The progression of cell death in wild-type (wt) and *ex1/ex2* seedlings 0, 3 and 5 days after the beginning of stress treatment as revealed by trypan blue staining. (C) Stress-induced decline of the maximum quantum efficiency (Fv/Fm) of wild-type (◇) and *ex1/ex2* (■) seedlings. Values represent the mean and standard deviations of three samples. For each sample 25 seedlings were analyzed. (D) Stress-induced lesion formation of wild-type (white bars) and *ex1/ex2* seedlings (black bars). Values represent the mean and standard deviations of four samples. For each sample 50 seedlings were analyzed. (E) Stress-induced changes in gene expression of *Ferritin, WRKY 46, FeSOD1* and *WRKY33* during 6 days of low temperature/high light treatment of wild-type (white bars) and *ex1/ex2* seedlings (black bars). Results are means of three replicates. Primers used for quantitative RT-PCR of each sample are shown in Table 1. Bars (A): 10 µm.

Previous studies of PCD in plants had shown that prior to the final collapse of cells cellular compartments lose their integrity and undergo structural changes that may, as suggested for mitochondria, reveal an active role of organelles in the initiation of cell death (Yao et al. 2004; Yoshinaga et al. 2005). Either chloroplasts or mitochondria may be the primary target of $^1O_2$-

mediated death signaling and after losing their structural integrity may play a key role in initiating and/or accelerating cell death. We have monitored the structural integrity of mitochondria first by expressing a reporter gene under the control of the 35S-CaMV promoter that encodes the GFP protein with an N-terminal extension of the mitochondria-specific signal sequence of the F1-ATPase delta subunit of Arabidopsis (DIPS) (Sakomoto and Hoshino 2004). Prior to the combined high light/low temperature stress, the GFP protein was confined to the mitochondria (Fig. 4.3A). During the following 7 days of stress treatment the GFP protein was retained within the mitochondria, whereas plastids had lost most of their SSU-GFP protein (Fig. 4.3A). Since it is conceivable that the GFP may still remain trapped inside damaged mitochondria, we also tested permeability changes of mitochondrial membranes by using Mito-tracker Red as a cell-permeable fluorescent probe (Oparka and Reed 1994). To allow a uniform and rapid uptake, protoplasts rather than intact seedlings were incubated with the chemical. To minimize possible artifacts due to the photosensitizing activity of the probe that has been reported to impede the membrane potential of mitochondria and to initiate apoptosis (Minamikawa et al. 1999), the chemical was added only at the very end of the incubation of protoplasts under very dim light conditions and structural changes of chloroplasts and mitochondria were always assessed in comparison to wild-type protoplasts treated in the same way. After 1 h of illumination of pre-darkened protoplasts, addition of Mito-tracker Red revealed that mitochondria remained intact and maintained their membrane potential both in wild type and *flu*, whereas chloroplast integrity of *flu* protoplasts was selectively perturbed (Fig. 4.4).

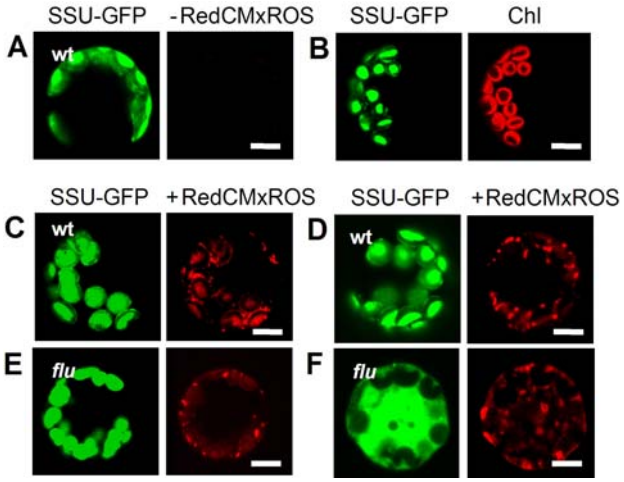

Fig. 4.4. $^1O_2$-mediated changes of chloroplast and mitochondria membrane integrity. Protoplast from 5-day-old light-grown wild-type (wt) (A, C, D) and *flu* seedlings (B, E, F) expressing the SSU-GFP transgene were shifted from the dark (C, E) for 1 h to the light (D, F). Plastid leakage occurred during re-illumination of protoplasts of *flu* (E, F) but not of wild type (C, D). The integrity of mitochondrial membranes was tested under the same conditions with Mito-tracker Red. Membrane integrity was retained during the stress treatment in wild-type and *flu* protoplasts (D, F). Bars: 10 µm.

The reliability of Mito-tracker Red staining was confirmed by co-treatment of protoplasts with cyclosporin A. In the presence of cyclosporine, Mito-tracker Red staining of mitochondria was no longer observed (data not shown). A possible conclusion that one may infer from these results is the coexistence of at least two distinct cell death programs in plant cells that are evoked by a disturbance of mitochondria and chloroplast homeostasis, respectively, and perturb directly only the structural intactness of the affected organelle. We have tested this prediction by expressing the BAX inhibitor (BI) in the *flu* mutant. *BAX* is a well known inducer of cell death in animals and yeast. Suppression of BAX-induced cell death in transgenic plants that over-express a BAX Inhibitor-GFP (AtBI-GFP) fusion protein had been attributed to a selective block of a mitochondrial cell death pathway (Kawai-Yamada et al. 2001) and had been shown to suppress the hypersensitive defense response against pathogens (Huckelhoven et al. 2003). We crossed *flu* with this transgenic line and isolated *flu*/*AtBI-GFP* double mutants. The AtBI-GFP fusion protein was associated with the endoplasmic reticulum (Supplementary Fig. 4.4), whereas $^1O_2$-generation occurred in *flu* chloroplasts. Seedlings of *flu* and *flu/AtBI-GFP* grew like wild type under continuous light, but were severely impaired in their development and showed lesion formation, when they were shifted to the dark for 8 h and re-exposed to light for 5 days. These experiments support our notion that $^1O_2$-mediated cell death is activated by a signaling pathway that operates separately from the mitochondrial cell death pathway and uses chloroplasts, but not mitochondria as a primary target.

4.4 Discussion

Thus far, initiation of most programmed cell death responses has been linked to a disturbance of mitochondrial homeostasis (Jones 2000; Tiwari et al. 2002; Green and Kroemer 2004). Our present study identifies chloroplasts as a source of an additional, plant-specific cell death signaling pathway. Even though in both cases the perturbance of membrane functions seems to play a key role in initiating cell death, mitochondria- and chloroplast-associated cell death signaling are distinct from each other. In mitochondria, superoxide and H_2O_2 modify directly mitochondrial membranes that release cell-death inducing proteins (Green and Reed 1998; Joza et al. 2001; Green and Kroemer 2004). In chloroplasts, leakage of envelope membranes is triggered by singlet oxygen, that first mediates the activation of $^1O_2$-responsive nuclear genes, rather than directly attacking the plastid envelope (op den Camp et al. 2003; Wagner et al. 2004).

If one interprets the evolution of mitochondria-associated cell death programs as a consequence of the invasion of an anaerobic progenitor of present-day eukaryotic cells by aerobic prokaryotes, one may speculate that the chloroplast-associated cell death program may originate from a second, independent endosymbiotic event, in which chloroplasts arose from a cyanobacterial ancestor acquired by a eukaryotic host, in which mitochondria were already established (Koonin and Aravind 2002). Generation of $^1O_2$ in cyanobacteria and plants may occur either within light-harvesting antenna complexes or the reaction centers of PSII. Whereas carotenoids of light-harvesting complexes effectively quench excess light energy and suppress singlet oxygen formation (Niyogi 1999), carotenoids of the reaction center of PSII fail to do so. In an apparent attempt to optimize the efficiency of the photosynthetic electron transport, ß-carotenes bound to the PSII reaction center are localized away from the reaction center P680 Chl (Kamiya and Shen 2003). Hence, $^1O_2$ production seems to be an inherent property of PSII even under low light conditions. The quenching of this ROS has been linked to the turnover of the D1 protein and to tocopherols that are oxidized and in this way act as scavengers of $^1O_2$ (Trebst 2003). Hyper-reduction of the electron transport chain in cells under stress enhances the level of $^1O_2$ that no longer can be fully quenched and may be perceived as a stress signal. During the subjugation of the cyanobacterial endosymbiont, the host cell might have refined by selection the function of this stress signal and subsequently used it to activate a cell death program that targets the chloroplast and impedes its integrity. Signal transfer from the chloroplast to the nucleus is under the control of the two plastid proteins EXECUTER1 and

EXECUTER2 that are highly conserved among all plants, for which genome sequence information is available, but are not present in prokaryotic cyanobacteria.

Our findings may help to explain two other, controversially discussed aspects of nuclear-chloroplast interactions. Tetrapyrrole intermediates have been proposed to act as retrograde signals that coordinate the activities of these two subcellular compartments (Gray 2003; Ankele et al. 2007) by moving out of the chloroplasts and directly regulating nuclear gene expression. Since free tetrapyrroles in light-grown plants act as very potent photosensitizers, it is difficult to understand how they may be exported from the plastid and reach the nucleus without generating $^1O_2$. $^1O_2$–mediated signaling may lead to nuclear gene expression changes that have been previously attributed to a signaling role of tetrapyrroles. Furthermore, $^1O_2$-mediated chloroplast leakage, as reported in the present study, would also impact the physiological relevance of tetrapyrroles reported previously to accumulate within the cytoplasm of seedlings fed with the precursor of tetrapyrroles δ-aminolevulinic acid (Ankele et al. 2007).

During evolution of plants, chloroplast genomes have undergone severe reduction and many genes of the cyanobacterial ancestor of plastids must have been transferred to the nucleus. On an evolutionary time scale, initially these gene transfers have been thought to be very rare events (Martin 2003). Recent work, however, has shown that chloroplast DNA escapes from the plastid and may recombine into nuclear chromosomes at an astonishingly high rate (Huang et al. 2003; Stegemann et al. 2003). The stress-induced leakage of chloroplasts may provide a mechanism that explains how and why so often chloroplast DNA physically may get into the nucleus.

4.5 Materials and Methods

4.5.1 Plant material and growth conditions

All experiments were performed with *Arabidopsis thaliana* ecotype *Columbia* (Col-0). Seeds were surface-sterilized and plated on Murashige and Skoog media with vitamins and 0.8% agar. Seeds were first kept at + 4°C for 4 days in the dark and then grown under continuous light (80 - 100 µmol m^{-2} s^{-1}) at 20 - 21°C. Light was provided by white light tubes (Philips Master TDL 36W, Philips Electronics N.V., Eindhoven, Netherlands and Sylvania Gro Lux F36W, SLI Lichtsysteme GmbH, Erlangen, Germany). In some of the experiments different light regimes were used as described under "Results". The mutants used in this study, *ex1*/*flu*, *ex2*/*flu*, *ex1*/*ex2*/*flu* have been described previously (Lee et al. 2007). Plants expressing the *35S (cauliflower mosaic virus, CaMV)–SSU-GFP* transgene described previously (Kim and Apel 2004) were crossed with *flu*, *ex1*/*flu*, *ex2*/*flu* and *ex1*/*ex2*/*flu* and the resulting double, triple, and quadruple mutants were selected from segregating F2-generations. Arabidopsis (Col 0) seeds expressing the *35S-DIPS-GFP-NOS* (nopaline synthase terminator) (Sakomoto and Hoshino 2004) and *35S-AtBI-GFP-NOS (Kawai-Yamada et al. 2001)* transgenes were kindly provided by W. Sakamoto (Okayama University, Japan), and H. Uchimiya (University of Tokyo, Japan), respectively. *DIPS* encodes the transit peptide of the mitochondrial F1-ATPase delta subunit and *AtBI* is a cDNA encoding the Bax Inhibitor-1 of *Arabidopsis thaliana*. Both transgenic lines were crossed and double mutants were isolated from segregating F2 populations. For the low temperature/high light experiments shown in Fig. 4.3, late embryogenesis of *ex1/ex2* and wild-type controls occurred in siliques that were kept in the dark by covering them with aluminum foil for 4 days prior to the onset of seed dormancy to ensure proper seed germination and seedling development of *ex1/ex2* (Lee et al., in preparation).

4.5.2 Confocal laser scanner microscopic (CLSM) analysis

The green fluorescence of GFP and the red fluorescence of Chl were monitored simultaneously using a confocal laser scanning microscope (TCS-NT; Leica, Heidelberg, Germany) with Kr/Ar laser excitation. GFP and Chl fluorescence were induced at an excitation wavelength of 488 nm. GFP and Chl were detected at fluorescence emission wavelengths of 507–520 nm and 620–700 nm, respectively. The TCS-NT software version 1.6.587 (Leica Microsystems) and Adobe Photoshop 5.5 (Adobe Systems, Inc., San Jose, CA, USA), respectively, were used for image acquiring and processing.

4.5.3 Protein analysis

Seedlings of *flu/SSU-GFP* double mutants were grown for 4 days under continuous light, transferred to the dark for 8 h and re-exposed to light for 1 h. Total protein was extracted with 20 mM Tris, pH 7.5, 10% (v/v) glycerol, 1 mM DTT, 1 mM phenylmethylsulfonyl fluoride and 0.5% Triton X-100 from seedlings at the end of the dark period and after re-illumination. Ten or thirty microgram of protein per sample was used for SDS PAGE and immunoblotting. An *HRP*-conjugated GFP antibody (Clontech) was used for the detection of SSU-GFP fusion proteins at a 1:10000 dilution. The detection assay (Immun-Star HRP, Bio-Rad) was based on chemi-luminescence.

4.5.4 $^1O_2$-mediated lesion formation

10-day-old seedlings (wt, *flu*, *ex*/*flu*, *ex2*/*flu*, and *ex1*/*ex2*/*flu*) kept under continuous light were transferred to the dark for various lengths of time and re-exposed to light for 24 h. Lesion formation was examined under a stereo microscope. The number of plants with white patches relative to the total number of plants was used to calculate the frequency of lesion formation.

4.5.5 Determination of cell death

Trypan blue staining (Keogh et al. 1980) was performed as described(Mauch-Mani and Slusarenko 1996). Seedlings were harvested and boiled in the staining solution for 2 min and left in the solution for 4 h at room temperature. They were then de-stained in chloral hydrate for 4 and 24 h. Seedlings were stored under 50% glycerol and examined under a Zeiss Axiophot microscope (Oberkochen, Germany). Propidium iodide (PI) staining and scanning was conducted with wild-type and *flu/SSU-GFP* seedlings after an 8 h dark to 1 h light transition and GFP/PI dual stained seedlings were examined under the confocal microscope. The DNA and PI complexes were visualized at an excitation wavelength of 488 nm and an emission wavelength of 610-620 nm (Zhang et al. 2003).

4.5.6 Low temperature/high light stress treatment

Wild-type and *ex1*/*ex2* seedlings were grown under continuous light at 12 µmol $m^{-2}s^{-1}$ for 6 days in E-66HO/2 growth chambers (Percival Scientific, Inc., Perry, Iowa, USA) equipped with compact fluorescent lamps F55BX/840 (GE Lighting AG, Zurich, Switzerland). At the end of the low light treatment, the Fv/Fm values of seedlings were recorded. The light intensity was then raised to 250 µmol m^{-2} s^{-1} and the temperature was reduced to 12°C. The effects of this low temperature/high light stress treatment were examined daily for up to 7 days. Chlorophyll a

fluorescence measurements were done with a closed FluorCam System (Photon Systems Instruments, Brno, Czech Republic) with a sample chamber containing a CCD video camera and an irradiation system. The maximum quantum efficiency of PSII was calculated using standard quenching analysis protocols provided by Photon Systems Instruments. Cell death responses were examined with Trypan Blue (TB) staining.

4.5.7 Extraction and measurement of Pchlide

Total Pchlide was extracted with 90% acetone/10% 0.1 M NH_4OH in water. Relative amounts of Pchlide were determined as previously described (Kim and Apel 2004).The relative units were normalized either per fresh weight of seedlings with five independent biological replicas or per chlorophyll content with three replicas.

4.5.8 RNA extraction and RT-PCR

Total RNA was extracted from seedlings by using an RNeasy plant mini kit (Qiagen, Hilden, Germany). cDNA was synthesized from 0.7*μg* of RNA, treated with DNase (Promega) by using oligo(dT)15 primers (Promega) and Improm II reverse transcriptase (Promega) according to the manufacturer's instructions. RT-PCR was performed with equal amounts of cDNAs by using the GeneAmp® PCR system 9700 (Applied Biosystems, Foster City, CA, USA). *WRKY33* and *WRKY46* were selected as early singlet-oxygen responsive genes (Lee et al. 2007) (GEO accretion number for microarray data, GSE10509; http://www.ncbi.nlm.nih.gov/geo/query/). *FeSOD1* and *Ferritin*, were selected as superoxide- and hydrogen peroxide-specific genes, respectively. Primer sequences for the selected genes are shown in Table I.

Table 4.1. List of selected genes and sequences of the primer

Common name	Forward Primer	Reverse Primer
WRKY33	5'- GAAACAAATGGTGGGAATGG-3'	5'- TGTCGTGTGATGCTCTCTCC -3'
WRKY46	5'- CATCCTTAAGCGAAGCCTTG -3'	5'- TCGATGCGTGCATCTGTAAT-3'
FeSOD1(*FSD1*)	5'- GAGCCGCATATGAGCAAACAAA-3'	5'- AGCCGAGCACAAGGGGATTCA-3'
Ferritin	5' -CGTTCACAAAGTGGCCTCAG-3'	5'- CAAACTCCGTGGCCTTTGC-3'
Profilin1	5'- AGAGCGCCAAATTTCCTCAG-3'	5'- CCTCCAGGTCCCTTCTTCC-3'

4.5.9 The isolation of protoplasts and chloroplast

All procedures were carried out in the dark or under green safe light conditions, unless mentioned otherwise. *Arabidopsis* protoplasts were isolated from 4-day-old seedlings grown on half strength MS solid medium under continuous light (70-80 µmol $m^{-2}sec^{-1}$) by harvesting seedlings and incubating them for 15 h in the dark in the presence of the digestion medium (0.4 M mannitol, 1% cellulase, 0.25% macerozyme, 8mM $CaCl_2$ 0.1% MES, pH 5.8). By the end of 15 h incubation period, free protoplasts were isolated as previously described (Danon et al. 2005). After washing protoplasts with W5A medium, they were resuspended in culture medium (half strength MS, 0.4M mannitol, 0.4M glucose, 0.1% MES pH 5.7). At time "0", aliquots were taken from the protoplast suspension prior to illumination (70 µmol $m^{-2}sec^{-1}$). During illumination aliquots were removed every hour and protoplasts were counted and examined under the confocal microscope. For chloroplast isolation, protoplasts were resuspended in resuspension buffer (400mM sorbitol, 20mM MES-KOH pH 6, 0.5mM $CaCl_2$), centrifuged again at 60 x *g* and suspended in 300mM sorbitol, 20mM Tricine-KOH pH 8.4, 10mM EDTA, 10mM $NaHCO_3$, 0.1% BSA. Chloroplasts were ruptured by pressing them with a 10ml syringe through a 20- and 10 µM- nylon mesh (from Sefar AG, Switzerland). This rupturing step was repeated and the ruptured protoplasts were centrifuged at 60 x *g* and resuspended either in culture medium to monitor the intactness of chloroplasts or in 90% acetone to extract the pigments. Protoplasts with intact or leaky chloroplasts were counted under the confocal microscope. Three biological replicas (50-100 protoplasts/100µl of cultures) were used for this experiment. In parallel, the number of chloroplasts with a SSU-GFP signal relative to the total number of chloroplasts was determined for each sample from 6 individual images covering 500 μm^2 of the confocal microscopic field. For pigment analysis by HPLC, the protoplast/chloroplast pellets were resuspended in 90% acetone, and kept at 4^0C overnight in the dark to facilitate complete extraction of pigments. The number of protoplasts taken for HPLC was normalized based on the total chlorophyll content of each protoplast sample.

4.5.10 Qualitative analysis of the mitochondrial membrane potential by Mito-tracker Red treatment

Mitochondrial membrane potentials of wild-type and *flu/SSU-GFP* protoplasts were monitored by using Mito-tracker Red CMX-ROS (lyophilized solid from Molecular probes™, Invitrogen™) before and after the release of singlet oxygen. The Mito-tracker was kept as a 1mM stock solution in DMSO. Aliquots of the stock solution were added to the protoplast culture immediately before the beginning of the scanning to reach a final concentration of 500 nM. Mito-

tracker signals were visualized with an excitation at 578 nm and an emission of 590–620 nm. The entire experiment was performed three times, providing independent biological replicates.

4.6 Acknowledgements

We are grateful to Drs. W. Sakamoto (Okayama University) and H. Uchimiya (University of Tokyo) for providing seeds of transgenic Arabidopsis (Col-0) expressing *35S-DIPS-GFP-NOS* and *35S-AtBI-GFP-NOS*, respectively. We are indebted to Dr. Dieter Rubli for art work, to André Imboden for taking care of plants, and to Drs. Christophe Laloi, Teresa Fitzpatrick, Frank Landgraf and Klara Simkova for helpful discussions during the completion of the manuscript. This study was supported by the Swiss Federal Institute of Technology and the Swiss National Science Foundation.

4.7 References

Ankele, E., Kindgren, P., Pesquet, E., and Strand, A. 2007. In vivo visualization of Mg-protoporphyrin IX, a coordinator of photosynthetic gene expression in the nucleus and the chloroplast. *Plant Cell* 19(6): 1964-1979.

Apel, K. and Hirt, H. 2004. Reactive oxygen species: metabolism, oxidative stress, and signal transduction. *Annu Rev Plant Biol* 55: 373-399.

Blackstone, N.W. and Green, D.R. 1999. The evolution of a mechanism of cell suicide. *Bioessays* 21(1): 84-88.

Danon, A., Miersch, O., Felix, G., Camp, R.G., and Apel, K. 2005. Concurrent activation of cell death-regulating signaling pathways by singlet oxygen in *Arabidopsis thaliana*. *Plant J* 41(1): 68-80.

Foyer, C.H. and Noctor, G. 2000. Oxygen processing in photosynthesis: regulation and signalling. *New Phytologist* 146(3): 359-388.

Gray, J.C. 2003. Chloroplast-to-nucleus signalling: a role for Mg-protoporphyrin. *Trends Genet* 19(10): 526-529.

Green, D.R. and Kroemer, G. 2004. The pathophysiology of mitochondrial cell death. *Science* 305(5684): 626-629.

Green, D.R. and Reed, J.C. 1998. Mitochondria and apoptosis. *Science* 281(5381): 1309-1312.

Huang, C.Y., Ayliffe, M.A., and Timmis, J.N. 2003. Direct measurement of the transfer rate of chloroplast DNA into the nucleus. *Nature* 422(6927): 72-76.

Huckelhoven, R., Dechert, C., and Kogel, K.H. 2003. Overexpression of barley BAX inhibitor 1 induces breakdown of mlo-mediated penetration resistance to Blumeria graminis. *Proc Natl Acad Sci U S A* 100(9): 5555-5560.

Jones, A. 2000. Does the plant mitochondrion integrate cellular stress and regulate programmed cell death? *Trends Plant Sci* 5(5): 225-230.

Joza, N., Susin, S.A., Daugas, E., Stanford, W.L., Cho, S.K., Li, C.Y., Sasaki, T., Elia, A.J., Cheng, H.Y., Ravagnan, L., Ferri, K.F., Zamzami, N., Wakeham, A., Hakem, R., Yoshida, H., Kong, Y.Y., Mak, T.W., Zuniga-Pflucker, J.C., Kroemer, G., and Penninger, J.M. 2001. Essential role of the mitochondrial apoptosis-inducing factor in programmed cell death. *Nature* 410(6828): 549-554.

Kamiya, N. and Shen, J.R. 2003. Crystal structure of oxygen-evolving photosystem II from Thermosynechococcus vulcanus at 3.7-A resolution. *Proc Natl Acad Sci U S A* 100(1): 98-103.

Kawai-Yamada, M., Jin, L., Yoshinaga, K., Hirata, A., and Uchimiya, H. 2001. Mammalian Bax-induced plant cell death can be down-regulated by overexpression of Arabidopsis Bax Inhibitor-1 (AtBI-1). *Proc Natl Acad Sci U S A* 98(21): 12295-12300.

Keogh, R.C., Deverall, B.J., and Mcleod, S. 1980. Comparison of histological and physiological-responses to Phakopsora-Pachyrhizi in resistant and susceptible soybean. *T Brit Mycol Soc* 74(Apr): 329-333.

Kim, C. and Apel, K. 2004. Substrate-dependent and organ-specific chloroplast protein import in planta. *Plant Cell* 16(1): 88-98.

Koonin, E.V. and Aravind, L. 2002. Origin and evolution of eukaryotic apoptosis: the bacterial connection. *Cell Death Differ* 9(4): 394-404.

Laloi, C., Stachowiak, M., Pers-Kamczyc, E., Warzych, E., Murgia, I., and Apel, K. 2007. Cross-talk between singlet oxygen- and hydrogen peroxide-dependent signaling of stress responses in *Arabidopsis thaliana*. *Proc Natl Acad Sci U S A* 104(2): 672-677.

Lee, K.P., Kim, C., Landgraf, F., and Apel, K. 2007. EXECUTER1- and EXECUTER2-dependent transfer of stress-related signals from the plastid to the nucleus of *Arabidopsis thaliana.* *Proc Natl Acad Sci U S A* 104(24): 10270-10275.

Liu, Y., Ren, D., Pike, S., Pallardy, S., Gassmann, W., and Zhang, S. 2007. Chloroplast-generated reactive oxygen species are involved in hypersensitive response-like cell death mediated by a mitogen-activated protein kinase cascade. *Plant J* 51(6): 941-954.

Martin, W. 2003. Gene transfer from organelles to the nucleus: frequent and in big chunks. *Proc Natl Acad Sci U S A* 100(15): 8612-8614.

Mauch-Mani, B. and Slusarenko, A.J. 1996. Production of salicylic acid precursors is a major function of phenylalanine ammonia-lyase in the resistance of Arabidopsis to *Peronospora parasitica*. *Plant Cell* 8(2): 203-212.

Meskauskiene, R., Nater, M., Goslings, D., Kessler, F., op den Camp, R., and Apel, K. 2001. FLU: a negative regulator of chlorophyll biosynthesis in *Arabidopsis thaliana*. *Proc Natl Acad Sci U S A* 98(22): 12826-12831.

Minamikawa, T., Sriratana, A., Williams, D.A., Bowser, D.N., Hill, J.S., and Nagley, P. 1999. Chloromethyl-X-rosamine (MitoTracker Red) photosensitises mitochondria and induces apoptosis in intact human cells. *J Cell Sci* 112 (Pt 14): 2419-2430.

Niyogi, K.K. 1999. PHOTOPROTECTION REVISITED: Genetic and Molecular Approaches. *Annu Rev Plant Physiol Plant Mol Biol* 50: 333-359.

op den Camp, R.G., Przybyla, D., Ochsenbein, C., Laloi, C., Kim, C., Danon, A., Wagner, D., Hideg, E., Gobel, C., Feussner, I., Nater, M., and Apel, K. 2003. Rapid induction of distinct stress responses after the release of singlet oxygen in Arabidopsis. *Plant Cell* 15(10): 2320-2332.

Oparka, K.J. and Reed, N.D. 1994. *The use of fluorescent probes for studies of living plant cells* IRL Press, Oxford University, UK, Oxford.

Przybyla, D., Gobel, C., Imboden, A., Hamberg, M., Feussner, I., and Apel, K. 2008. Enzymatic, but not non-enzymatic, $^1O_2$-mediated peroxidation of polyunsaturated fatty acids forms part of the EXECUTER1-dependent stress response program in the flu mutant of *Arabidopsis thaliana*. *Plant J* 54(2): 236-248.

Sakomoto, W. and Hoshino, T. 2004. An approach to screen mitochondrial mutants in *Arabidopsis thaliana*. *Endocytobiosis Cell Res* 15(1): 101-109.

Stegemann, S., Hartmann, S., Ruf, S., and Bock, R. 2003. High-frequency gene transfer from the chloroplast genome to the nucleus. *Proc Natl Acad Sci U S A* 100(15): 8828-8833.

Tiwari, B.S., Belenghi, B., and Levine, A. 2002. Oxidative stress increased respiration and generation of reactive oxygen species, resulting in ATP depletion, opening of mitochondrial permeability transition, and programmed cell death. *Plant Physiol* 128(4): 1271-1281.

Trebst, A. 2003. Function of beta-carotene and tocopherol in photosystem II. *Z Naturforsch [C]* 58(9-10): 609-620.

Wagner, D., Przybyla, D., Op den Camp, R., Kim, C., Landgraf, F., Lee, K.P., Wursch, M., Laloi, C., Nater, M., Hideg, E., and Apel, K. 2004. The genetic basis of singlet oxygen-induced stress responses of *Arabidopsis thaliana*. *Science* 306(5699): 1183-1185.

Yao, N., Eisfelder, B.J., Marvin, J., and Greenberg, J.T. 2004. The mitochondrion--an organelle commonly involved in programmed cell death in *Arabidopsis thaliana*. *Plant J* 40(4): 596-610.

Yoshinaga, K., Arimura, S.I., Hirata, A., Niwa, Y., Yun, D.J., Tsutsumi, N., Uchimiya, H., and Kawai-Yamada, M. 2005. Mammalian Bax initiates plant cell death through organelle destruction. *Plant Cell Rep* 24(7): 408-417.

Zhang, C., Czymmek, K.J., and Shapiro, A.D. 2003. Nitric oxide does not trigger early programmed cell death events but may contribute to cell-to-cell signaling governing progression of the Arabidopsis hypersensitive response. *Mol Plant Microbe Interact* 16(11): 962-972.

Supplementary Materials

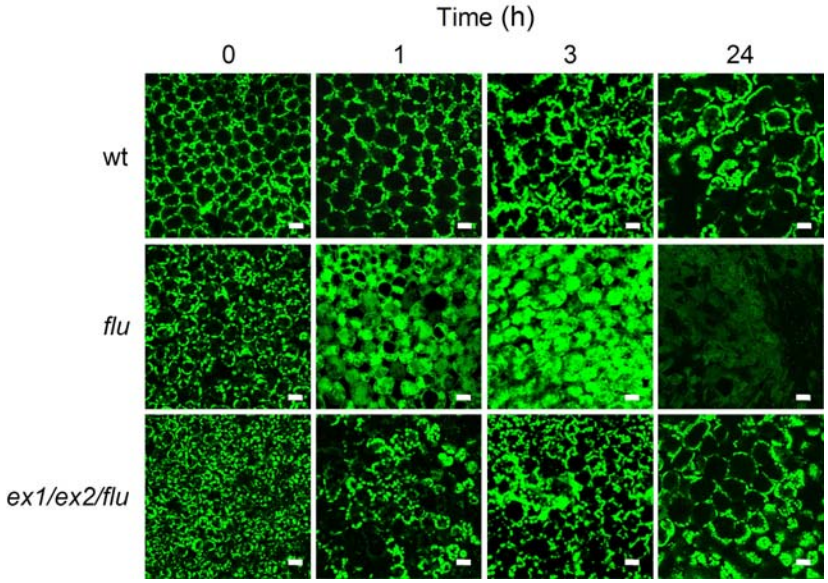

Supplementary Fig. 4.1. $^1O_2$-mediated plastid leakage. *flu*, *ex1/ex2/flu* and wild-type seedlings expressing the ribulose-1.5-bisphosphate carboxylase small subunit (SSU)-GFP fusion protein were shifted from continuous light to the dark for 8 h and re-illuminated for various lengths of time. Immediately before the onset of re-illumination larger amounts of SSU-GFP had accumulated in all three lines and were confined to chloroplasts (0). After 1 h of re-illumination most of the SSU-GFP had already been released to the cytosol in the *flu* mutant, whereas in the triple mutant the SSU-GFP was retained within chloroplasts throughout 24 h of re-illumination, similar to wild type. Bars: 30µm

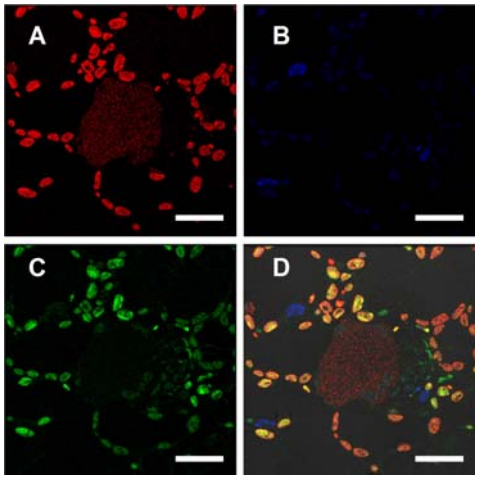

Supplementary Fig. 4.2. Immunological localization of SSU during $^1O_2$-mediated plastid leakage in light-grown *flu* seedlings after a 1h dark/1h re-illumination treatment. A) Distribution of red fluorescent anti-SSU. B) DAPI-staining of DNA. C) Autofluorescence of GFP. D) Merger of all three images. Arrows mark a single collapsed cell. Bars: 15µm

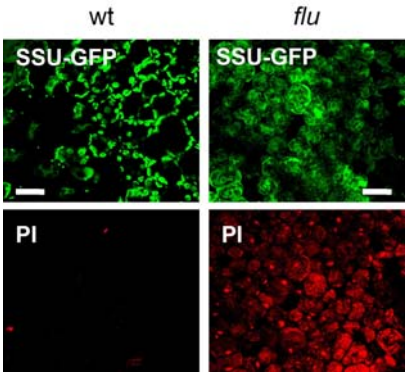

Supplementary Fig. 4.3. $^1O_2$-mediated cell death in seedlings expressing the SSU-GFP fusion protein. *flu* and wild-type seedlings were grown under continuous light, shifted to the dark for 8 h and re-exposed to light for one hour. Plastid leakage occurred in *flu* but not in wild-type seedlings. Similarly, staining of seedlings with propidium iodide (PI) revealed cell death by cellular PI up-take and its intercalation into double-stranded DNA, whereas PI is excluded from viable cells of wild-type controls. Bars: 30 µm.

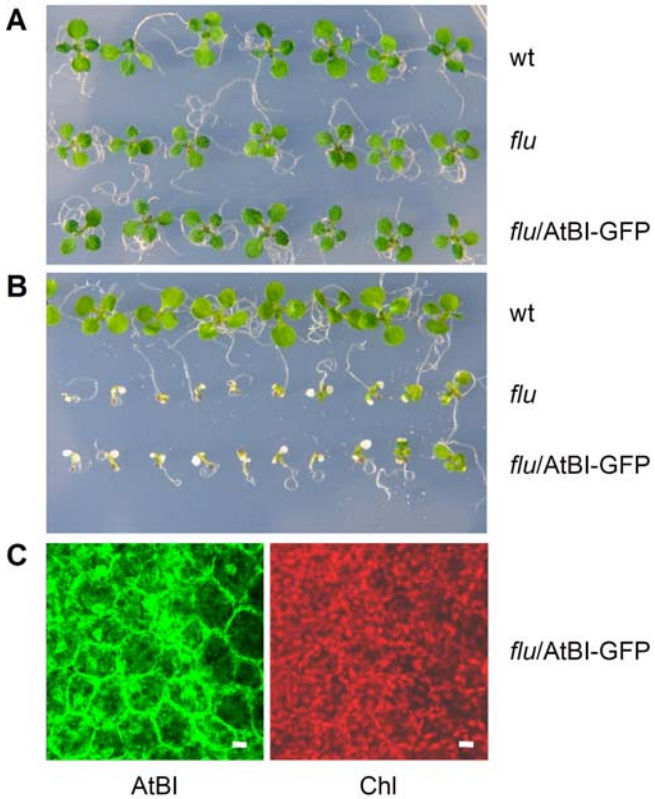

Supplementary Fig. 4.4. Distinction between $^1O_2$-mediated and BAX-induced cell death in Arabidopsis seedlings. *flu* seedlings that over-express a BAX-inhibitor (AtBI)-GFP fusion protein and *flu* and wild-type seedlings were grown under continuous light (A) or shifted to the dark for 8 h and re-exposed to light for 48 h (B). Expression of AtBI-GFP had previously been shown to inhibit the onset of BAX-induced cell death in Arabidopsis seedlings. However, $^1O_2$-mediated cell death in *flu* seedlings was not detectably affected by *AtBI-GFP* expression (B). (C) AtBI-GFP was outside of chloroplasts (Chl) and associated with the endoplasmic reticulum. Bars (C): 10 µm

5. General conclusions

Abiotic stress conditions such as high light, high or low temperatures, drought, high or low salt, or nutrient stress, may limit the ability of a plant to use light energy for photosynthesis. Under such stress conditions hyper-reduction of the photosynthetic electron transport chain and photo-inhibition may occur even at moderate light intensities, often causing a reduction in the growth and productivity of the plant.

The emergence of these stress symptoms has been closely associated with the enhanced production of chemically distinct reactive oxygen species (ROS) (Apel and Hirt 2004). However, it is not clear, whether the biological activity of ROS is the result of its cytotoxic effect or reflects the more indirect role of a second messenger that signals further cellular responses, or both (Dangl et al. 1996). Because different ROS are generated almost simultaneously and in different subcellular compartments, it is difficult to determine the biological activity and mode of action of each of these ROS separately. In order to address this problem, the conditional *flu* mutant of *Arabidopsis*, which generates singlet oxygen in plastids during a dark-to-light transition, has been used to study the biological activity of singlet oxygen and to distinguish between cytotoxicity and signaling of this ROS. To be able to further study the biological activity of singlet oxygen, the research described in this thesis was mainly focused on elucidating the function of EXECUTER1 and EXECUTER2 that are required for transmitting singlet oxygen-dependent signals from the plastid to the nucleus.

Generation of singlet oxygen rapidly occurs in the chloroplasts of the *flu* mutant after a dark-to-light shift, due to the overaccumulation of the photosensitizer Pchlide in the dark. Immediately after the release of singlet oxygen, mature *flu* plants stop growing, while seedlings bleach and die (op den Camp et al. 2003). This genetic stress program has been analyzed by mutagenizing *flu* a second time and identifying second site mutations that suppress seedling lethality and growth inhibition of mature plants. Inactivation of a single gene, *EXECUTER1 (EX1)*, is sufficient to abrogate both of these stress reactions in *flu* (Wagner et al. 2004). After the *ex1/flu* double mutant had been complemented with the wild-type copy of *EX1*, seedlings died again under non-permissive light/dark cycles like seedlings of the parental *flu* line, whereas seedlings of plants transformed with control DNA continued to be unaffected by the release of $^1O_2$ and grew like *ex1/flu* seedlings. Mature *ex1/flu* double mutant plants initially grown under continuous light were not visibly affected by a shift to light/dark cycles and continued to grow like wild-type plants, whereas *ex1/flu* plants complemented with the *EX1* wild-type copy ceased their growth and their

leaves developed necrotic lesions similar to the response of the parental *flu* line. Both experiments show that bleaching of *flu* seedlings and growth inhibition and lesion formation of mature *flu* plants cannot be ascribed to photooxidative damage by singlet oxygen, but instead reflect the $^1O_2$-mediated activation of genetically controlled response programs that require the activity of the *EX1* gene.

Enhanced levels of $^1O_2$ within plastids of the *flu* mutant that trigger drastic phenotypic changes would be expected to modulate nuclear gene expression as well. Indeed, within the first 30 min after the release of $^1O_2$ rapid changes in nuclear gene expression occur (op den Camp et al. 2003). Inactivation of the plastid protein EX1 attenuated the upregulation of $^1O_2$-responsive nuclear genes, but did not fully eliminate these changes. This result suggests that other signaling pathways may exist that respond to $^1O_2$ in an EX1-independent manner. A second related nuclear-encoded protein, dubbed EXECUTER2 (EX2), has been identified that also appears to be implicated with the signaling of $^1O_2$-dependent nuclear gene expression changes. Like EX1, EX2 is confined to the plastid. Upon inactivation of EX2 in the *flu* mutant, additional $^1O_2$-responsive genes emerge and genes that were already up-regulated in *flu* are either further stimulated or down-regulated. In the absence of EX1, EX2 has only a relatively minor effect on the expression of $^1O_2$-responsive genes. Thus, the primary function of EX2 seems to be that of a modulator attenuating and controlling the activity of EX1. Only when both EXECUTER proteins are inactive is the up-regulation of the vast majority of $^1O_2$-responsive genes abolished. It is not clear yet whether EX1 and EX2 act independently or do physically interact with each other (**Chapter 2**).

Activation of seedling lethality and growth inhibition in mature plants as seen in *flu* have not been reported to occur in wild-type plants even under conditions that would be expected to stimulate the release of $^1O_2$. EX1 and EX2 are highly conserved among all higher plants for which sequence data are available. The conservation of these genes points to an essential function of the two EXECUTER proteins that must offer some benefits to the plant. EX1- and EX2-dependent signaling of stress responses in wild-type plants seems to form an integral part of a complex stress-related signaling network and to be subject to modulation by other signaling pathways that weaken the extreme consequences of $^1O_2$-signaling as seen in the *flu* mutant. The analysis of the biological function of EX1 and EX2 in a wild-type background has been described in **Chapter 3**.

When grown under continuous light (100 µE $m^{-2}sec^{-1}$), cotyledons of the *ex1*/*ex2* double mutant are unable to green. This phenotype is not seen in single *ex1* or *ex2* mutant lines. As this

phenotype is also detected in seedlings of *ex1*/*ex2* grown at a lower light intensity (10 µE $m^{-2}sec^{-1}$) the impairment of chlorophyll accumulation does not seem to be due to an enhanced sensitivity of the double mutant to light stress that might cause the bleaching of cotyledons. Instead, suppression of chlorophyll accumulation in *ex1*/*ex2* seedlings can be attributed to the disruption of normal plastid development. Indeed, in seedlings of the *ex1/ex2* double mutant, chloroplast formation was severely disturbed. However, all these deficiencies were observed in cotyledons, but not in true leaves of the mutant. These results indicate that $^1O_2$-mediated signaling may be involved in controlling plastid development during early seedling development.

Interestingly, even though the generation of $^1O_2$ in plastids by energy transfer occurs under aerobic conditions only in the light (Apel and Hirt 2004; Krieger-Liszkay 2005), plastid development is arrested not only in light-grown but also in etiolated seedlings of *ex1*/*ex2*. Therefore, an *EX1* and *EX2*-dependent signaling pathway controlling plastid development must occur during embryogenesis prior to seedling development, while embryos are still exposed to light. Since the chlorophyll contents and the size distributions of chloroplasts during early embryogenesis in wild type and ex1/ex2 mutant plants grown under continuous light were indistinguishable the impact of the *ex1/ex2* mutations on plastid differentiation is likely to be confined to a short period during late embryogenesis just prior to the onset of seed dormancy when developmental changes are expected to enhance the release of free chlorophyll and the formation of chlorophyll catabolites, both potent photosensitizers that in the light generate singlet oxygen.

Using the reporter system described in Chapter 3 in wild-type plants, generation of $^1O_2$ was assessed noninvasively at four different stages of embryogenesis, four days after anthesis (DAA) during the morphogenetic phase (“pale”), seven DAA when embryos start to green and develop functional chloroplasts (“pale-green”), thirteen DAA with embryos accumulating storage reserves and having fully developed photoheterotrophic chloroplasts (“green”), and eighteen DAA when seed coats are no longer transparent but turn brownish (“brown”). In *AAA:LUC* wild-type plants grown under continuous light, only “green” seeds showed luciferase activity. When these seeds were shifted to the dark for four hours prior to the luciferase assay, the activity in “green” seeds had vanished, suggesting that luciferase activity in immature wild-type seeds depends on the generation of $^1O_2$ that occurs only in the light by energy transfer from excited photosensitizing pigments onto oxygen..

As $^1O_2$ production starts to occur first in “green” seeds of wild-type plants, $^1O_2$-mediated and EX1- and EX2-dependent signaling should affect gene expression only during late stages of seed development. During early embryogenesis, inactivation of EX1 and EX2 had almost no

detectable effect on the expression of nuclear genes, whereas during late embryogenesis the expression of a small group of genes was affected by these mutations. Only few of these genes had previously been found among the $^1O_2$-responsive genes expressed in leaves of the *flu* mutant (op den Camp et al. 2003).

Since generation of $^1O_2$ during embryogenesis occurs only in the light, the proposed impact of $^1O_2$-mediated signaling on plastid differentiation in seedlings should be suppressed not only by inactivation of EX1 and EX2 that blocks $^1O_2$-mediated plastid signaling, but also by keeping developing seeds away from light to prevent $^1O_2$ production. Contrary to what was predicted, proplastid differentiation in wild-type seedlings derived from seeds that had been transferred to the dark during embryogenesis to prevent $^1O_2$ production was not disturbed. However, plastid differentiation in *ex1/ex2* seedlings derived from seeds transferred to the dark during their development was no longer impaired, very much in contrast to the arrest of proplastid differentiation in seedlings derived from seeds of the same plant that had developed under continuous illumination. Collectively, these data indicate that in light-grown plants lacking EX1 and EX2 proteins generation of $^1O_2$ prior to seed dormancy results in the severe disturbance of plastid formation during seedling development, while maintenance of EX1/EX2-dependent signaling in these plants suppresses this negative impact of $^1O_2$. In immature seeds transferred to the dark, however, $^1O_2$ production does not occur and plastid differentiation during post-embryonic development is not impaired regardless of the genetic background of the seeds. Changes during late embryogenesis that impact plastid differentiation in seedlings and that are associated with the light-dependent release of $^1O_2$ seem to be controlled by two different signaling routes. One proceeds independently of EX1 and EX2 and impedes plastid differentiation during postembryonic development, whereas the second signaling pathway depends on EX1 and EX2 and suppresses the negative impact of the former signaling on plastid differentiation. This seemingly complex interaction of two opposing signaling events may help the plant to coordinate and separate two conflicting developmental steps that take place during late embryogenesis in the same cell, chloroplast disintegration and chlorophyll catabolism on the one hand, and the conservation and protection of proplastids on the other. Plastid differentiation in seedlings may be due to the activation of transcripts during seed germination that had been already synthesized during late embryogenesis and stored in quiescent embryos prior to dormancy.

Since the arrest of proplastid differentiation occurs only in *ex1/ex2* seedlings derived from light-exposed seeds, formation of this regulator may be linked to gene transcripts that are selectively up-regulated during late embryogenesis of light-grown *ex1/ex2* plants but not in wild-type plants.

Genes, whose expression during late embryogenesis was enhanced in light-grown *ex1/ex2* relative to wild type, were reexamined. Transcripts of twelve of them reached at least ten-fold higher levels in *ex1/ex2* than in wild type. One of them, *At5g45340*, was of particular interest. It forms part of a small family of four genes encoding cytochrome P450 proteins with ABA 8-hydroxylase activity that are involved in ABA catabolism (Millar et al. 2006; Umezawa et al. 2006). ABA had been implicated previously with the control of chloroplast formation in young seedlings (Rohde et al. 2000; Penfield et al. 2006) . Transcripts of three members of this gene family reached five- to 30-fold higher levels in fifteen to sixteen DAA than in six to seven DAA old immature seeds, whereas the expression level of the fourth member remained constant between these two stages of seed development. Among the three up-regulated cytochrome P450 genes only the expression of *CYP707A3* was differentially affected during late embryogenesis and reached a more than ten-fold higher level in *ex1/ex2*. When seedlings derived from seeds of light-grown *ex1/ex2/cyp707a3* triple mutants were compared with seedlings of the parental *ex1/ex2* line, plastid differentiation in these two groups of seedlings clearly differed. Inactivation of *CYP707A3* in *ex1/ex2* partially restored the capacity of proplastids to differentiate into chloroplasts.

A similar recovery of plastid formation was also observed in *ex1/ex2* seedlings growing on ABA medium. ABA has previously been shown to regulate several key steps of seed formation. Its role as a positive regulator of plastid differentiation during post-embryonic development, however, has remained unnoticed (Finkelstein et al. 2008). How the spatial and temporal specificities of these different ABA-dependent processes during seed formation and germination are controlled and coordinated is not known. The concentrations of ABA in immature and mature seeds, respectively, of light-grown *ex1/ex2* and wild-type plants were similar. Hence, ABA-dependent control of plastid differentiation during seedling development cannot be attributed to overall changes in total ABA content, but calls for a more selective regulatory principle. Multiple perception sites have been implicated with the sensing of ABA in different intra- and extracellular compartments and recently the first ABA receptors have been identified (Verslues and Zhu 2007). One of them, the Mg^{2+} chelatase H subunit, is confined to the plastid compartment (Shen et al. 2006) and may be involved in ABA-dependent control of post-embryonic plastid differentiation. In this case, it is not clear yet, how the upregulation of a gene encoding an ABA catabolizing enzyme that has been assigned to extraplastidic membranes can impinge on ABA-sensing within the plastid compartment.

A novel $^1O_2$-specific genetically controlled programmed cell death response has been described in **Chapter 4**. $^1O_2$-mediated signaling may evoke two seemingly contradictory visible stress responses, acclimation and programmed cell death (PCD) (Kim et al. 2008). In order to identify factors that may be closely involved in determining which way the plant responds to the release of $^1O_2$, experimental conditions must be established under which either acclimation or cell death prevails. By varying the length of the dark period, one can modulate in the *flu* mutant the level of the photosensitizer Pchlide and define conditions that minimize the cytotoxicity of $^1O_2$ and either endorse acclimation in *flu* plants exposed to a very short dark period or trigger a programmed cell death response in plants shifted for a longer period to the dark. In order to distinguish between these two modes of action of $^1O_2$, the impact of the *ex1* and *ex2* mutations was combined. In the *flu/ex1/ex2* triple mutant and also in the *flu/ex1* double mutant visible cell death responses were completely or almost completely abolished. Similar results were obtained, when the spreading of cell death in different mutant lines and wild type was visualized by trypan blue staining. A very sensitive indicator of the $^1O_2$-mediated onset of cell death in the *flu* mutant is the loss of plastid integrity. The initiation of plastid leakage can be monitored in a transgenic *flu* line that accumulates the small subunit of the ribulose-1,5-bisphosphate carboxylase (SSU) fused to the green fluorescent protein (GFP) in the stroma of plastids. Upon a dark/light transition, leakage of the soluble SSU-GFP fusion protein from the plastid to the surrounding cytoplasm was followed non-invasively in intact plants under the confocal microscope. Leakage of individual plastids was detected even after a very short dark period of less than 1 hour that does not result in visible stress responses of the *flu* mutant during reillumination. Extending the length of the intervening dark period led to a steady increase in the number of plastids that leaked and eventually resulted in microlesions or larger lesions on leaves that could also be detected by trypan blue staining. These $^1O_2$-mediated cell death responses of the *flu* mutant were suppressed, when both EX1 and EX2 were inactive. Therefore, plastid leakage cannot be attributed to a direct damage of the plastid envelope by $^1O_2$ but seems to depend on $^1O_2$-signaling of nuclear gene expression changes that subsequently evoke the release of stroma proteins from the plastid compartment. The requirement of nuclear gene expression changes for the $^1O_2$-mediated leakage of plastids was supported by comparing the impact of $^1O_2$ on plastid integrity in *flu* protoplasts and on chloroplasts isolated from these protoplasts. At the end of the dark period, SSU-GFP fusion proteins were found exclusively within chloroplasts of protoplasts. However, during re-illumination of *flu* protoplasts, the chloroplast integrity was rapidly lost as indicated by the extensive translocation of the SSU-GFP fusion protein from the chloroplast to the surrounding cytoplasm. However, chloroplasts isolated from these *flu* protoplasts remained

intact during reillumination despite the release of $^1O_2$. These results provide additional evidence that chloroplast leakage in the *flu* mutant was not caused by a direct reaction of $^1O_2$ with constituents of chloroplast envelope membranes, but resulted from $^1O_2$-mediated activation of a PCD signaling pathway that depended on the intactness of the whole cell.

A similar chloroplast leakage also occurred in wild-type plants that grew under a combined high light/low temperature stress (described in Chapter 4). Under these conditions, wild-type seedlings bleached and collapsed after 5 to 6 days of stress treatment, whereas .most of the *ex1/ex2* seedlings were still not visibly damaged. Trypan blue staining revealed the spreading of cell death in wild-type seedlings, but not in *ex1/ex2* seedlings. Additionally, chloroplast integrity of ex1/ex2 seedlings had not been impaired, whereas in wild type seedlings most of the fusion protein had been translocated to the extraplastidic cytoplasm.

Under the combined low temperature/higher light stress, chloroplasts would be expected to enhance not only the generation of $^1O_2$, but also the production of H_2O_2 and superoxide (Foyer and Noctor 2000). To determine which of these ROS triggers the observed plastid leakage in wild-type seedlings during high light/low temperature stress, changes in transcript levels of genes known to be controlled by either $^1O_2$ or H_2O_2 or superoxide were recorded in wild-type and *ex1/ex2* seedlings after different lengths of stress. Transcript levels of the superoxide-responsive gene *Fe SOD1* and the H_2O_2-responsive gene *Ferritin* (*FER1*) were up-regulated during the first 3 to 4 days of stress treatment and remained constant thereafter (*Fe SOD1*) or declined again (*FER1*). These transcript changes were similar in wild type and *ex1/ex2*, supporting the previous finding that H_2O_2/superoxide-dependent retrograde signaling from the plastid to the nucleus does not involve EX1- and EX2-dependent signaling steps (op den Camp et al. 2003; Laloi et al. 2007). Relative to the H_2O_2- and superoxide-dependent up-regulation of genes, activation of the $^1O_2$-responsive marker genes *WRKY33* and *WRKY46* was delayed and started between the third and fourth day of stress treatment shortly before first visible damages of seedlings were detectable. These transcript changes were suppressed in *ex1/ex2* seedlings. The kinetics of transcript accumulation of different ROS-responsive genes revealed that H_2O_2 and superoxide production preceded the release of singlet oxygen. As the up-regulation of $^1O_2$-responsive genes, but not H_2O_2- or superoxide-responsive genes was suppressed in *ex1/ex2* and correlated with a similar suppressive effect of *ex1/ex2* on plastid leakage and seedling lethality, these latter stress responses of wild type seem to be under the control of $^1O_2$.

PCD in plants causes several physiological changes in the cell: a loss of cellular membrane potential, the cessation of cytoplasmic streaming, and organelle destruction (Yoshinaga et al. 2005). Either chloroplasts or mitochondria may be the primary target of $^1O_2$-mediated death

signaling and after losing their structural integrity may play a key role in initiating and/or accelerating cell death. The structural integrity of mitochondria and chloroplasts was monitored in two different transgenic lines which expressed the DIPS-GFP localized in mitochondria (Sakomoto and Hoshino 2004) and SSU-GFP localized in chloroplast. Under the combined high light/low temperature stress condition, the DIPS-GFP protein remained within the mitochondria, whereas plastids lost most of their SSU-GFP protein.

Since it is conceivable that the GFP may still remain trapped inside damaged mitochondria, we also tested permeability changes of mitochondrial membranes by using Mito-tracker Red as a cell-permeable fluorescent probe (Oparka and Reed 1994). After 1 hour of illumination of pre-darkened protoplasts, addition of Mito-tracker Red revealed that mitochondria remained intact and maintained their membrane potential both in wild type and *flu*, whereas chloroplast integrity of *flu* protoplasts was selectively perturbed. A possible conclusion that one may infer from these results is the coexistence of at least two distinct cell death programs in plant cells that are evoked by a disturbance of mitochondria and chloroplast homeostasis, respectively, and perturb directly only the structural intactness of the affected organelle. This prediction was tested by using transgenic *flu* mutants overexpressing the BAX inhibitor (AtBI). BAX is a well known inducer of PCD in animals and yeast. When BAX protein is translocated from the cytosol to the outer membrane of the mitochondria, it induces the release of proteins, such as cytochrome *c*, to the cytosol, and consequently triggers the PCD in animal system (Liu et al. 1996; Jurgensmeier et al. 1998). Even though a *BAX*-like gene has not been found in plants, heterologous expression of this gene in plants induces PCD (Yoshinaga et al. 2005). Suppression of BAX-induced cell death in transgenic plants that over-express a BAX Inhibitor-GFP (AtBI-GFP) fusion protein had been attributed to a selective block of a mitochondrial cell death pathway (Kawai-Yamada et al. 2001). The AtBI-GFP fusion protein was associated with the endoplasmic reticulum, whereas $^1O_2$-generation occurred in *flu* chloroplasts. Seedlings of *flu* and *flu/AtBI-GFP* grew like wild type under continuous light, but were severely impaired in their development and showed lesion formation, when they were shifted to the dark for 8 hours and re-exposed to light for 5 days. These results support that $^1O_2$-mediated cell death is activated by a signaling pathway that operates separately from the mitochondrial cell death pathway and uses chloroplasts, but not mitochondria as a primary target.

5.1 References

Apel, K. and Hirt, H. 2004. Reactive oxygen species: metabolism, oxidative stress, and signal transduction. *Annu Rev Plant Biol* 55: 373-399.

Brocard-Gifford, I.M., Lynch, T.J., and Finkelstein, R.R. 2003. Regulatory networks in seeds integrating developmental, abscisic acid, sugar, and light signaling. *Plant Physiol* 131(1): 78-92.

Dangl, J.L., Dietrich, R.A., and Richberg, M.H. 1996. Death don't have no mercy: cell death programs in plant-microbe interactions. *Plant Cell* 8(10): 1793-1807.

Finkelstein, R., Reeves, W., Ariizumi, T., and Steber, C. 2008. Molecular aspects of seed dormancy. *Annu Rev Plant Biol* 59: 387-415.

Finkelstein, R.R. and Gibson, S.I. 2002. ABA and sugar interactions regulating development: cross-talk or voices in a crowd? *Curr Opin Plant Biol* 5(1): 26-32.

Foyer, C.H. and Noctor, G. 2000. Oxygen processing in photosynthesis: regulation and signalling. *New Phytologist* 146(3): 359-388.

Jurgensmeier, J.M., Xie, Z., Deveraux, Q., Ellerby, L., Bredesen, D., and Reed, J.C. 1998. Bax directly induces release of cytochrome c from isolated mitochondria. *Proc Natl Acad Sci U S A* 95(9): 4997-5002.

Kawai-Yamada, M., Jin, L., Yoshinaga, K., Hirata, A., and Uchimiya, H. 2001. Mammalian Bax-induced plant cell death can be down-regulated by overexpression of Arabidopsis Bax Inhibitor-1 (AtBI-1). *Proc Natl Acad Sci U S A* 98(21): 12295-12300.

Kim, C., Meskauskiene, R., Apel, K., and Laloi, C. 2008. No single way to understand singlet oxygen signalling in plants. *EMBO Rep* 9(5): 435-439.

Krieger-Liszkay, A. 2005. Singlet oxygen production in photosynthesis. *J Exp Bot* 56(411): 337-346.

Laloi, C., Stachowiak, M., Pers-Kamczyc, E., Warzych, E., Murgia, I., and Apel, K. 2007. Cross-talk between singlet oxygen- and hydrogen peroxide-dependent signaling of stress responses in Arabidopsis thaliana. *Proc Natl Acad Sci U S A* 104(2): 672-677.

Liu, X., Kim, C.N., Yang, J., Jemmerson, R., and Wang, X. 1996. Induction of apoptotic program in cell-free extracts: requirement for dATP and cytochrome c. *Cell* 86(1): 147-157.

Meskauskiene, R., Nater, M., Goslings, D., Kessler, F., op den Camp, R., and Apel, K. 2001. FLU: a negative regulator of chlorophyll biosynthesis in Arabidopsis thaliana. *Proc Natl Acad Sci U S A* 98(22): 12826-12831.

Millar, A.A., Jacobsen, J.V., Ross, J.J., Helliwell, C.A., Poole, A.T., Scofield, G., Reid, J.B., and Gubler, F. 2006. Seed dormancy and ABA metabolism in Arabidopsis and barley: the role of ABA 8'-hydroxylase. *Plant J* 45(6): 942-954.

op den Camp, R.G., Przybyla, D., Ochsenbein, C., Laloi, C., Kim, C., Danon, A., Wagner, D., Hideg, E., Gobel, C., Feussner, I., Nater, M., and Apel, K. 2003. Rapid induction of distinct stress responses after the release of singlet oxygen in Arabidopsis. *Plant Cell* 15(10): 2320-2332.

Oparka, K.J. and Reed, N.D. 1994. *The use of fluorescent probes for studies of living plant cells* IRL Press, Oxford University, UK, Oxford.

Penfield, S., Li, Y., Gilday, A.D., Graham, S., and Graham, I.A. 2006. Arabidopsis ABA INSENSITIVE4 regulates lipid mobilization in the embryo and reveals repression of seed germination by the endosperm. *Plant Cell* 18(8): 1887-1899.

Rohde, A., De Rycke, R., Beeckman, T., Engler, G., Van Montagu, M., and Boerjan, W. 2000. ABI3 affects plastid differentiation in dark-grown Arabidopsis seedlings. *Plant Cell* 12(1): 35-52.

Sakomoto, W. and Hoshino, T. 2004. An approach to screen mitochondrial mutants in *Arabidopsis thaliana*. *Endocytobiosis Cell Res* 15(1): 101-109.

Shen, Y.Y., Wang, X.F., Wu, F.Q., Du, S.Y., Cao, Z., Shang, Y., Wang, X.L., Peng, C.C., Yu, X.C., Zhu, S.Y., Fan, R.C., Xu, Y.H., and Zhang, D.P. 2006. The Mg-chelatase H subunit is an abscisic acid receptor. *Nature* 443(7113): 823-826.

Umezawa, T., Okamoto, M., Kushiro, T., Nambara, E., Oono, Y., Seki, M., Kobayashi, M., Koshiba, T., Kamiya, Y., and Shinozaki, K. 2006. CYP707A3, a major ABA 8'-hydroxylase involved in dehydration and rehydration response in Arabidopsis thaliana. *Plant J* 46(2): 171-182.

Verslues, P.E. and Zhu, J.K. 2007. New developments in abscisic acid perception and metabolism. *Curr Opin Plant Biol* 10(5): 447-452.

Wagner, D., Przybyla, D., Op den Camp, R., Kim, C., Landgraf, F., Lee, K.P., Würsch, M., Laloi, C., Nater, M., Hideg, E., and Apel, K. 2004. The genetic basis of singlet oxygen-induced stress responses of Arabidopsis thaliana. *Science* 306(5699): 1183-1185.

Yoshinaga, K., Arimura, S.I., Hirata, A., Niwa, Y., Yun, D.J., Tsutsumi, N., Uchimiya, H., and Kawai-Yamada, M. 2005. Mammalian Bax initiates plant cell death through organelle destruction. *Plant Cell Rep* 24(7): 408-417.

Acknowledgements

There are lots of people I would like to thank for a huge variety of reasons.

First of all, I would like to thank Prof. Dr. Klaus Apel for giving me the opportunity to perform my PhD, and I could not have imagined having a better advisor and mentor for my PhD, and without his common-sense, knowledge and perceptiveness I would never have finished.

I am also very grateful to co-examiner, Prof. Dr. Nikolaus Amrhein, for managing to read my thesis.

All the people of the Plant Genetics Group (Dr. Frank Landgraf, Dr. Christophe Laloi, Dr. Rase Meskauskiene, Dr. Aiswarya Baruah, Dr. Dieter Rubli, Dr. Veronica Albrecht, Dr. Dominika Przybyla, Dr. Marco Würsch, Dr. Antoine Danon, André Imboden, Dominika Kauss, Hanno Mahler, Geetanjali Saini, Klara Simkova, Jean-Charles Isner, Mena Nater) are thanked for numerous stimulating discussions, help with experimental setup and general advice. In particular, I would like to acknowledge the help of Dr. Chanhong Kim for his support and for supervising my PhD work. Words cannot express his help. Thanks to group secretaries, Martha and Ursula, for being always helpful and going good advice.

Special thanks ETH Zurich and the Swiss National Science Foundation for funding my PhD work.

Finally, I have to say “thank you” to all my friends and family wherever they are; particularly my parents, brother, brother’s wife and nephews for their love.
And I can’t leave out my fiancé, Jung Hee, for her endless love and for waiting for me until I have finished my PhD without any complaint.

May, 2008

Keun Pyo Lee

Curriculum vitae

Name: **Lee, Keun Pyo**

Date of birth: **April 7th, 1975**

Place of birth: **Pusan**

Nationality: **Republic of Korea**

11.2003-06.2008 **Ph.D. thesis, Prof. Dr. Klaus Apel**

Thesis title: "The role of Executer1-and Executer2-dependent retrograde signaling after release of singlet oxygen in *Arabidopsis thaliana*"
Institute of Plant Science, Plant Genetics, Swiss Federal Institute of Technology (ETH), Switzerland

03.2001-08.2003 **M.sc. in Applied Biology, Prof. Dr. Dae Won Lee**

Thesis title: "Identification and purification of lectin from induced callus in Korean mistletoe (*Viscum album* var. *coloratum*)"
Department of Applied Biology, Dongguk University, Republic of Korea

03.1994-02.2001 **B.sc. in Natural Sciences**

Department of Biology, Dongguk University, Republic of Korea

01.1996-03.1998 **Military Service**

The Republic of Korea Army

03.1991-02.1994 **High School**

Kaya High School, Pusan, Republic of Korea

Publication List

- **Keun Pyo Lee**, Chanhong Kim, Aiswarya Baruah, Christophe Laloi, Mena Nater, Ivo Feussner and Klaus Apel (2008). Singlet oxygen-mediated signaling during late embryogenesis of Arabidopsis primes the fate of plastid differentiation by modulating the level of abscisic acid. In preparation.

- Chanhong Kim, **Keun Pyo Lee**, Ashok M.L., Karolina Blajecka, Magdalena Obazanek-Fojt, Hyesung Jeon, Rasa Meskauskiene, Hye Min Ham, Ji Young Kim, Diana Marcela Pazmiño Mantilla, Mena Nater, Karin Krupinska and Klaus Apel (2008) A new role of chloroplasts as the *alpha* and *omega* of a plant-specific programmed cell death pathway. In preparation.

- **Keun Pyo Lee**, Chanhong Kim, Frank Landgraf and Klaus Apel (2007) EXECUTER1- and EXECUTER2-dependent transfer of stress-related signals from the plastid to nucleus of *Arabidopsis thaliana*. ***Proc Natl Acad Sci USA***, 104(24), 10270-10275

- David Goslings, Rasa Meskauskiene, Chanhong Kim, **Keun Pyo Lee**, Mena Nater and Klaus Apel (2004) Concurrent interactions of heme and FLU with Glu-tRNA reductase (HEMA1), the target of metabolic feedback inhibition of tetrapyrrole biosynthesis, in dark- and light-grown Arabidopsis plants. ***Plant Journal***, 40, 957-67

- Daniela Wagner, Dominika Przybyla, Roel op den Camp, Chanhong Kim, Frank Landgraf, **Keun Pyo Lee**, Marco Würsch, Christophe Laloi, Mena Nater, Eva Hideg and Klaus Apel (2004) The genetic basis of singlet oxygen-Induced stress responses of *Arabidopsis thaliana*. ***Science***, 306, 1183-5

- **Keun Pyo Lee**, Chanhong Kim, Dae Won Lee and Klaus Apel (2003), *TIGRINA d*, required for regulating the biosynthesis of tetrapyrroles in barley, is an ortholog of the *FLU* gene of *Arabidopsis thaliana*, ***FEBS Letter***, 553, 119-124

- **Keun Pyo Lee** and Dae Won Lee (2003), Somatic embryogenesis and plant regeneration from seeds of wild *Dicentra spectabilis* (L.), ***Plant Cell Reports***, 22(2), 105-109